ROUTING AND TRAFFIC-ENGINEERING IN MULTI-HOP WIRELESS NETWORKS: AN OPTIMIZATION BASED APPROACH

BY

VINAY KOLAR

B.E., Bangalore University, 2000
M.S., Binghamton University, 2004

DISSERTATION

Submitted in partial fulfillment of the requirements for
the degree of Doctor of Philosophy in Computer Science
in the Graduate School of
Binghamton University
State University of New York
2007

Accepted in partial fulfillment of the requirements for
the degree of Doctor of Philosophy in Computer Science
in the Graduate School of
Binghamton University
State University of New York
2007

Dr. Nael B. Abu-Ghazaleh _____ November 28, 2007
Department of Computer Science
Binghamton University

Dr. Michael J. Lewis _____ November 28, 2007
Department of Computer Science
Binghamton University

Dr. Kenneth Chiu _____ November 28, 2007
Department of Computer Science
Binghamton University

Dr. Kartik Gopalan _____ November 28, 2007
Department of Computer Science
Binghamton University

Abstract

Multi-hop wireless networks (MHWNs) attract significant interest due to the minimal infrastructure demands and their potential in supporting mobile and pervasive computing. The high demand placed by a growing user base on the limited available bandwidth places a premium on effective communication and networking for MHWNs. Recent studies in protocol development have improved the network performance considerably. However, effective networking under sparse bandwidth remains a difficult problem. Traffic-engineering techniques have been used to solve this problem in conventional networks. One of the key challenges in traffic-engineering in MHWNs is the routing problem – a problem of delivering packets across multiple wireless hops, considering the complex interference patterns and interactions in MHWNs.

The dissertation targets *developing a formally grounded approach for solving routing problems in MHWNs, while taking into account the effects of interference.* The work builds on recent efforts in the networking community to express a network behavior as an optimization problem, and decomposing the formulation to provide distributed protocols. A successful model can then be applied to: (1) analyze the performance and capacity of existing protocols; (2) develop protocols for traffic engineering and admission for static networks; and (3) develop formally grounded and near-optimal distributed routing protocols.

In MHWNs, the routing problem is substantially more complicated than the wired problem because of interference. Interference is exhibited at many levels, leading to effects such as uncontrolled contention and unfairness. The approach proposed in this dissertation breaks the problem into multiple layers. Firstly, *a Multi-commodity flow based routing model that produces interference-separated routes* is developed. The study analyzes the interaction of multiple routes and proposes effective objective functions to improve the throughput and delay metrics of the connections. Simulation results show significant improvement in performance over a traditional routing protocol.

However, the assumption of an ideal scheduling model in the routing model discounts for the scheduling effects, that limits the applicability of the model. Existing accurate CSMA scheduling

models cannot be directly applied as part of a routing formulation due to their complexity and underlying assumptions. *A low-complexity scheduling model is proposed to capture the key scheduling interactions in CSMA based schedulers, like IEEE 802.11, and this model is integrated with the routing model.* Simulations demonstrate large performance improvements (around 40%) when compared to the scheduling-unaware routing model.

The above routing models are NP-hard, thus limiting their applicability to larger networks. *The third contribution of the dissertation is to approximate the routing model to a polynomial time algorithm.* A *decomposition* based approach is followed to formulate a low-complexity model by applying domain-specific heuristics. We show that such a model is orders of magnitude faster than the above routing models, while being able to maintain efficient solutions.

An approach to account for the effect of scheduling, while preserving a low run-time, is presented. *Interaction graphs* are proposed to capture the scheduling characteristics of CSMA based schedulers. Using the interaction graph framework, we capture a fundamental fairness property of CSMA scheduling called *Contention fairness*. The dissertation proposes a detailed throughput estimation model to capture contention fairness by applying Renewal Theory and Continuous-time Markov chain. Based on the insights gained, we propose a distributed mechanism to mitigate unfairness. Simulation results validate the accuracy of the model and demonstrate the significant improvement in fairness obtained by the proposed distributed scheme.

The next contribution of the dissertation is to characterize the interactions between two competing links in CSMA. *Throughput estimation models are proposed for various categories of interactions that have been identified in MHWNs and are validated by simulations.* We show that such a model can accurately capture the certain frequently occurring categories.

We discuss the future work towards realizing the formulation as an online traffic-engineering tool in deployed networks. Finally, we sketch our plans towards formally deriving routing layer functionality in distributed protocols using the above framework.

Acknowledgements

It gives me immense pleasure to express my gratitude to all the people who helped me actualize this thesis. I am deeply indebted to my advisor, Dr. Nael Abu-Ghazaleh, for his guidance and support extended to me during the course of my graduate student life. His creative suggestions along with his words of encouragement, patience and time went a long way in my dissertation. I consider it my good fortune to be advised under a person of such intellect, yet so humble and down-to-earth. My heart felt thanks to Nael.

All this would have not been possible without the invaluable encouragement of my parents and Smitha. Their constant moral support has been the foundations of my progress. Thanks for standing by me in all good and bad times!

My special thanks to Dr. Michael Lewis for his guidance on research and academics; and also for being on my dissertation committee. I enjoyed being his teaching-assistant for more than 2 years. I am grateful for his confidence in me. His suggestions were very helpful for improving my research and teaching abilities, though I have much more to learn in these areas. I also would like to thank my other dissertation committee members: Dr. Kenneth Chiu, Dr. Kartik Gopalan, and Dr. Nagen Nagarur for being in my committee, and for their feedback and suggestions. I thank Dr. Kanad Ghose, Dr. Madhusudhan Govindaraju and Dr. Dmitry Ponomarev for all the support extended. In addition to valuable research suggestions, the faculty in Department of Computer Science were very supportive for my personal growth and showed great interest to shape my career goals. It was an great experience to be with a group of such people. Thank you, CS department.

My thanks to Kaushik Balasubramanian, Kartik Bharat, Ameya Agnihotri and Gurudutt Chennagiri for making my graduate life more interesting. I would like to thank all my friends in the

networking lab – Sameer Tilak, Saquib Razak, Ke Liu, Weishuai Yang, Adnan Majeed, Vikram Munishwar and SeonYeong Han– for providing their thought-provoking comments and creating a pleasurable environment in the lab during the course of this dissertation.

Contents

List of Tables

List of Figures

List of Algorithms

Chapter 1

Introduction

Wireless communication is a critical enabler of mobile computing and communication, where users use portable devices to access information anywhere and anytime. Freedom from wires lowers the infrastructure needs for creating a network, facilitating inexpensive and fast deployment of networks. As a result, wireless networks will play an important role in an Internet that is increasingly wireless at the periphery. In addition, the ability to communicate on the move introduces new applications and opportunities.

Multi-hop wireless networks (MHWNs), a branch of wireless networks that can be deployed with minimal infrastructure, are emerging as a critical technology that plays an important role at the edge of the Internet. Mesh networks [8, 90] provide an extremely cost-effective last mile technology for broadband access; ad hoc networks have many applications in the military, industry and everyday life [89]; and sensor networks hold the promise of revolutionizing sensing across a broad range of applications and scientific disciplines – they are forecast to play a critical role as the bridge between the physical and digital worlds [56]. This range of applications results in MHWNs with widely different properties in terms of scales, traffic patterns, radio capabilities and node capabilities. While a wide variety of applications has created a high-demand for the growth of MHWNs, many unique challenges have to be addressed to enable effective use of MHWNs. Thus, effective networking of MHWNs has attracted significant research interest.

1.0.1 Routing in MHWNs

One of the primary challenges in networking MHWNs is the routing problem; how to construct efficient routes for a network that is self-configuring and potentially mobile. Routing protocols have a determining effect on the application throughput [17, 83]. Improving the performance of these protocols in MHWNs has been given considerable attention in the past decade. **An important step for designing high-performance routing protocols is *characterizing* and *quantifying* the effects that play a prominent role in determining the performance of the network.**

A formal specification or verification of a routing protocol functionality aids in reasoning the effectiveness and limitations of a routing protocol under a network requirement. The first generation of routing algorithms for MHWNs attempted to specialize classical routing algorithms developed for wired networks to work in MHWNs. Essentially, these protocols must account for mobility and pay careful attention to the bandwidth and resource limitations that exist in MHWNs. Many flavors of protocols including proactive protocols [101, 103], reactive protocols [65, 102], hybrids [51], as well as geometric protocols [71] emerged. Common across these protocols is that they route connections greedily, taking local decisions without coordination. Typically, decisions are made for each connection considering metrics such as shortest path; such policies may lead to routing connections to mutually interfering nodes when, perhaps, other regions of the network are idle. While some new routing protocols attempt to adaptively switch away from paths where the quality of the links is low (due to signal propagation as well as interference), a formal reasoning for demonstrating the optimality of such routes is not investigated. Without considering the effect of interference, the routes produced by these protocols can result in inefficient routing configurations.

The available bandwidth between a pair of communicating nodes is influenced not only by the nominal communication bandwidth, but also by ongoing communication in nearby regions of the network. More specifically, neighboring transmissions contribute interference power, which may make it impossible to exchange packets between a given pair of nodes. An important paper by Gupta and Kumar [47] has quantified the available capacity in a MHWNs as of the size of the network, assuming a given density. However, the above derivation assumes *optimal routing*, along

with *optimal transmission schedule* and *idealized propagation model*, using uniform deployment and traffic pattern. As a result, this is an asymptotic analysis that is not capable of determining the achievable limit for a specific deployment and traffic pattern. In addition, it is not helpful in deriving the shape of an effective routing and packet transmission schedules that approaches this limit.

Recent research studies have proposed optimal routing models [63, 76]. However, these models are not directly applicable to static MHWN since they do not capture interference modes under existing MAC protocols. Models for existing MAC protocols [16, 18, 41, 123] can capture the interference details but cannot be used for computing optimal routes due to their complexity.

1.0.2 Dissertation problem

In wired networks, traffic engineering has been used to plan traffic with an eye for overall performance (rather than the local per-connection perspective of routing protocols); traffic engineering in wired networks is a fairly mature technology (e.g., [28, 73, 109]). In the context of MHWNs, such approaches cannot be directly applied because of the impact of interference. More precisely, in wired networks, flows only interact when they share the same links and routers. Their interaction is then well understood based on queueing theory, providing the necessary tools for the traffic engineering.

In contrast, flows interfere in much more complex ways in wireless environments. Links interfere only if an interfering sender is close enough to another receiver to cause a collision. In addition, the wireless channel gives rise to a number of different modes of interactions between interfering links, which can cause poor performance and short term or sustained unfairness [42]. **Thus, the main goal of the dissertation is to develop models of MHWN operation that account accurately and efficiently for how connections interfere in a wireless environment.**

The applications for such a model range far wider than just traffic engineering. It can also be applied directly for QoS admission control in static MHWNs and for guiding provisioning decisions for planning static networks. In addition, accurate modeling of interference and of MHWN networks is critical for better understanding of their operation, which can lead to more effective distributed

protocols that are based on these observations. Depending on the structure of the optimization problem, distributed protocols may be derivable from it using decomposition.

It has recently been argued that effective distributed protocols can be developed by viewing the network as an optimization problem against an objective function consisting of some measures of the utility of the users [22]; the research in this dissertation takes this approach. An interesting corollary is that both layering and distributed protocols can be viewed as a decomposition problem of the "centralized" optimization problem. Of course, various decomposition strategies can be devised, leading to different tradeoffs in the resulting distributed solutions. Thus, both our work in modeling the problem, and in exploring decomposition for accelerating its solution can be viewed as steps towards developing effective, analytically grounded, distributed protocols for MHWNs.

1.0.3 Contributions and relation to existing work

Traffic-engineering has been applied for solving specific problems in MHWNs. Optimal routing models have been proposed in the existing literature [63,76] assuming an optimal scheduling component. This limits the the applicability of the models in realistic networks that use CSMA based MAC protocols. Analysis and models for CSMA protocols has been studied in great detail [16,18,40,41,118]. But, such solutions cannot be integrated into the optimal routing model because of high-complexity (explained in Section 3.4). **In a nutshell, while some individual models exist to compute the elements of optimal routing, a cohesive model for evaluating optimal routing configuration in realistic MHWNs is absent.** Development of such an integrated routing model will assist in the applicability of the theoretical models in the realistic MHWNs. Moreover, the insights obtained from the model can be effectively used in designing the distributed protocols.

Towards this end, we first create routing models that optimizes performance metrics of the connection like throughput and end-to-end delay. Such models are infeasible due to two main reasons: the high complexity and the ineffectiveness to capture the realistic CSMA scheduling. In order to overcome these deficiencies, we model: (1) A low-complexity CSMA scheduler with reasonable accuracy and propose an integrated routing and scheduling model. (2) A approximate polynomial time routing model that has enables a formal approach to develop efficient distributed

protocols. Finally, we improve the accuracy of the scheduling model by capturing various CSMA specific properties, while still preserving the low-runtime of the solution. We now discuss the contributions in detail.

The first contribution of the dissertation is to develop a network flow based routing model under optimal scheduling assumption. While studies [63, 76] have explored optimal routing with such assumption, several facets of the routing problem have not been analyzed. Multiple routes interact in complicated ways which have not been analyzed by the existing studies. In this dissertation, we first develop a *Multi-commodity flow (MCF)* model [7], a well-known network flow methodology, for optimal routing in the presence of interference. The distinct features of the proposed model that differentiates it from the existing studies like [63, 76] are: (1) The model analyzes the various interactions, both intra and inter-route interactions; (2) An indepth analysis of the objective function formulation and the drawbacks of simple extentions of the existing objective functions are discussed; and (3) The model proposes a node-based approach to capture the interference effects. We refer to the above model as *Interference Aware Routing (IAR) Model* in this dissertation. Simulation results show significant improvement in performance over a traditional routing protocol in terms of throughput, goodput, and end-to-end delay. Chapter 4 describes the IAR model.

The second contribution of the dissertation is to extend the optimal routing model for realistic schedulers. The realistic schedulers like IEEE 802.11 [117], described in Section 2.2, follow a distinctively different policy than the optimal scheduling ones [54, 124, 125]. Hence, the assumption of an optimal scheduler has a high impact on the derived optimal routes. Several complex scheduling interactions occur due to interference in MHWNs [42, 110]. Existing studies model such realistic schedulers [16, 18, 40, 41, 118, 123] and are summarized in Section 3.4. Such models input a set of active routes and evaluate the scheduling effectiveness. However, the necessity for an optimal routing model is orthogonal to this objective – a route-set has to be determined for a given deployment of nodes. While such scheduling models can be used in routing model to find the scheduling effectiveness, the combination of various active edges that forms a route-set in a given scenario is large – it grows exponentially with the number of nodes and connections. Hence, a

direct approach of evaluating each route-set for optimality conditions is infeasible. Another fundamental limitation is the runtime of such scheduling models. Majority of the schedulers, while being accurate, are computationally expensive. Evaluating scheduling effectiveness of different route-sets using such expensive scheduling component further increases the complexity of the optimal routing model, which is already NP-hard. The dissertation proposes a two-level approach: (1) A routing framework separates the routes into interference-separated paths; (2) A low-complexity scheduling model captures the key scheduling interactions that are detrimental. A feedback mechanism from the scheduling component to the routing component is used to eliminate such harmful interactions and the routing model is re-evaluated. Chapter 5 describes the above *Scheduling-Aware Routing (SAR) Model*. Simulation results show that accounting for scheduling effects leads to large improvements in the quality of the solution.

The above two contributions provides a framework for formulating an interference-separated and scheduling-aware routing model. The contributions that follow are geared towards a thorough characterization of the models, primarily by increasing the accuracy, reducing the complexity and extending the scope of the models. Chapters 6 and 7 improves the network flow based routing model, while chapters 8 , 9 and 10 deals with accurate capturing of the CSMA scheduling.

Extensions to the network flow based routing models

Routing models that minimize the end-to-end delay caters to a wide variety of delay sensitive applications in static MHWNs. *Towards this goal, we formulate a delay sensitive routing model using an end-to-end delay based objective.* Chapter 6 describes the multi-commodity flow based routing model that optimizes the end-to-end delay of the connections. The proposed formulation yields routes that significantly outperform the best routes obtained by current routing protocols under a real-time traffic.

The complexity of the network flow based routing model, which is NP-hard, severely limits the applicability of the model only to small networks. *The dissertation approximates the NP-hard optimal routing model into a polynomial time algorithm.* Realistic evaluation of moderate to dense networks is impractical under the IAR based routing model, thus making the model ineffective

for practical purposes. Due to the same reason, it is unrealistic to extend the IAR model to incorporate other complex elements of traffic-engineering, such as the scheduling component. The dissertation proposes a *Decomposition* based approach, where a large problem is broken down into smaller problems and sub-problems are solved individually. Such a low-complexity model makes the optimal routing framework practical and extensible. Chapter 7 explains the *Decomposition based IAR (d-IAR) model* in detail. The study shows, experimentally as well as with analysis, that the resulting formulation achieves orders of magnitude lower run times while maintaining the ability to find efficient solutions.

Extensions to the CSMA scheduling models

The next set of contributions enhance the accuracy of the scheduling component, while maintaining a low-complexity. As explained in the previous paragraphs, capturing the complex scheduling interactions in a low-complexity model is non-trivial. We improve on the scheduling model to capture several key effects described in the below paragraphs.

Fairness among a set of competing links is known to be one of the key problems of realistic MAC protocols like IEEE 802.11 [84, 125]. Fairness issues in IEEE 802.11 raise due to several reasons, namely (1) Certain spatial arrangements of the active edges cause fairness issues while contending for the wireless channel. We term the unfairness resulting from such unfair contention as *Contention fairness*; and (2) *Hidden-terminals* [119], where a node experiences packet collision due to simultaneous transmission by two unsynchronized sources, causes unfairness issues. The contention fairness is explained in Chapter 8 and the hidden terminal problem and its effects are outlined in Section 2.2.3.

The dissertation analyzes the causes for "Contention unfairness" in MHWNs and proposes a low-complexity model to evaluate the effect of such unfairness. Existing studies on the analysis and modeling of fairness do not explicitly differentiate between the causes of such unfairness. Moreover, the models have the above discussed limitations of high-complexity. Chapter 8 describes the model and evaluates the unfairness in IEEE 802.11 MHWNs. The model is verified for its accuracy and efficiency. Such a model is directly applicable in networks where the packet collisions are prevented

due to advanced CSMA protocol mechanisms [37] or by external routing protocols. Based on the insights gained from the contention fairness model, we propose a distributed approach to alter the backoff mechanism in IEEE 802.11. Simulation studies demonstrate that such an approach can lead to approximately 25% improvement in the fairness properties.

The next contribution of the dissertation is to characterize the fundamental interactions between two competing links in CSMA. Existing studies have analyzed the possible interactions in MHWNs consisting of only two links and have categorized them based on the type of interactions [108]. *Chapter 9 proposes a model to compute the throughput in each of these categories.* We show that such a model can accurately capture the certain categories of interaction that occur most frequently in MHWNs.

Chapter 10 proposes *Interaction graphs (IGs)* to capture the scheduling characteristics of CSMA based schedulers. We show that such graphs are useful for capturing spatial and temporal relationships between the active edges of the network. In addition to the ability to characterize the CSMA interactions, IGs also enable comparison of the specific CSMA protocol with an ideal CSMA behavior. This ability is demonstrated by modeling the impact of hidden and exposed terminals in IEEE 802.11.

While individual scheduling models have been proposed, an integrated scheduling model that accounts for the primary artifacts of the CSMA will be beneficial for various applications, including the construction of an accurate and low-complexity routing model. We wish to extend the dissertation in the future work. The long-term directions for extending the dissertation is to develop an online traffic-engineering tool in static MHWNs. Various applications like admission control, provisioning and QoS will be benefitted from such a tool. We also like to extend the model towards developing near-optimal distributed protocols by using formal approaches. Chapter 11 discusses these future work along with the conclusions of the dissertation.

Chapter 2

Background

In this chapter, we overview necessary background for MHWN. Section 2.1 describes the characteristics of multi-hop wireless networks and their unique challenges. The physical and the Medium Access Control(MAC) layer is described in Section 2.2. The routing layer background is provided in Section 2.3.

2.1 Multi-hop Wireless Networks

In Multi-hop wireless networks (MHWNs), the devices self-configure to cooperatively communicate without the need for access points. The wireless nodes cooperate to route each others packet to provide connectivity. MHWNs lower the barrier for coverage as existing devices can self-configure to provide access to each other. However, the architecture is quite different from conventional networks. For example, in such settings, the devices are often mobile, causing the topology of the network to frequently change, and making it difficult to use ideas such as hierarchy and address aggregation that have served us well in wired networks. There is also a great variety in the architecture, scale and other characteristics of MHWNs: for example, Mesh networks, Mobile Ad-hoc (MANETs) networks, Vehicular Networks, sensor networks and other types of networks are structurally MHWNs. Each of these types of networks may in turn vary in scale, radio and medium access technologies, traffic patterns and other important operational characteristics.

The properties of the lower layers, like physical and Medium Access Control (MAC) layers, has

a high impact on the higher layers. The routing layer has to tackle the issues due to high channel error rate, lack of infrastructure, mobility and power-constrained devices. This prohibits the direct application of routing ideas present in single-hop [62, 121] and wired networks [60]. Transport protocols like TCP fail to work effectively in MHWNs [57, 125] due to various assumptions of such protocols. Modified versions of TCP to suit MHWN have been studied [9, 10].

It has been concluded that the core of the issues lie centered in the uniqueness of the MHWN interactions that break the assumption of the existing higher level protocols. This dissertation is an attempt to address this broad set of challenges by understanding the key interactions of MHWNs at primarily two levels: the MAC and the Routing layer. The rest of the chapter reviews the development of MAC protocols that regulate the channel access. A review of the routing layer is presented in Chapter 2.3.

2.2 Wireless Communication and Medium Access

In this section, we briefly overview the wireless signal propagation and describe the Medium Access Protocol that regulates the channel access in wireless networks.

2.2.1 Wireless signal propagation

In wireless communication, as the signal from a sender propagates over the channel, it attenuates with distance; it also suffers from physical propagation effects due to interactions with the physical environment (e.g., passing through obstacles). A receiver receives the signal after attenuation and other propagation effects, and attempts to decode it. If the ratio of the received signal strength to the sum of the noise and signal from interfering signals, is sufficiently high the signal can be decoded successfully; otherwise, the transmission cannot be received. Thus, interference from concurrently transmitting nodes plays an important effect in determining whether correct reception or a collision occurs. We now briefly state the various models that have been used in simulation and modelling studies to approximate the interference.

Models for interference calculation

Accounting for detailed signal propagation and interference needs considerations of many environmental and signal propagation parameters. Simplistic approximations are used to infer the effect of interference in modeling wireless networks. In this section, we discuss the popular simplistic models that the modeling literature has used to account for the effect of interference.

The first model is very simplistic and assumes that a receiver can receive and decode all the packets sent by any of the node within a certain radius. Any simultaneous transmission by two or more nodes within this circle can interfere with the packet reception at the receiver. Such a model is henceforth referred as *Unit Disc Model*. However, it has been observed that a significant power level is needed to receive and decode the packet, while signal with lesser power can interferere with the ongoing reception, causing packet collision. To represent this effect, a model was proposed where each node is able to receive and decode the packet from any of the node within a certain range, called *reception range*. However, any node within a greater radius , called interference range, is capable of interfering with the packet reception. A receiver cannot receive the packets from the nodes lying within the reception range and interference range, but such nodes can interfere with the packet reception. We refer to such a model as *Two Disc Model*.

While the above models simplify the interference calculation, it does not account for the relationship between the signal strength of the active reception and the interfering signal strength. Gupta and Kumar [47] proposed two models to depict this relationship for calculating the reception success (and the effect of interference): (1) *Protocol model:* Under this model, a node can successfully receive a packet from a sender if there is no other actively sending node within certain factor of d, where d is the distance between the sender and the receiver. The difference between the two disc Model and the protocol model is that the latter model is sensitive to the signal strength between the sender and receiver, while the former one has fixed reception and interference ranges. (2) *Physical model:* A node can successfully receive a packet if signal strength is a factor of times higher than the *combined* strength of the interfering signals and the noise. Such model is also referred as *Signal to Interference and Noise ratio (SINR) model*.

2.2.2 Medium Access Protocols

The initial applications of wireless communications used simple protocols to access the wireless medium. The characteristics of these protocols evolved from the wired protocols, due to its similarity in sharing the transmission medium between multiple nodes. The MAC protocols can be broadly categorized into two approaches (1) A reservation based approach; and (2) A contention based approach. Protocols like Time Division Multiple Access (TDMA) and Frequency division multiple access (FDMA) fall under former category. However, the advanced wireless protocols are contention based protocols. Hence, in this chapter, we review the evolution of contention based protocols in greater detail.

Aloha [2] was one of the first channel access protocols to be studied in systems using shared medium. Under an Aloha protocol, a node transmits the data as soon as it gets the data and retransmits it if it is deduced that the data is lost. A very high packet loss, thus leading to inefficient bandwidth usage, was observed under Aloha due to "instant" transmission, without considering the currently active transmissions. *Slotted Aloha* was proposed where a node can send a packet only at the start of discrete time slot boundaries. While this reduced the packet loss percentage, it still did not account for the currently active transmissions.

Carrier sense (*Carrier Sense Multiple Access (CSMA)*) where the medium is sensed before a transmission is initiated to attempt to avoid collisions, is often used to improve operation in shared media. For example, Ethernet [91] uses CSMA, resulting in significant performance advantages over Aloha. However, in wireless networks, CSMA is imprecise since the channel is sensed at the sender, but the reception occurs at the receiver. This gives rise to the hidden terminal and exposed terminal problems (discussed below). A wireless node is able to sense that the channel is busy if the sum of the noise and the signal from the transmissions is above a given power threshold, called the Receiver Sensitivity Threshold (T_{RX}). This is a constant parameter in most of the wireless cards, but higher end cards can tune this parameter.

It is important to note that collision detection (another technique used in wired shared media) cannot be used in wireless networks: because the signal power attenuates very quickly with distance, the transmission power at a sender is orders of magnitude higher than the power received from an

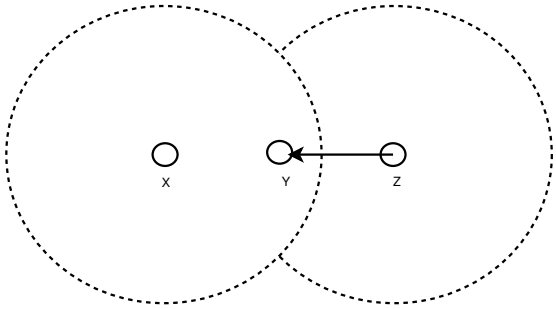

Figure 2.1: Hidden terminal: Node X is a hidden terminal for Z-Y transmission

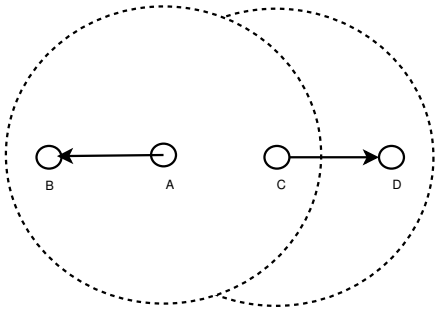

Figure 2.2: Exposed terminal: Node A and Node C are the exposed terminals for each links C-D and A-B respectively

interfering packet. This makes it impossible to discern the presence of a collision.

2.2.3 Drawbacks of CSMA in wireless networks

Because CSMA is carried out at the sender, instead of the receiver, it cannot prevent all collisions in wireless environments, leading to several modes of interactions between the interfering links. Inefficient bandwidth usage [119] were studied in CSMA protocols and its variants. *Hidden terminal* and *Exposed terminal* are two prominent adverse effects of CSMA, both of which stem from the inconsistent channel state between transmitter and the receiver. These effects often arise while discussing the drawbacks of even advanced wireless protocols, and hence we review them briefly in this paragraph.

A hidden terminal is a node whose transmission may interfere with another receiver, thus causing a packet collision. Figure 2.1 shows a hidden terminal X causing a packet drop at Z. Nodes X and Y cannot sense each other, thus enabling concurrent transmissions, which leads

to packet drop at C. While hidden terminal leads to packet drops by a relatively aggressive transmission strategy, exposed terminals are caused due to conservative use of the channel. Certain transmissions (for example transmissions $A-B$ and $C-D$ in Figure 2.2), which can ideally proceed concurrently without interfering with each other. However, the CSMA protocol prevents concurrent transmissions of the nodes A and C.

2.2.4 Advanced CSMA protocols

The field of packet radio networks, which studied the above protocols, was dormant for a decade and a new rise interest in ad-hoc networks rejuvenated research in MHWNs. Advanced protocols were proposed [13, 36, 70, 75, 116, 117, 119] and analyzed [3, 5, 15, 124, 125]. *Carrier Sense Multiple Access / Collision Avoidance (CSMA/CA)* was proposed, in which various mechanisms to avoid packet collision were adopted. This set of protocols forms the base for current generation MAC protocols. Avoiding hidden terminals and exposed terminals were proposed by a variety of mechanisms [36, 119]. A popular version of collision avoidance mechanism was proposed in the MACAW protocol [13], where collision avoidance is attempted by a 4-way handshake between the sender and the receiver. The protocol also supports another mechanism of collision avoidance by waiting for a longer time (back-off) before transmitting a packet if the previous packet experiences a collision. The IEEE 802.11 [117] is an extention of the MACAW protocol and is reviewed in detail in the next section.

2.2.5 IEEE 802.11 protocol

A modified version of MACAW protocol was the IEEE 802.11 [117] which was proposed as the de-facto standard for MAC protocol in both Single-hop and Multi-Hop Wireless Networks. We review the IEEE 802.11 in this section.

IEEE 802.11 has two access modes: (1) Point Co-ordination Function (PCF) (2) Distributed Co-ordination Function (DCF). PCF uses a mixture of contention based access and reservation based access, and is not currently not being used in majority of the wireless networks. We concentrate on the IEEE 802.11 DCF, which is a mainly a contention based protocol, in this dissertation and

is further discussed in this section.

Basic handshake

A sender node that has packets to transmit first transmits a *Request to Send* (RTS) control packet. Upon successful reception of RTS and a clear channel at the receiver, it sends *Clear to Send(CTS)* packet to the sender. The purpose of the RTS/CTS control packets is to ensure that the medium is idle at the both the receiver and the sender. The neighbors overhearing the RTS/CTS exchange mark that there is an ongoing transmission, and thus defer to initiate their transmissions. This process of "virtually" marking the medium as busy to enable neighboring transmissions is termed as *Virtual Carrier Sensing (VCS)* and thus acting as a *Collision Avoidance(CA)* mechanism.

After a successful RTS/CTS exchange, it is ensured that the medium is idle at both ends of the transmissions. The sender now sends the actual DATA packet and the receiver acknowledges the DATA reception by ACK packet. This 4-way RTS-CTS-DATA-ACK handshake is borrowed from the MACAW protocol [13]. Another mode of handshake that is used in IEEE 802.11 is the *Basic Mode*, where the RTS and CTS packets are not transmitted. The node that is ready to transmit a packet transmits the DATA packet first and waits for the ACK packet from the receiver. Recent studies have indicated that *Basic Access* mechanism provides greater throughput in a majority of the scenarios [124].

Advanced Collision avoidance techniques

The above handshake would suffice under an "ideal" wireless propagation where a transmission from a node can be lead to only two possible effects on the other nodes[1]: (1) The transmission can be deciphered completely; or (2) The transmission cannot be sensed and will not interfere with the other transmissions that a node is receiving. However, the wireless medium is far from the above ideal nature. Under a realistic signal propagation, there can be nodes which might not be able to decipher the transmission from a node, but which might cause a packet collision by interference. In such scenarios, the VCS cannot avoid all the collisions, thus demanding better *Collision Avoidance*

[1]Propagation delay of the signal is assumed to be negligible for simplicity

(CA) strategies.

Transmitting at discrete time boundaries Conservative packet transmission techniques were proposed to avoid collisions. A simple mechanism, with similarities from "Slotted Aloha" protocol, was proposed where a node sends a packet only at the start of discrete time intervals, called *slots*. Slot duration is fixed and is represented by s_t in this dissertation.

Wait before transmitting The IEEE standard proposes to wait for *atleast* certain slots before it transmits any packet. Before transmitting an RTS packet (or the DATA packet in IEEE 802.11 *Basic Mode*), the node waits for *Distributed Coordination Function Inter-frame Space (DIFS)* number of slots (i_{DIFS}). And transmission of CTS/DATA/ACK packets (ACK packet in *Basic Mode*) observes a shorter waiting time, given by *Short Inter-frame space (SIFS)* parameter (i_{SIFS}). The shorter duration of SIFS is to enable higher priority to the ongoing transmissions (that observe SIFS waiting period) rather than the ones that have to initiate the transmission (such nodes observe DIFS waiting period). If the channel is idle for this waiting period, then the node steps to next stage of transmitting the packet. If the channel is observed to be busy during the DIFS wait period (for RTS packet), then the transmission of the packet is deferred and the DIFS period of wait is re-started.

Backoff mechanism In dense networks, regulation of the collision by SIFS and DIFS fail to prevent collisions to a large extent. Hence, further conservative schemes were adopted in IEEE 802.11 to reduce the collisions. It is mandated that a node waits for certain number of slots before it starts sending the RTS packet (or the DATA packet in the Basic Mode). The number of slots to wait was uniformly chosen in the interval $[0, \text{CW}_{\text{min}}]$ where CW_{min} is a threshold parameter. A counter, known as *Backoff counter (*BO*)*, is initialized to this random number. If the DIFS wait time was successful (i.e. the channel did not become busy during the wait), then the node starts decrementing the BO counter for each time slot. The node starts transmitting the packet when this backoff counter(BO) reaches zero. If the channel is sensed to be busy in this waiting duration, then the node "freezes" BO value and will start decrementing BO only after successful DIFS waiting

Parameter/Variable name	Notation	Default values
Slot time	s_t	$20\mu s$
SIFS interval	i_{SIFS}	$10\mu s$
DIFS interval	i_{DIFS}	$i_{\text{SIFS}} + 2s_t$
Minimum Congestion window	CW_{min}	31
Maximum Congestion window	CW_{max}	1023
Maximum number of retransmits	R_{max}	7
Backoff counter	BO	- N.A. -

Table 2.1: IEEE 802.11 parameters and variables

period.

Exponential Backoff on collision The selection of the random number of slots to wait in the duration $[0, \text{CW}_{\text{min}}]$ is observed while there are no packet collisions experienced. However, upon detection of an unsuccessful packet transmission attempt, the node uses aggressive wait mechanisms to prevent further collisions. Unsuccessful packet transmissions can be as a result of packet collision or the receiver failing to continue the handshake (e.g.: Failing to send a CTS due to a busy channel at receiver). The sender node will wait for longer periods for the next transmission attempt. Instead of choosing a random wait interval between $[0, \text{CW}_{\text{min}}]$, it doubles the interval to pick a random number, thus resulting in larger expected wait times. In order to avoid a very large interval, a maximum interval from $[0, \text{CW}_{\text{max}}]$ (where $\text{CW}_{\text{min}} \geq \text{CW}_{\text{max}}$) is set as a threshold to choose random wait times. This exponential increase in the interval at each packet transmission (increasing it by a factor of 2) is called *Exponential Backoff*. Frequent collisions may suggest failure of the receiver node to intercept packets from the source. To account for this fact, a packet is attempted for R_{max} number of times. Upon failure to deliver the packets, the MAC layer relinquishes its attempt to transmit a packet. Similar mechanisms is also observed in MACAW protocol.

The detailed mechanisms for the IEEE 802.11 can be found in the standard document [117]. The table 2.1 summarizes the IEEE 802.11 parameters/variables and their common values.

The increasing demand for the wireless networks lead to a concrete analysis of IEEE 802.11 protocol. We focus on the performance and effects of IEEE 802.11 in MHWNs [3, 5, 15, 124, 125]. The hidden terminals and the exposed terminals can still occur in IEEE 802.11 based networks. The

fairness for the channel access is also questionable in such networks. In this dissertation, we study the behavior of IEEE 802.11 in MHWNs and specifically analyze the issues of hidden terminals, exposed terminals and certain fairness issues.

2.3 Routing

In this section, we discuss one of the primary challenges in MHWNs, the routing problem. Routing ideas in Single hop wireless networks [62, 121] or wired networks [60] cannot be applied directly to MHWNs due to the unique MHWN characteristics that were discussed in Section 2.1. The routing problem in MHWNs targets constructing efficient routes for a network that is self-configuring and potentially mobile. The evolution of the routing protocols in MHWNs, their characteristics and limitations are discussed in this section.

The first group of proposed routing protocols, which is referred as *First-Generation Routing Protocols*, focused on deriving efficient routes using conventional metrics such as hop count, at low overhead. The failure of such routing metrics to account for the quality of the wireless channel causes severe under-utilization of the channel. Section 2.3.1 briefly overviews hop-count based protocols and discusses their shortcomings in more details.

The development of "link-quality" aware routing protocols emerged to address the drawbacks of First-Generation routing protocols. We discuss the routing protocols in this *Second-Generation Routing Protocols* in Section 2.3.2.

The limitations of link quality aware routing protocols and the characteristics of an ideal routing protocol is discussed in the Section 2.3.2. The modelling attempts for designing such an ideal protocol is later studied in Chapter 3.

2.3.1 First Generation: Greedy Hop-count Based Routing

Routing protocols for MHWNs can be broadly divided into two categories based on *when the routes are constructed*: (1) Proactive routing protocols, and (2) Reactive Routing Protocols. Proactive routing protocols construct the "routing tables" apriori to packet transmission for all possible destinations; examples of proactive routing protocols in MHWNs include DSDV [103] and WRP [93].

Reactive Routing protocols compute routes on-demand for destinations towards which they have packets by conducting a route discovery process. Examples of reactive routing protocols include AODV [102] and DSR [65]. Reactive routing protocols can be more efficient than proactive ones because they only search for routes on-demand. However, because route construction is only started when a packet transmission is needed, there is a delay before the route is available. In a dynamic topology where the nodes are mobile, proactively computing routes may be counter-productive as many routes become invalid before they are used.

Initial routing protocols such as DSDV [103], DSR [65] and AODV [102], select routes strictly favoring the shortest hop ones. The routing protocols makes local route selection decisions greedily, attempting to find the shortest hop routes for its active connections. The advantage of this approach is the distributed operation that allows simple local decisions to be taken. The intuition behind choosing the minimum hop-count path is that a shorter path translates to: (1) Higher Capacity: The number of transmissions necessary to move a packet from source to a destination is a function of the number of hops. A shorter path, means fewer retransmissions, reducing competition for the channel and increasing end to end capacity; (2) Lower Energy Consumption: Fewer retransmissions also lead to lower energy expenditure in delivering the packet to the destination; (3) Shorter end to end delay: With a smaller number of hops, each packet experiences fewer retransmissions, and fewer queueing delays at each intermediate hop. This results in a reduction in the end-to-end delay. This general observation is true for all packet switched networks; for this reason, hop count is used as a path quality discriminator by some wired routing protocols.

The effectiveness of hop count as a measure of route quality has recently been brought into question [26]. More specifically, there is a large variation in link qualities and a metric like hop count which does not account for this variation will not accurately predict a route quality. In fact, hop-count tends to pick poorer quality links: since it uses fewer hops, these hops tend to be *longer*, where length is the physical distance between the sender and receiver forming a hop. As the distance between the sender and receiver increases, the signal strength received at the receiver decreases, which induces higher packet error rates– longer hops tend to be poorer in quality than shorter ones.

The prevalence of hop-count as a routing metric was assisted by simulation results which relied on simplistic propagation models. Most simulators initially had a simple *Protocol model* [47] which specified that all the nodes within a reception range receive a transmission correctly. This model favors hop-count as an effective parameter since it does not model variations in link quality; it was shown by Li et al [83] that the number of hops does determine the effectiveness of the route if all the other parameters (like channel capacity of links in different routes) are the same.

Several early works recognized that that not all the routes of the same hop-count are equal. Goff et al [46] analyzed mobile scenarios and proposed mechanisms to stop using the route when the signal strength of a link goes below a fixed threshold. New routes were discovered before a route breaks down, thus switching to a better quality route. As more sophisticated simulation models evolved [19, 115], these effects were also clear in simulations. The added evidence from experimental testbeds finally demonstrated that link quality cannot be ignored when carrying out routing decisions. Yarvis et al [130] show that the hop count provides an unrealistic estimation as a routing metric in a real world sensor network and motivate the need for a routing metric which quantifies the route based on the quality of the links present in the route. De Couto et al. [26] discovered in the experimental mesh network testbed that there is substantial difference in throughput among the routes that had the same number of hops and proposed to use link quality to estimate the route effectiveness rather than just the hop-count. Other studies have reached similar conclusions [3,25,31]. These observations motivated a second generation of routing protocols which take into account link quality. These are discussed in the next section.

2.3.2 Second Generation: Link-quality based routing

The advantages of link-quality based routing was explained in the earlier section. In this section we discuss the ideas behind link-quality based routing, popular protocols and their limitations.

The core idea of a link-quality aware routing protocols are: (1) To estimate the quality of each link; and (2) To measure the quality of the overall route as a weighted sum of the quality of the intermediate hops. In the below sections, we discuss these ideas with respect to certain key link-quality aware routing protocols.

Link Quality Aware Routing

In this section, we overview efforts in developing effective link-quality aware routing protocols. The general philosophy of these protocols are to replace hop-count in conventional protocols with an estimate of route quality, which itself is based on a function that combines the qualities of the links making up the route. Thus, the primary challenge in these protocols are: (1) how to estimate link quality; and (2) how to combine these estimates into a route quality metric. In this section, we focus on these issues, and also discuss the general properties of this class of routing protocols.

Factors Affecting Link Quality

The problem of estimating link quality in the presence of a fading wireless channel and interference is difficult. Channel parameters such as the nominal bandwidth play a role in determining the link quality and are often or slowly changing. Other parameters like the amount of contention due to interference from competing links and the effectiveness the MAC handshake are topology and traffic specific, which makes them difficult to estimate. In the remainder of this section, we assume that wireless channel nominal quality, which accounts for issues such as fading, is known. We focus on the interference related factors that influence link quality.

Assume an ideal channel where the channel state is predictable and an ideal MAC protocol which is able to schedule the packets collisions. The throughput for each link is affected by the contention for the common channel by neighboring transmissions. Hence, the quality of the link depends only upon the *available capacity*. CSMA based schedulers (like IEEE 802.11) are not ideal, and therefore unable to eliminate collisions completely under realistic carrier sense levels, due to the inherent difference in the channel state observed at the sender and the receiver. The limitations of CSMA based schedulers were identified by Xu et al [124]. Thus, under such schedulers, the *percentage of packet losses* are an additional factor determining the link throughput.

Impact of CSMA scheduling on the link throughput

To illustrate the effect of packet losses in a practical CSMA based scheduler, we simulated different sets of 144 uniformly distributed nodes with 25 arbitrarily chosen *one-hop* connections. The

simulation was carried out in QualNet simulator [105]. The aim of this experiment is to show the effect of CSMA based scheduling at different interference levels. One hop connections were chosen to eliminate multi-hop artifacts such as self-interference and pipelining and isolate link-level interactions. Each source sends CBR data at a rate high enough to ensure that it always has packets to send. Each node measures the amount of time the channel is busy (busy time). The ideal available capacity at a node can be approximated by the idle time observed at either source or destination.

Figure 2.3(a) plots the busy time at the source of a link [2] against the observed throughput of the link. In general, as interference increases, the achievable capacity decreases. However, it can be seen that at higher busy times (enlarged for clarity in Figure 2.3(b)), large variations in throughput arise for the same observed busy time. The scheduling effectiveness starts to play a determining effect on the throughput of the link at high interference levels.

Let t_i be the throughput achieved by an ideal scheduler; intuitively t_i is proportional to the amount of *available capacity*, which is in turn proportional to the busy time observed at the link. Let t_o be the observed throughput in the CSMA based scheduler, IEEE 802.11. The ratio of $\frac{t_o}{t_i}$, called *normalized throughput* provides a measure of the scheduling efficiency relative to an ideal scheduler independently of the available transmission time. Figure 2.3(c) plots the normalized throughput as a function of observed percentage of IEEE 802.11 MAC level transmissions that experience RTS or ACK timeouts (which represents the packet losses) for *all* the links. It can be seen that as the fraction of packet timeouts increases, the normalized throughput decreases almost linearly. Thus *the reason for variations in observed capacity from the nominal capacity predicted by the interference metric is the scheduling as observed in MAC level timeouts.* This shows that aggregate interference metrics quantifying the available capacity (such as busy time) cannot predict scheduling effects and correlate poorly with scheduling efficiency.

Measuring the link quality is complicated by other MAC layer effects. We discuss two key factors under such secondary effects:

- *Data rate* – Most of the advanced MAC protocols, like IEEE 802.11, are enhanced to use different data rates based on the estimated channel noise [58, 67, 111]. Since the channel

[2] Other metrics such as busy time at destination were also explored with very similar results.

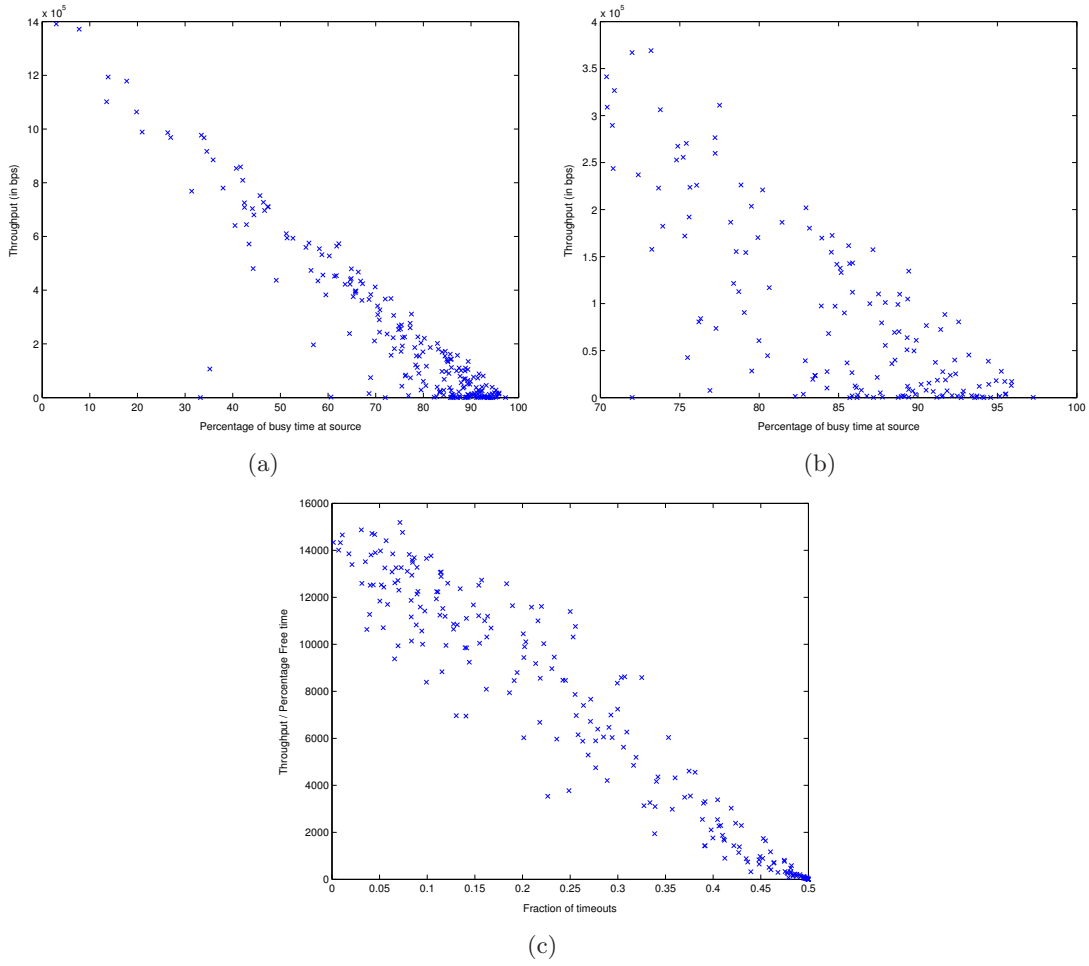

Figure 2.3: Effect of Interference and Scheduling on Capacity. (a) shows the effect of source busy time on throughput; (b) enlarges the high interference region of (a); (c) shows that normalized throughput is a function of scheduling/MAC level timeouts. (The results were presented in the study [79])

noise variance over time is significant, due to either dynamic interference from the neighboring nodes or environmental variations, the data rate between the sender and the receiver is not constant. Many protocols that use broadcast packets to notify the neighbors about the link quality may be vulnerable to the data rate variations. All the broadcast packets are sent at the lowest possible data rate. Receiving such a packet does not always ensure that the neighbor will be able to receive the actual data packets (which may be sent at higher data rates). Thus, an added requirement for the the metric is to estimate the link quality given that the actual packets will be transmitted at a higher data rate.

- *Packet size* – The efficiency of the packet transfer on a link is also a factor of the size of the packet being transmitted. Larger packets require a longer transmission time and suffer a correspondingly larger chance of errors. The measurement of the link quality with smaller control packets, may be inaccurate for larger data packets. Hence, the link quality metric should also account for the packet size that is being transmitted over the link.

The explicit measurement of the available capacity and the percentage of packet losses in a distributed routing protocol is a hard problem because the measurement at routing layer will be distorted by secondary effects (such as the amount of time the packet resides in the queue) and inability of accessing the information present at the MAC layer (since, typically, MAC is implemented on the hardware). To summarize, the important properties that the link quality metric has to capture under the assumptions of a predictable channel are:

- Property 1 – The available channel capacity of a link
- Property 2 – The packet loss observed on a link

While the first property estimates the amount of contention for a given link, the second property measures the efficiency of the MAC protocol in using the available capacity.

Environment Effects on Link Quality

In the above discussion, we assumed a predictable channel and focussed on the challenges in capturing interference related effects that affect link quality. However, link quality in a realis-

tic environment is subject to unpredictable channel state changes. Experiments in the real world testbeds [5, 23, 25, 86, 130] show that the quality of the link between a pair of nodes regularly fluctuates, thus making it harder to statically assign a single quality metric for the link[3].

One of the first approaches attempted to estimate link quality was to measure parameters of the channel such as the signal strength [32, 46, 66]. De Couto et al. [25, 26] provided experimental evidence from testbeds that signal strength is a poor predictor of the loss rate. Aguayo et al. [5] also found that the the use of simple metrics like *Signal to Noise ratio* (SNR) is not a good estimator of the quality of the link. The experiment measured the average SNR at the nodes and the delivery probability of the packets were found not to confirm with the observed SNR results. Various routing metrics which accounted for the link quality were proposed to solve the routing issues in testbeds [3, 20, 25, 31, 100, 132]. Other research studies [30, 129] evaluate various link-quality aware routing protocols and summarize certain key properties of the routing metrics. The routing metrics that are proposed for networks using multiple channels and multiple-radios (e.g. [3,31]) are different from a single channel wireless network, even though they share the key ideas. Since a single channel and single radio networks are predominantly used in static wireless multi-hop networks (like mesh networks) and share certain fundamental ideas with the multiple channel and radio counterpart, we focus on the routing metrics that are suitable for such networks.

Review of Existing Link Quality Metrics

In this section, various link quality metrics are studied and their effectiveness and deficiencies are summarized.

- **Expected Transmission Count (ETX)** [25] – The intuition behind ETX is that the cost of a link is proportional to the expected number of attempts required to successfully transmit a packet. The ETX of a link is defined as $\frac{1}{d_f d_r}$ where d_f is the probability that the packet is successfully received over a link in forward direction (for data transmission) and d_r is the success probability of packet transfer in the reverse direction (for ACK transmission). Each

[3]While most of the testbeds show this variation, the results from other testbeds ([34,82]) show that the error rate and the quality of a link is relatively constant. We conjecture the effect of topology and traffic account for differences in conclusions.

Algorithm 1 Algorithm to compute ETX of a link

Require: Node X receives an ETX probe packet from Node Y
{// W = *Number of probe packets sent by a node in 1 second*}
{// n_{xy} = *number of probe packets heard by Y that was sent by X in the last w seconds*}
{// n_{yx} = *Number of probe packets heard by X that was sent by Y in the last w seconds*}
Extract n_{xy} from the received packet
$r_{xy} \leftarrow \frac{n_{xy}}{wW}$ {// *Rating of XY*}
Update n_y
$r_{yx} \leftarrow \frac{n_{yx}}{wW}$ {//*Rating of YX*}
$\text{etx}_{xy} \leftarrow \frac{1}{r_{xy} r_{yx}}$ {//*ETX for the link XY*}

node periodically broadcasts a probe packet at a constant rate of W packets per second. The nodes record the number of probe packets received from each neighbor. This count is included in the periodic probe packet sent by the node in order to return the link information to the sources. The packet loss rate is calculated from the data recorded by the node and the data from the probe packet of neighboring nodes as described in Algorithm 1.

The metric for the route is the sum of the ETXs of its links. While ETX measures packet loss (Property 2), it fails to account for the available capacity (Property 1). A link with a higher handshake effectiveness of the MAC protocol is always favored, without considering the contention present over the link. Also, since the ETX uses "probe" broadcast packets to inform the neighbors about their reception, the metric does not measure the link quality of the actual packets which are usually larger and transmitted at a higher data rate. While transmitting control packets of different lengths will overcome the problem, this leads to an added control overhead. Also, the estimation of the route quality based on summing the ETX of the links is a simple metric which does not account for the bottleneck links. However, the performance studies by Draves et al. [30] has shown that ETX outperforms other metrics.[4]

- **Round trip time (RTT)** [3] – RTT is measured by sending a *probe packet* by a sender (say X). The time of packet generation (t_x) is included in the packet. The receiver (say Y) will acknowledge the probe packet by transmitting a *probe-ACK* packet back to the sender.

[4]Under a multiple channel scenario, each with different bandwidths and data rate, an extended version of ETX called *Weighted Cumulative Estimated Transmission Time* (WCETT) was proposed by Draves et al. [31]. However, under a single channel model, which is the focus of the chapter, WCETT measurement will identical to ETX measurement

It includes the t_x inside the probe-ACK packet. The sender estimates the time required for the packet to traverse the link (rtt_{xy}); this measurement incorporates the combined effect of the available capacity (Property 1), the packet losses (Packet 2) and the queueing delay of the packet. In order to avoid oscillations and temporary link quality variations, *Smoothed RTT(SRTT)* is calculated by associating a weight of α to the most recently measured RTT. Algorithm 2 demonstrates the steps involved in calculating the RTT of a link. Study of

Algorithm 2 Algorithm to compute RTT of a link

Require: Node X has sent the probe packet and receives a probe-ACK packet from Node Y
{// α = *Weight given for accounting for the most recent round trip time*}
{// t_x = *Time when the probe packet was sent by X. This is marked in the probe packet*}
Extract t_x from the probe-ACK packet
$\text{rtt}_{xy} \leftarrow$ *Current time* $- t_x$
{// *Update the Smoothed RTT (SRTT)*}
$\text{srtt}_{xy} \leftarrow \alpha\,\text{rtt}_{xy} + (1-\alpha) srtt_{xy}$

RTT under different traffic pattern in [30] indicates that RTT is useful for measuring links with very high loss rates, but not for other links. Since the RTT uses fixed sized packets for measurement it is susceptible for packet size. Also, the control packets are unicast to each of the neighbor and flows twice between a pair of nodes. This leads to higher measurement overhead making it unscalable for dense networks.

- **Packet pair** is a standard approach used in estimating the bandwidth in traditional networks [72]. The sender transmits two packets back-to-back, one with smaller packet size and another with a larger packet size. The measurement of the delay between the packets at the receiver will indicate the one-way contention across the link and this delay is conveyed to the sender. Since the receiver measures the time-interval between the packet pair, it is possible to avoid the effect of queueing delays in measuring the contention at the link. Packet pair is close relative of RTT that eliminates the queue delay factor from the metric. Draves et al [30] compared packet pair metric with the above metrics. While the packet pair metric eliminates the queueing delays, the other drawbacks of the RTT are still present. An additional problem of delays associated with possible packet retransmission of the second control packet can cause this approach to underestimate the link quality.

- **Estimated Data Rate (EDR)** [100] – EDR proposes to address the deficiency of the ETX to measure the available capacity (Property 1). EDR assumes that the effectiveness of the route depends upon the available capacity and the packet loss of the bottleneck link. The bottleneck link is determined by considering the amount of queue build up at the nodes of a route. The ETX of the bottleneck link and the MAC layer effects like backoff is approximated and the EDR metric is proposed for measuring the quality of the route. While EDR accounts for the available capacity, it bases the metric on the bottleneck link, thus not optimizing the other hops of the route. EDR is not sensitive to adaptive data rate and varying packet sizes of the actual data.

- **Required Number of Packets (RNP)** [20] – Cerpa et al. [20] study of temporal properties of links and observe that there is a significant variation of the link properties over larger time frames. The above mentioned metrics are insensitive to temporal variations and thus fail to depict the link quality. They propose a metric called Required Number of Packets (RNP) which is sensitive to distribution of the packet losses and thus will avoid links with temporal instability. RNP is estimated by periodically broadcasting control packets for a small duration of time and measuring the temporal variation of the reception rate at all the neighbors. While this metric captures the temporal properties, the measurement overhead of such broadcasts over a period of time is high. Observing the effect of interfering links using RNP is difficult since it requires all the interfering links to transmit in a *time synchronized* manner. Such measurements fail to capture the real traffic on the contending links, thus estimating the available capacity (Property 1) and packet loss (Property 2). Moreover, since broadcast is being used such measurement is prone to the effects of adaptive data rate changes and packet size variations. However, temporal changes in link quality will place a higher emphasis on deciding the measurement time frames for all the above metrics and thus play a significant role in deciding the throughput of the link.

- **Expected MAC latency (ELR)** [132] – ETX and EDR not only require additional beacon based broadcast packets, but also fail to account for the changes of the data rate (by the MAC protocol) and packet sizes (by the application). The unicast link properties, which are

inherently different from the broadcast link properties, cannot be accurately estimated using broadcast packets. Also, the temporal changes in the traffic, which occurs frequently, are not captured by the above metrics. Expected MAC latency (ELR) proposes to overcome this problem by learning the link quality as the data packets are forwarded. The key idea of ELR is to eliminate the broadcast control packets by combining the properties of the geography unaware routing protocols with the geography aware routing protocols [71].

ELR measures *expected MAC latency per unit-distance(LD)* to the destination by a one-time initialization of the node locations and periodically calculates the link effectiveness by switching to different probable next hops. Continuous measurement of the link effectiveness is used to calculate the probability with which the neighbor may be the best forwarder. Upon a successful packet transfer to a next hop, the LD is updated to account for the newly observed latency. If the link observes a packet loss, the previously observed latency is incremented based on the *delivery rate* on the link. Since the LD is log-normally distributed, the logarithm of LD ($\log(LD)$) is estimated (described in Algorithm 3).

Algorithm 3 Algorithm to compute MAC latency per unit distance(LD) of a link

Require: Node X has sent the unicast packet to send and the set of possible forwarders is non-empty

{// α *is the weight associated for the older samples to avoid random fluctuations*}
{// p_{xy} = *Unicast delivery rate on the link* XY}
{// LD_{xy} = *Estimated MAC latency between the link* XY }
Probabilistically choose the next hop forwarder Y among the set of possible forwarders and transmit the packet to Y.
if Packet is successfully transmitted to Y **then**
  $p'_{xy} \leftarrow$ Update the unicast delivery rate on the link due to packet success
  $l_{xy} \leftarrow$ Compute the latency of this packet delivery X to Y
  $\log(\mathrm{LD}_{xy}) \leftarrow \alpha \log(\mathrm{LD}_{xy}) + (1-\alpha)\log(\mathrm{LD}_{xy})'$
else {Packet transmission is not successful}
  $p'_{xy} \leftarrow$ Update the unicast delivery rate on the link due to packet failure
  {// *Expected number of retries for packet success* $= \frac{1}{p_{xy}}$. *Increase the latency accordingly*}
  $l_{xy} \leftarrow (1 + \frac{1}{p_{xy}})l_{xy}$
  $\log(\mathrm{LD}_{xy}) \leftarrow \alpha \log(\mathrm{LD}_{xy}) + (1-\alpha)\log(l_{xy})'$
end if

ELR accounts for the temporal variations of the link quality by sampling different neighbors

Metric \ Property	Contention	Packet loss	Varying Data rates	Varying Packet sizes
ETX	No	Yes	No	No
RTT	Yes	No	No	No
Packet Pair	Yes	No	No	No
EDR	Yes	Yes	No	No
RNP	No	Yes	No	No
ELR	Yes	No	Yes	Yes

Table 2.2: Comparing different link estimation metrics

adaptively. The drawback of ELR is the inability to calculate the the packet loss information since unicasts are associated with packet retries which cannot be obtained from the MAC hardware in realistic deployment.

Table 2.2 summarizes the properties of the different link quality estimation metrics. It is to be noted that some metrics may reflect some components affecting link quality, but in a very coarse form. For example, RTT may capture the packet drops since the packet drops will lead to a higher RTT. ELR cannot capture the required number of retransmissions (even though theoretically it is possible) since it uses unicast packets and the packet loss due to retransmission cannot be captured. We do not explicitly consider such secondary effects in the table.

Route Quality estimation

Once the individual link qualities are estimated, the next problem is how to combine them to reach a measure of an overall route quality. The quality of the route depends upon the quality of the individual links present in the route. The multi-hop route can be imagined as pipe, with each link representing a part of the pipe with constant diameter which represents the link quality. The overall throughput of the route is the amount of data that can be pushed in the pipe. It can be seen that the throughput is affected by the *bottleneck link* which has the least diameter. Multiple routes may exist between a given source and destination. The routing protocol is responsible for the choice of the route which can support maximum throughput for the connection. Yang, Wang and Kravets [129] suggest that "Isotonicity" is an important property for combining the link-quality into a single route quality. Isotonocity refers to the property that the cost of a route strictly increases

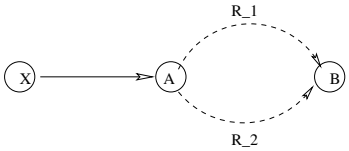

Figure 2.4: Isotonicity

when it is prefixed with additional hops. For example, consider two routes between node A and node B, say R_1 and R_2 as shown in Figure 2.4. Let the combined link metrics of R_1 and R_2 be represented as r_1 and r_2. Let there be another path that is prefixed to route $A \ldots B$, say from node X to A denoted by $X \ldots A \ldots B$. Consider the two routes between X and B in $X \ldots A \ldots B$, one passing through R_1 and the other through R_2. Let us denote them by $X \ldots R_1$ and $X \ldots R_2$ respectively, and their metrics by xr_1 and xr_2 respectively. The isotonicity property says that if the metric $r_1 \leq r_2$, then $xr_1 \leq xr_2$. In essence, this property says that each part of the route should have a equal value when included in a larger route.

Limitations of Link-Quality Aware Routing

In this section, we summarize the disadvantages of the link-quality estimation techniques. The majority of the link-quality estimation mechanisms require probe packets (broadcast or unicast) to sample the link quality. The accuracy of the estimates obtained via probes is limited because the actual data packets can be transmitted in different data rates and have different packet sizes; both these factors affect the perceived quality of the channel. The use of broadcast control packets fails to capture the link quality at different data rates. Capturing the link-quality for all the data packet sizes makes the measurement technique infeasible.

The second disadvantage of such measurement techniques is the inability to predict the future load of the networks. Let us assume that the link-quality reflects the data packet transfer and the variance of link-quality is captured at a fine level. Based on the metrics, a route with a set of links is selected and the data packets flow through this route. The transmission of these data packets will change the interference patterns and packet loss rates at other links. Thus, the past estimation of the link qualities are invalid and the measurements have to be re-initiated at the nodes that are affected.

Zhang et al [132] discuss the disadvantages of measurement of packet losses using a broadcast medium (other than the known issues of variable data rate and packet sizes). The number of packets lost can be measured in a broadcast environment. However, the MAC layer uses retransmissions if the packet transmission is unsuccessful in unicast packets. The discrepancy arises due to the inability of the routing layer to know the number of retransmissions that have occurred at the MAC layer. The MAC protocol, that is implemented in the hardware, does not expose such information to the above layers. Hence, measurements such as ETX, that use broadcast packets for measuring packet loss, cannot be easily transformed to measure the packet loss rate of unicast traffic.

In summary, the link-quality aware routing protocols discussed above are based on a methodology for estimating the quality of links. The links quality of the links forming a route are then combined to produce an estimate of the quality of the route. This estimate is used, in place of hop-count, in what are otherwise traditional routing protocols.

2.3.3 Towards an ideal routing protocol in MHWNs

While the objective of link-quality aware routing is to maximize the efficiency of a route, these protocols operate greedily and do not coordinate routing across routes to achieve overall network performance optimization. In an MHWN, multiple connections exist that are each made of multiple links. These links compete with other links in their neighborhood for access to the common channel. The aim of the *Globally-aware routing* is to find the routing configuration that would provide an optimal (or near optimal) overall network performance across all the connections. Globally coordinated routing requires global (or at least, non-local) state information. Thus, developing such solutions for dynamic networks is challenging.

2.3.4 Traffic-engineering in MHWNs

Solving the optimal routing problem in general MHWN is a challenging problem. The definition of 'optimal' network performance varies largely owing to different varieties of traffic demands on the network. For example, certain video and audio applications may prefer a route with least delay and tolerable packet loss, whereas a network for file transfer applications may require a low packet

loss path which is not highly sensitive to delay. A commonly used technique to solve the problem of achieving optimal performance for given traffic demands is known as *traffic-engineering*. Traffic-engineering in telephone (also referred as *Teletraffic engineering*) and data networks (like internet) has been well-studied and has proved beneficial [28, 73, 109].

Traffic-engineering under static topology and constant traffic demands uses a 'modeling component' to compute the allocation of the resources for optimal network performance. While the modeling component forms a integral part of traffic-engineering, there are several other components that enable the model to solve the problem. For example, *NetScope* [35] solves the traffic-engineering problem in wired networks with 'dynamic' traffic demands using other components like traffic monitoring tools. In this dissertation, we focus on the modeling components to enable traffic-engineering in MHWNs.

Modeling the problem of globally-aware routing can directly traffic engineering in MHWNs. The dissertation focusses a model that enables traffic-engineering in static, or slowly dynamic, networks. Static MHWNs are an important subset of MHWNs that includes mesh networks, some sensor networks, and potentially portions of ad hoc networks. Apart from solving the traffic-engineering problem, the modeling of optimal routing problem and evaluating the global solutions relative to the local solutions is important for the following reasons: (1) it provides realistic tight limits on the achievable performance for different networks, that can be used to guide provisioning decisions and provide an upper limit on protocol performance; and (2) experience with the nature of optimal configurations and understanding the type of coordination required across connections can provide insight into designing a next generation of distributed routing protocols. Thus, it provides a flexible and effective tool for evaluating and optimizing MHWNs.

We discuss the initial attempts to understand the behavior of such an ideal routing protocol by modeling various aspects of MHWNs in Chapter 3.

Chapter 3

Motivation and Related Work

The MAC layer intricacies and the routing layer challenges in multi-hop wireless networks were discussed in the previous chapters. In this chapter the characteristics of an ideal routing protocol, henceforth referred as *Globally coordinated routing*, is discussed. In this chapter, we discuss different efforts to model MHWNs that enable characterization of network performance, as well as derivation of effective routing configurations. Given that the problem is similar to classical traffic engineering, with the exception of the effect of the wireless channel (susceptible to fading and the effect of interference), a critical component of these schemes is how they model the channel and capture the interference effects.

3.1 Motivation for Globally coordinated routing

The necessity for a routing protocol to consider the physical layer and the MAC layer characteristics was illustrated in Section 2.3.3. The seminal work by Gupta and Kumar [47] calculated the asymptotic limit on the performance of the MHWNs. However, it assumed an "optimal transmission schedule". Similar modeling efforts assuming an ideal scheduler has been studied [63, 76]. However, in a contention based protocol like IEEE 802.11, guaranteeing optimal scheduling is impossible. Thus, it is important for the routing decisions to be aware of the scheduling implications. In this section, we motivate globally coordinated routing, discuss the basic model for expressing the globally coordinated routing problem and expressing the desired objective function.

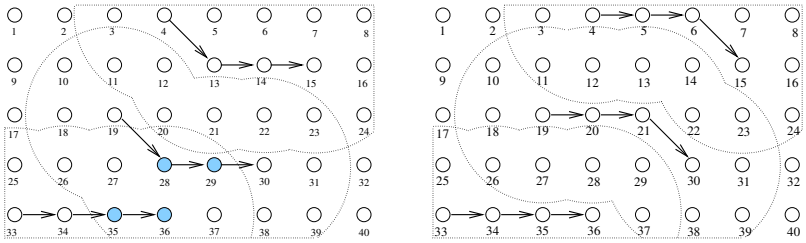

(a) Suboptimal routes (b) Optimal routes

Figure 3.1: Example Illustrating Coordinated Routing

Configurations obtained via globally coordinated routing will generally achieve a substantial improvement over greedy protocols. For example, in the small scenario depicted in Figure 3.1, coordinated routing yields a 33% more throughput *without* a decrease in any of the individual connection throughput. The reduction in interference bottlenecks will have other beneficial advantages such as reducing the end-to-end delays and packet drops, which benefit upper layer protocols such as TCP. It is likely that the advantages of this approach will be amplified by larger, more complex, scenarios where greedy solutions are likely to be far off from optimality. Further, the objective function can be manipulated to incorporate QoS, fairness or other desired considerations.

As a motivating example, consider the network shown in Figure 3.1. There are three connections between nodes *4-15, 19-30* and *33-36*. Consider the routing configuration in Figure 3.1(a). The dotted lines denote the interference range of the active nodes. An ideal unit disc interference range is used for illustrative purpose. Let us assume that all the links used by the connection are of the same quality and connections get started in the sequence *4-15, 19-30* and *33-36*. The connection *19-30* is able to choose an interference separated path from the connection *4-15*. However, when the connection *33-36* starts, the nodes *28,29, 35* and *36* experience interference from the other connection. The routing configuration shown in Figure 3.1(b) shows the optimal routes which do not interfere with each other. In the suboptimal route configuration (Figure 3.1(a)), there is no incentive for the connection *28-29* to change the route, since any route will either be interfered by connection *4-15* or *33-36*. The connection *4-15* will also not change route since none of the nodes in the connection face interference from the neighboring connection. Hence, in the suboptimal scenario, ideally both the connections *19-30* and *33-36* will have half the throughput of the ones

in the optimal scenario. This example illustrates that a greedy local view of the network scenario does not always lead to a globally optimal routing configuration.

3.2 Asymptotic Capacity Estimation of MHWNs

Some of the earliest effort in modeling MHWNs targeted formulation of asymptotic limits of capacity. Gupta and Kumar [47] considered a general wireless network and derived bounds on the capacity of such networks. They studied two kinds of networks: (1) Arbitrary networks where each node can choose an arbitrary destination, packet sending rate and transmission range, but nodes transmit at a constant rate of W bits per second over the channel; and (2) Random networks where the transmission range for each node is fixed, but each node chooses a random destination and transmission rate. In their derivation, n nodes are located in a unit disk area of a plane in the case of arbitrary networks. Under random network, n nodes are placed either on a surface of a 3-dimensional surface of sphere with surface area 1 sq. meter or a plane disk of area 1 sq. meter. While the analysis under arbitrary networks provide the capacity of the network allowing flexibility for the nodes to choose the network parameters, random networks reflect a more realistic network setting by fixing the transmission ranges (or transmission power) and variable data sizes that need to be sent to different destinations. They proposed and used the Protocol model and the Physical model of interference.

Using the above assumptions, the bounds on the channel capacity derived under different networks and models. Of interest to the study of the effect of interference on routing in realistic setting of networks, we focus the results in random networks. With fixed reception range, the Protocol model gives the interference region as a factor of reception range. The interference from all the currently active sources are added up in the Physical model. The upper bound on the random network is shown to be $\theta\big(\frac{W}{\sqrt{n \log n}}\big)$ under the Protocol model and is $\theta\big(\frac{W}{\sqrt{n}}\big)$ in the Physical model where W is the channel capacity in *bits/second*. This quantifies the reduction in the capacity as the number of active nodes per unit area increase. The above study was based on all single hop connections between two nodes which are within the reception range of each other. Explicit capacity estimation for a multi-hop connection is treated by Gastpar and Vetterli [44] who indicate

that under a relay based traffic the achievable capacity is $O(\log n)$, a more encouraging result than the study by Gupta and Kumar [47]. However, both the studies consider a random network and propose the asymptotic bounds; the throughput bound for a given network under a given set of connections is desirable in most practical cases.

3.3 Modeling for Interference Aware Routing

Jain et al. [63] revisit the problem of finding the bounds on the throughput with the goal of quantifying the capacity for a given topology and traffic pattern, rather than asymptotic bounds for general networks. The main idea is to identify the set of links that cannot be active together considering the effect of interference. Each link in the network is represented as a vertex in a transformed graph called *Conflict Graph*. If two links interfere with each other, then there is an edge present between the two vertices representing the links.

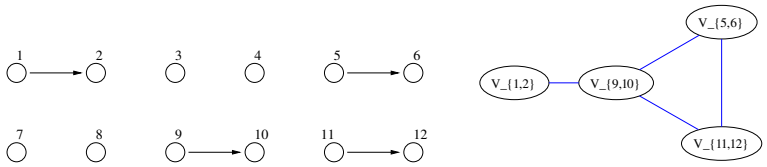

(a) Scenario (b) Conflict Graph

Figure 3.2: Conflict graphs

Consider a scenario with 4 active links as shown in Figure 3.2(a). Figure 3.2(b) shows the conflict graph for the given scenario. A vertex $v_{(i,j)}$ in Figure 3.2(b) represents the link (i, j) in the scenario and the edge between two vertices in the conflict graph represents the interference between the edges. An *independent set* is a set of vertices that are not connected to any of the vertices in the set (E.g. $\{v_{(1,2)}, v_{(5,6)}\}$). Independent set of vertices in a conflict graph represents the set of links that do not interfere and thus can be scheduled simultaneously. A *maximal independent set* is an independent set such that no other vertex can be added to the set that results in another independent set. Thus, the maximum number of links that can be scheduled together can be represented as a maximal independent set of a conflict graph. Let $I = \{I_1, \ldots, I_k\}$ be the set of all maximal indepen-

dent sets I_i where $1 \leq i \leq k$. In the above example, $I = \{\{v_{(1,2)}, v_{(5,6)}\}, \{v_{(1,2)}, v_{(11,12)}\}, \{v_{(9,10)}\}\}$.

Let $d_{i,j}$ denote the distance between the two nodes i and j and let R'_j represent the interference range of node j. Conflicting links are found by Protocol model [47] of interference. Two edges $l_{i,j}$ and $l_{p,q}$ interference with each other if $d_{iq} \leq R'_i$ or $d_{pj} \leq R'_p$.

Basic max-flow formulation: The problem of finding the throughput is modeled as a max-flow problem which maximizes the amount of flow out of the source node (maximum sending rate). The basic model for finding the maximum flow from a source to the destination considers maximizing the sum of outgoing flows from the source (or incoming flows at destination) by constraining that (1) the source generates the traffic, destination is the flow sink and no other nodes generating other traffic; and (2) The flow at each link is non-negative and does not exceed the capacity.

Optimal throughput: The maximum throughput depends upon the number of links that can be active concurrently. At any instant of time only one maximal independent set $I_i \in I$ can be active. Let λ_i denote the amount of time allocated to a I_i. The utilization of a maximal independent set is the amount of time each maximal independent set is active. If we normalize the overall utilization of all the maximal independent sets, then $0 \leq \lambda_i \leq 1$. A schedule to activate the maximal independent sets restricts the λ values. The constraint in Equation 3.1 restricts the scheduling policy by not allowing multiple maximal independent sets to be active concurrently.

$$\sum_{i=1}^{k} \lambda_i \leq 1 \tag{3.1}$$

While Equation 3.1 restricts the schedule of the maximal independent sets, it does not limit the usage of each link. The maximum flow at the link should not exceed the utilization periods of all the maximum independent sets that it belongs. If C_{ij} denotes the capacity of the link l_{ij}, then Equation 3.2 expresses this constraint.

$$f_{ij} \leq \sum_{l_{ij} \in I_i} \lambda_i C_{ij} \tag{3.2}$$

The optimal throughput is given by adding the constraints in Equations 3.1 and 3.2 to the basic max-flow formulation.

Lower and upper bound constraints: While the above formulation yields the optimal throughput, calculation of *all* the maximal independent sets takes an exponential time. Hence, maximal independent sets are heuristically calculated. The resulting routing and scheduling formulation gives the *lower bound* of the throughput.

In a conflict graph, a clique (set of vertices that are all connected to each other) represents the links that mutually interfere. A *maximal clique*, similar to maximal independent sets, is a clique for which an additional vertex cannot be added such that the resulting set forms another clique. Due to mutual interference, only one vertex of a clique can be active at a given time. Such *Clique constraints* are used to restrict the interfering links. A clique constraint states that the sum of normalized utilization of all the vertices in the maximal clique is lesser than one, which restricts the the upper bound of throughput.

Kodialam et al. [76,77] consider the same problem but use a different approach. They model the problem as a linear programming problem identifying the constraints that specify the interference between the links. They also propose algorithms to obtain the set of feasible schedules of channels (in a multi-channel environment) based on the result obtained from the linear program. However, unlike the model in [63], the model proposed by Kodialam et al. [77] can identify the sets of links that interfere with each other in $O(|E|)$ where E is the number of edges in the conflict graph.

3.3.1 Accounting for Interaction Among Connections

While studies by Jain et al. [63] and Kodialam et al. [76, 77] consider the problem of estimating the throughput of a single multi-hop connection, they propose a simple extension to the model to handle multiple connection scenarios. The main component of a globally aware routing protocol is the interaction between the routes of different connections to enhance the network performance. The proposed frameworks in the above studies were constructed and are best used to study the throughput of a single connection. The linear programming model has to considerably altered to account for the various interactions between the connections. The resulting effects lead to a

non-linear programming model which are very difficult to solve computationally. Also, the above studies only consider aggregate throughput as a metric, focusing on feasible throughput bounds, rather than providing usable routing configurations.

A contribution of the dissertation, we formulate a model for finding the optimal routing configurations in multiple connection MHWNs with a single channel in Chapter 4. The model is based on a *Multi-Commodity Flow (MCF)* formulation [7]; a network flow modeling approach that has been applied to traffic engineering in conventional networks. However, such a routing model is infeasible for analysis of routing in denser networks owing to the high complexity. Chapter 7 analyzes the complexity of such model and proposes a low-complexity model based on decomposition approach; an approach to divide a large problem into several smaller problems. We illustrate the run-time gains of such an algorithm and compare the quality of the routes with the MCF formulation.

3.4 MAC modeling–Accounting for the Effect of Scheduling

The formulations discussed thusfar ignore the effect of the scheduler; they assume that aggregate interference metrics such as busy time are the sole factor influencing link capacity (as would be the case, for example, under an ideal scheduler). Such formulations measure the *available capacity* of the links (Property 1 discussed in Section 2.3.2), but do not account for the effect of imperfect CSMA based schedulers (Property 2 in the same section). The effect of packet drops is considerable in realistic environments which operate under a contention based MAC schedulers like IEEE 802.11 (as explained in Section 2.3.2). Modeling the effect of routing by considering such MAC protocol would require not only the formulation discussed above, but also a model of characterizing the MAC protocol that can then be combined with the nominal capacity to estimate link quality more accurately.

IEEE 802.11 uses a two-way handshake between the source and the receiver to let the neighbors of both the nodes know about the communication going on between the source and the receiver (Section 2.2.5). The nodes which are able to *receive* the packet will defer their transmission. Under the Protocol model, all the nodes within the receiving range of source and receiver will listen to the handshake and defer their transmissions. The only nodes that interfere with the ongoing

transmission are the nodes which are within the interference range, but not within the receiving range. A crude model to estimate the destructive effect of these interferes that are not prevented by the MAC protocol is to estimate the channel busy time contributed by such interferes as a measure of their scheduling impact on each link they interfere with.

Approximating the busy time of the node at a higher layers, like the MCF model proposed in Chapter 4, do not model the MAC specific interactions at a great detail. This has two key disadvantages: (1) The throughput of the link correlates well with busy time in low interference regions. However, as seen in Figure 2.3 in Section 2.3.2, at moderate to high interference regions the busy time and the throughput of the link fail to correlate. Thus the estimation of throughput by using the above models at high interference regions may be incorrect. (2) The variation of the quality of the links on a small scale time frame in a real testbed was studied in [5]. Capturing such interactions will need a precise formulation of the MAC protocol.

Modeling the contention based MAC protocol is an active research area. Bianchi [14] modeled the IEEE 802.11 protocol and a throughput estimation using the proposed model was analyzed. Various other research work like [18, 41] propose new frameworks for modeling the CSMA/CA based MAC protocols. Garetto, Salonidis and Knighitly [41] model the fairness and throughput. They formulate the starvation of the link in a multi-hop wireless network. Such estimation of MAC factors can be used in the formulation of the routing. However, the certain restrictions make their application infeasible in routing models. The dissertation proposes a scheduling component that helps in modelling globally-aware routing. The limitations of the existing approaches and the contribution of the dissertation is described below:

- *High complexity* – Most of the recent studies are iterative in nature, thus requiring long runtime. The dissertation focus on creating a scheduling model that has faster runtime. While the existing models can be used for an accurate characterization of scheduling effects, they are infeasible to be used in the integrated *scheduling-aware routing model* due to their high runtime. This implies that scheduling effects of MHWN can be analyzed using the current models, but improving the performance of MHWN by finding alternative route configurations is infeasible since *each set of routes* has to be evaluated for its scheduling effectiveness. The

dissertation attempts to develop a scheduling model that can be integrated into a routing model.

- *Advanced Physical Model* – The dissertation assumes an advanced model of physical layer which is based on *Signal-to-Interference Noise Ratio* (SINR). Many new interactions are observed due to the change in physical model.

- *Relaxation of some primary assumptions* – The scheduling model proposed by the dissertation relaxes other assumptions in the related work, like a Poission Point Process based scheduling traffic.

Chapter 5 proposes a *Scheduling Aware Routing (SAR) model* to overcome the above problems and to capture a detailed link behavior. The idea is to capture the MAC interactions by identifying the patterns of interactions between the links. The resulting scheduling model is integrated with the routing model to account for scheduling effects.

While the SAR model is not as accurate as the scheduling-only models [18, 41], it provides a feasible scheduling component for a routing model. An accurate, low-complexity model for accounting for scheduling would be beneficial in the construction of a globally-aware routing model.

Chapter 4

Interference Aware Routing Model

The need and motivation for a globally coordinated routing in the context of MHWN was discussed in Chapter 3. In this chapter, we discuss a contribution of the dissertation in formulating such Globally Coordinated routing in MHWNs using a network flow based model.

4.1 Introduction and Motivation

Modeling routing with a complete set of interference constraints is a complex problem. For example, it has been shown that an optimal constrained routing with just the bandwidth constraints for a multi-commodity problem is NP-hard [43]. We build on recent works that model the routing and scheduling problem in MHWNs as a network flow problem [63, 76]. Chapter 3 had briefly reviewed the modeling efforts for Globally-Coordinated routing. In this chapter, Section 4.2 specifically relates our work to previous efforts as well as others.

We model the network, including interference, as an extensible Linear Programming (LP) model and investigate objective functions that lead to routes which are *interference separated*. We identify: (1) crucial parameters that affect the overall connection health; and (2) unexpected effects from a standard formulation that arise especially in multiple connection environment. We propose alternative formulations that address these effects. The basic model is presented in Section 4.3, and the objective function formulation is analyzed in Section 4.4.

While the proposed approach is not directly usable in dynamic networks, which are better suited

to distributed solutions, this formulation is beneficial because:

- It provides methodology and experience with achievable performance relative to existing routing protocols.
- It provides an environment to refine the model based on observed behavior (for example, to capture the effect of scheduling), and further our understanding of the problem
- The formulated model can serve as the starting point for developing distributed routing protocols that approximate the behavior of globally aware routing protocols. Design decisions in the formulation were taken with an eye for future development of distributed versions (e.g., the selection of a node based, rather than an edge-based, interference model).
- Developing distributed globally aware protocols is a future direction for our work
- The proposed approach is feasible for static or slowly changing networks, which represent an important subset of MHWNs, including mesh networks and static sensor networks.

Our analysis assumes Protocol model of interference [47]. We believe that it can be extended to capture other propagation models like Signal to Interference Noise ratio (SINR), Bit Error Rate (BER) and fading channels, or incorporate measurement data, in the future.

We evaluate the formulation in Section 4.5 by simulating routes obtained from the linear programming solver against the best routes obtained by Dynamic Source Routing. We observe considerable improvement in performance for most cases. However, we observe that scheduling plays an important effect in determing interactions between interfering links; nodes that are in interference range but not in reception range cause more difficulty for the MAC protocol. We show in Section 4.6 that by exposing this relationship to the scheduler, more effective routing is achieved leading to impressive gains in performance, especially under high loads. Finally, Section 4.7 presents the concluding remarks with the possible improvements and extentions of the model.

4.2 Related work

Routing in MHWNs is a well-studied topic and routing protocols were reviewed in Chapter 2.3. It was discussed that the first and the second generation routing protocols fail to yield optimal routing configurations and the need for a globally-coordinated "ideal" routing protocol was motivated in Chapter 3.

The impact of interference on routing performance is studied by Kodialam et al [76, 77] and Jain et al [63]. These works model a MHWN using a network flow formulation; they form the basis of our work. The general problem of routing multiple flows in a finite capacity network with additional QoS constraints is a complex integer nonlinear optimization problem. A well-known network flow formulation, *Multi-commodity flow (MCF)* [7], has been used successfully in traffic-engineering of wired networks to derive the theoretic bounds, and as the basis for heuristics to develop fast-runtime approximation algorithms in these traditional networks [45]. However, this formulation cannot be directly adapted to MHWNs because of the presence of interference. MCF has been used in other contexts for multi-hop wireless networks. Sankar et al use an MCF formulation to derive routes that maximize the lifetime of power-constrained networks [112]. This work uses a conventional formulation that does not account for interference since it is not concerned with network performance aspects of the problem. The presence of interference and bandwidth constraints significantly complicates the problem.

Our work is most related to recent work on calculating the capacity bounds of ad-hoc networks with interference. Specifically, the wireless version of the MCF formulation must account for interference. Interference effects can be captured by extending the linear programming constraints of the MCF formulation as demonstrated by Jain et al [63]. In the same paper, the authors show that it is NP-hard to compute the path with least interference. They model interference as a conflict graph and derive the upper and lower bounds on the throughput for a static topology with a pre-specified connection set, assuming idealized scheduling. They show that theoretically optimal routes yield much better throughput than the existing routing protocols do. However, most of their analysis is carried out with a single-connection model. In contrast, our work explicitly accounts for the modeling requirements under multiple connections. Further, we use a more sophisticated

model, and investigate the choice of objective functions which yield more effective routing that maximizes reuse and reduces hot-spotting.

Kodialam et al. propose a joint routing and scheduling problem in [76] which promises 67% of the optimal throughput. However, they consider a very simple model of interference where nodes experience interference only from the immediate neighbors.

The work presented in this chapter extends these previous works that use a network flow formulation in several important ways.

1. The proposed formulation is based on a node-centric model, which models the interference at each node. This approach is different from existing models that are edge-centric. We believe that the node-centric model offers significant advantages because nodes are the active entities in the network where transmission decisions are taken. Thus, it becomes possible to consider of scheduling effects (which we show play a major role). Further, the node-centric approach makes the development of distributed protocols more straightforward.

2. The existing models assume an ideal scheduling protocol which prevents the packet drops. Such a formulation may not be directly applicable to the contention based scheduling protocols like IEEE 802.11. We explore the effect of scheduling, and show that it plays an important role in determining the effect of interference.

3. Existing works focus mostly on the effect of interference on a single connection, with cursory treatment of the more complex case of multiple connections whereas this chapter focuses on analyzing and modeling interference with the multiple connection interaction as one of the main parameters.

4. We explore objective-function formulation issues, and implications on run-time and quality of the solution.

5. Existing studies only consider aggregate throughput as a metric, focusing on feasible throughput bounds where as the proposed model focuses on deriving optimal routing configurations that are tunable to application objectives.

6. We investigate the path elongation effects and heuristics to reduce the complexity of the objective function.

Gupta et al. [48] use the basic algorithm derived by Jain et al [63] and derive a simpler means of calculating cliques and reach a distributed version of the formulation [48]. Our work is different in terms of the underlying model and solution methodology, as discussed above with regards to original formulation in [63]. Discussion of the types of interference and its effect on scheduling has been done in past research work like [47,124]. These types have been modeled in Kodialam et al [77]. Such a model has been used in this chapter to describe various kinds of interference. Raniwala et al. introduce the definition of interference period and show that interference is one of the main limiting performance factors [106]. However, their objective is effective channel assignment in a multi-channel system.

4.3 Multi-Commodity Flow Formulation

Consider a static MHWN where packets for a particular connection may flow through multiple intermediate wireless links. A node m can directly transmit to another node n if the quality of the signal received by n is above a given threshold. We denote such tuple of nodes (m, n) as an *edge*[1]. To represent this network as a graph, let N be the set of nodes where each node constitute a *vertex* of the graph and E be the set of *directed edges*. Let $G(N, E)$ represent the graph of the network. In this section we present our formulation of the routing problem as a network flow problem and distinguish it from existing network flow formulations.

4.3.1 Basic Routing

The problem of routing in MHWNs can be transformed into a Multi-commodity flow problem [7]; we describe this basic formulation here. Let (s_n, d_n, r_n) denote source, destination and the rate of the n^{th} connection. The rate of connection, r_n, is the number of bits to be sent per unit time. Let C be the set of connections. The demand for a given node is the difference between the total

[1]The definition of the edge can be adapted to capture alternative propagation models, or to be based on measured data.

outflow from the node and total amount of inflow to the node. The demand at a node for n^{th} connection is represented by b_i^n as

$$b_i^n = \begin{cases} r_n, & \textit{if } i = s_n \\ -r_n, & \textit{if } i = d_n \\ 0, & \textit{otherwise.} \end{cases} \tag{4.1}$$

To analyze the flow at each edge, we break the flows into a set of n disjoint flows, one for each connection. Let x_{ij}^n denote the flow at edge (i, j) for the n^{th} connection. Let the maximum capacity of an edge (i, j) be denoted by $u_{i,j}$.

4.3.2 Feasibility of flows

The basic feasibility test on whether all n flows can be accommodated is the standard multi-commodity flow problem. Equations 4.2 to 4.4 describe the constraints that need to be satisfied for feasibility. Equation 4.2 describes the limiting bound of each flow to be the maximum rate of the connection. For a given connection, each edge can carry a maximum load corresponding to the rate of the given connection. The bundle constraint for the given graph is given by Equation 4.3 which limits the total flow at an edge not to exceed its capacity. The flow constraint in Equation 4.4 specifies the demand requirement to be met at each node as the difference between the outflow and inflow (Equation 4.1).

$$0 \leq x_{ij}^n \leq r_n \forall n \in C, \forall (i, j) \in E \tag{4.2}$$

$$l_{ij} \leq \sum_{n \in C} x_{ij}^n \leq u_{ij} \forall (i, j) \in E \tag{4.3}$$

$$b_i^n = \Big(\sum_{(i,j)\in E} x_{ij}^n \Big) - \Big(\sum_{(j,i)\in E} x_{ji}^n \Big)$$
$$\forall n \in C, \forall i \in N \tag{4.4}$$

The above model assumes that a flow can be split into multiple routes (multi-path routing [95]). However, a single route per connection is desirable in majority of networks to reduce the overhead of routing protocol and avoid side-effects that occur due to multi-path routing such as packet reordering. Under such conditions, the problem transforms into a integer MCF problem. Each edge can either carry the full traffic for a given connection or none of it; this constraint is represented by Equation 4.5. The variable y_{ij}^n is a boolean variable which is set to 1 if the edge carries the traffic for the nth connection and 0 otherwise.

Integer flow constraint:

$$x_{ij}^n = r_n \cdot y_{ij}^n \quad \forall n \in C, \forall (i,j) \in E \tag{4.5}$$

4.3.3 Traffic parameters and auxiliary constraints

Additional parameters are needed to allow effective traffic characterization. This section models these critical parameters and introduces supplementary constraints to account for the feasibility of the parameters. Traffic parameters and constraints associated with them have not investigated by previous network flow formulations for MHWNs.

Node Based Model of Signal and Interference

In contrast to the conflict graph model used in [63] and the edge-based approach in [77], the formulation in this chapter adopts a more flexible *node-based interference model*. More specifically, interference is tracked at nodes, rather than edges, since the nodes are the physical entities in the network; performance viewed by the nodes allows more effective optimization of the network as viewed by its users. An additional advantage of the node-centric formulation is a more direct and simpler transition to distributed protocols as we directly optimize performance from the communicating node's perspective.

A basic model of the flow and the interference experienced at the node is studied in this section. We first define the busy, or committed, time of the node into *Signal* (flows carried by the node at incoming and outgoing edges) and *Interference* (the silent period of a node to enable the neighboring flows). Differentiating between the signal and interference is useful in objective function formulation and helps the extensibility of the model. For example, we use the *Signal* part of the busy time to restrict the number of hops taken by the node. The amount of signal carried by a node i, denoted by S_i, is the sum of flows that enter or leave the node. This is denoted by Equation 4.6.

$$S_i = \sum_{n \in C} \left(\sum_{(i,j) \in E} x_{ij}^n + \sum_{(j,i) \in E} x_{j,i}^n \right) \quad \forall i \in N \tag{4.6}$$

Let Γ_{ij} be a two dimensional matrix of boolean values which is set to 1 if there is an interference at node j when node i is transmitting. Γ_{ij} can be derived based on node location assuming some propagation model, or experimentally based on observed connectivity and interference. The use of Γ allows later extension of the model, for example, to account for fading channels; we use a "Two Disk" interference model (explained in Section 2.2.1) as proof of concept in this chapter.

Modeling Interference

The interference at a given node can be viewed as the amount of time the node has to be silent in deference to neighboring flows. If there exists a scheduling mechanism which perfectly schedules the transmissions, then the node has to be silent if none of the nodes which are currently receiving can be interfered with the node's transmission: we call this model the *Receiver Conflict Avoidance (RCA)* [77]. Under RCA, the interference at a node i ($\ddot{\mathrm{I}}_i$) will be equal the sum of inflow to all the nodes which interfere with i, as described in Equation 4.7:

$$\ddot{\mathrm{I}}_i = \sum_{n \in C, \Gamma_{iz}=1, (w,z) \in E, w \neq i, z \neq i} x_{wz}^n \quad \forall i \in N \tag{4.7}$$

Even though RCA describes an imperative condition, it is not sufficient for protocols in which scheduling is based on contention. Generally, the two way handshake of RTS-CTS in protocols like 802.11 would extend the time for which the node i will be silent. To inform the hidden nodes

around the receiver about the ongoing communication, the receiver also sends a small packet to the transmitter. This two-way communication gives rise to reception of packets at both the transmitter and receiver. To avoid interference at both ends, node i has to be silent if a node which is within the interference range (R_i) is either transmitting or receiving. This interference period is called *Transmitter-Receiver Conflict Avoidance (TRCA) model of interference* [77], denoted by I_i. The value of I_i is the sum of inflows and outflows of all the nodes which interfere with node i, and is given by Equation 4.8. given by the equation 4.8.

$$I_i = \sum_{n \in C, \Gamma_{wi}=1, (w,z) \in E, y \neq i, z \neq i} x_{wz}^n + \sum_{n \in C, \Gamma_{wi}=0, \Gamma_{iz}=1, (w,z) \in E, y \neq i, z \neq i} x_{wz}^n \quad \forall i \in N \tag{4.8}$$

Active and Passive nodes

If a node does not carry traffic, the amount of interference it experiences is immaterial; thus, there is a need to minimize interference only at active nodes that participate in sending, receiving or relaying packets. Let us denote such nodes which have $S_i > 0$ as *Active* and other nodes as *Passive*. We introduce the concept of *Normalized interference* to differentiate between the two kinds of nodes as given in Equation 4.9. Let *Normalized Interference* at a node i, denoted by $\hat{\mathrm{I}}_i$, be the interference at the node if its carrying any traffic; otherwise, it is zero. The interference in Equation 4.9 can be computed using either the RCA or TRCA model.

$$\hat{\mathrm{I}}_i = \begin{cases} I_i, & \textit{if } S_i > 0, \\ 0, & \textit{otherwise} \end{cases} \tag{4.9}$$

Node Commitment Period

In a fixed reference time period, the time the node spends in transmission/reception can be represented by S_i. The time that the node i has to reserve to be idle for enabling the flow of interfering traffic can be represented by $\hat{\mathrm{I}}_i$. We call the sum of these two values, the *Commitment Period* (A_i) of the node (Equation 4.10). For all the active nodes, the *Commitment Period* should be lesser

than or equal to the reference period; otherwise, the node will be unable to fit all the flows as expressed by:

$$A_i = S_i + \hat{\mathrm{I}}_i \tag{4.10}$$

Interference Constraint:

$$A_i \leq U \quad \forall i \in N \tag{4.11}$$

The constraints given by Equations 4.2,4.3, 4.4, 4.5 and 4.11 collectively state the feasibility constraints for a single path traffic considering interference. We use *interference* to mean *TRCA interference* in the remainder of the chapter.

4.4 Objective Function Formulation

The choice of the *optimal path set* depends on the definition of optimality as expressed by the objective function. While it is necessary for an objective function to consider the interactions between connections, the complexity of the formulation should be manageable for practical use in moderate to large size networks. This section explores the interaction between multiple connections that need to be captured by the objective function and builds a simple, yet effective, objective function in a step-by-step manner.

4.4.1 Tradeoffs in Objective Function Specification

The combination of Normalized interference ($\hat{\mathrm{I}}_i$) and signal (S_i), that represents the time a node is communicating, provide the basis to construct different objective functions that foster path separation.

The choice of the objective function has significant implications on the difficulty of the optimization problem. A multiple objective formulation leads to an excessively difficult optimization problem. Thus, we attempt to combine the objectives into a simpler form. However, we show that

the intuitive approaches to objective function expression lead to some unintended and harmful effects in the solution. For example, minimizing the total interference leads to excessive hot-spotting as the solver routes connections using the same nodes (minimizing the number of active nodes). We explore these alternatives in this section, and develop a per-connection objective function expression that is free of these undesirable effects. We also discuss the tradeoff between minimizing interference and limiting path stretch (which is known to be harmful in MHWNs).

Multiple Objectives Consider the objective of trying to minimize *Commitment period* at each node as shown in Equation 4.12.

$$\textit{Minimize} \quad A_i \quad \forall i \in N \tag{4.12}$$

This equation has the drawback of *Multiple Objective Functions*, since A_i has to be minimized across all the nodes; a formulation with multiple objective functions significantly complicates the optimization task. The individual objectives, either as observed at a single node or by a single connection, should be combined into a single objective that would approximate the effect of the multiple objectives. Our goal is to find such *Pareto Optimum* by combining multiple objectives into one. Such *Multiple Objective Mathematical Programs (MOMP)* can generally be solved by either having a *Weighted Sum* or *Lexicographic* approach [114]. The *Weighted sum* approach with equal weights is well suited to our problem since the aim is to reduce the interference across all the nodes and connections without a set priority to each node or connection. We would like to investigate the effects of varying weights and *Lexicographic approaches* in the future.

We introduce two simple approaches to combining the multiple objectives: minimizing the sum of the commitment periods, and minimizing their maximum.

Total Commitment Period Minimization Equation 4.13 represents an objective function that minimizes the sum of *Commitment Periods* of all nodes in the network.

$$\textit{Minimize} \quad \textstyle\sum_{i \in N} A_i \tag{4.13}$$

Peak Commitment Period Minimization The commitment period is an estimate of the channel state around a node: the higher the commitment period, the greater is the bottleneck created at that node. The *Bottleneck Node* is the active node with the maximum commitment period. Under optimal scheduling, the bottleneck node is the one which dictates the end to end delay of the packet. Even in more realistic schedulers (e.g., contention based 802.11), the bottleneck node experiences maximum demand and will often be the critical link in determining properties such as the end-to-end delay and effective throughput. Accordingly, an objective function can be constructed that targets reducing the commitment period of the bottleneck node (Equation 4.14). Note that while *max* leads to a non-linear objective; however, there are well known approaches for linearizing it.

$$Minimize \quad max\{A_i | \forall i \in N\} \tag{4.14}$$

The disadvantage of the combined functions is that they collapse some aspects of the objective functions captured by the multiple objective formulation. This results in some undesirable effects. For example, in the case of the peak commitment minimization, the focus is only on the *Bottleneck node* and the other nodes are ignored. We explain such issues in the next section and motivate our final, per-connection objective function.

4.4.2 Problems in Combined Objective Functions

Problems may arise in the combined objective function formulation. We show examples of such problems in this section.

Conjoint node effect: Consider a topology with multiple connections. The objective functions in Eq. 4.12, Eq. 4.13 and Eq. 4.14 use the commitment period *Normalized Interference*. Consider Equation 4.13 where we minimize the sum of commitment periods. If a new node is added to carry the flow for any connection, then its commitment period would rise from zero to the sum of its signal and interference (by definition of commitment period). This would increase the objective value by a significant amount. Thus, the formulation favors keeping the number of active nodes to the minimum. While this is helpful in single connection scenario to keep the number of hops to the

minimum, the multiple connection scenario ends up with overloaded nodes which carry more than one connection while there exists another path with same number of hops and lesser interference. This effect is termed as *Conjoint node effect*.

Connection Coupling: Consider the Equation 4.14 where the *bottleneck node's* commitment periods is minimized. If there exists a node in at least one of the connection with a very high value of commitment period and which cannot be reduced, then the other connections are unoptimized. This problem is termed, *Connection coupling*.

Path Inflation: Most MANET routing protocols attempt to minimize the hop count of a connection; it is well known that the performance of an isolated multi-hop connection is directly related to the number of hops under idealized propagation assumptions [83]. Even though a longer route may be preferable to avoid the interference hot-spots, some objective functions fail to take the shorter path when one is available at the same or lower cost. Objective functions which ignore the hop-count metric may suffer from *Path Inflation*. In many cases, this objective function fails to restrict the number of hops. Adding more nodes in the connection, adds active nodes, hop-count and the interference at the other active nodes, thus leading to a greater commitment period. Thus, a simple equation like 4.13 restricts the flow to the shorter number of hops. This is not the case in the objective function 4.14. The objective minimizes the maximum commitment period of all the nodes.

To illustrate the path inflation effect, consider a single connection between nodes *25-30* in a 6x6 grid topology (similar to node placement in Figure 4.1(b)). Once the bottleneck node of maximum commitment period is found, there is no restriction by the formulation to the number of nodes in the flow provided they have a commitment period lesser than or equal to the bottle node. Based on the approach of the solver, the routes obtained by objective function in Equation 4.14 can be inflated; an 8 hops path in taken in the above example. Equation 4.14 fails to restrict the commitment periods of other nodes, which leads to path inflation.

4.4.3 Per-connection Objective Function

This section describes an alternative objective function that mitigates the effects observed with a single combined objective function. The *Connection Coupling* and the *Conjoint node effect* suggest the need for splitting the objective function used on a *Per-connection* basis. Let *Per-connection Signal* ($\hat{\mathrm{S}}_i^n$) be the signal carried for the n^{th} connection at node i. Let $\hat{\mathrm{y}}_i^n$ be the boolean variable as described in Equation 4.15 which is set to 1 if the node i is a part of the n^{th} connection. The *Active* and *Passive* nodes can also be defined on a *per-connection* basis based on the value if $\hat{\mathrm{y}}_i^n$.

$$\hat{\mathrm{y}}_i^n = \begin{cases} 1, & \textit{if } \hat{\mathrm{S}}_i^n > 0 \\ 0, & \textit{otherwise.} \end{cases} \tag{4.15}$$

Let *Per-connection Commitment Period* ($\hat{\mathrm{A}}_i^n$) be the commitment period of a node i for connection n which is defined as follows. Let $\hat{\mathrm{A}}_i^n$ be A_i, if it is involved in carrying the flow for the n^{th} connection; otherwise, it is zero. Once the notion of $\hat{\mathrm{A}}_i^n$ is introduced, the effect of *Connection Coupling* can be directly eliminated since we can now minimize the per-connection based activity periods. Equation 4.16 shows an objective function that minimizes the peak commitment per connection.

$$\textit{Minimize} \quad max\ \{\hat{\mathrm{A}}_i^n \,|i \in N\} \quad \forall n \in C \tag{4.16}$$

It can be seen that equation 4.16 represents a *Multiple Objective Function*. This multi-objective function can be transformed into a single objective function as explained in Section 4.4.1. Let $\hat{\mathrm{A}}_{\max}^n$ be the maximum value of the Normalized Commitment Period for a given connection n. This would describe the *Bottleneck link* of the n^{th} connection.

$$\textit{Minimize} \quad \textstyle\sum_{\forall n \in C} \hat{\mathrm{A}}_{\max}^n \tag{4.17}$$

Equation 4.17 gives the objective function which decouples the commitment periods of connections and combines them as shown in 4.4.1.

Controlling path inflation: Even though Equation 4.17 avoids interference hot-spots and Connection Coupling, the Path Inflation effect can still arise. This section evaluates the balance between the shorter number of hops and the avoidance of interference and explores two schemes to overcome this problem.

For a constant number of hops h, the sum of the per connection signals at all nodes is constant and is given by:

$$\sum_{i \in N} \hat{\mathrm{S}}_i^n = 2hr_n \tag{4.18}$$

The source and the destination of the connection carry signal equal to the rate of the connection r_n. The router nodes carry signal equal to $2r_n$, for receiving and forwarding the signal. The premise of both approaches is to limit the sum of $\hat{\mathrm{S}}_i^n$ across all connections and to choose the best route among the set of routes selected. The first approach tries to minimize the sum by adding it in the objective function and the latter by adding linear constraints.

1. *Including the signal in objective function:* To dictate the shortest number of hops in a given set of connection is relatively easier. It can be observed that the sum of normalized signals at a node for different connections is equal to the total signal carried by the node. The objective function of the formulation has two functions (1) Minimize the normalized signal across all the connections; and (2) Minimize the objective function in Equation 4.17. We reduce this multiple objective functions into a single objective function by using the weighted sum approach. the. If we assign a high weight(say, a weight of α) to this sum of signal carried, such that it is much larger than the Commitment Period experienced by the node, then, by combining this sum with equation 4.17 would result in a new objective function given by equation 4.19.

$$\textit{Minimize} \quad \alpha \textstyle\sum_{i \in N} S_i + \sum_{\forall n \in C} \hat{\mathrm{A}}_{\max}^n \tag{4.19}$$

   Suitable value of α would force to choose the path set which not only has the shortest hops but also minimizes the interference among the flows. A relatively high value of α is assigned.

The maximum interference experienced by an active node in a linear placement of nodes is assigned as the value of α serves as a acceptable value. We compute the value of α as shown below:

For a topology where nodes are placed linearly, the minimum value of α can be shown to be bounded by the equation 4.21 where R_i is the Interference Range and R_r is the Reception Range of the signal.

Proof: The maximum activity period for a given node is when all the traffic flows through its interference range, R_i with maximum possible hops. Let $h_{\max}$ be the maximum number of hops in the interference region. The maximum number of hops happens in a circle of radius R_i can happen when the distance between the *alternate* nodes is just above R_r. Let us denote this value by R_r^+. Hence, if the nodes are placed in a straight line, $h_{\max}$ is given by the Equation 4.20. The node in such a region should be quiet for transmission from all the hops and for the time of reception. Thus, the lower bound for α is given by Equation 4.21.

$$h_{\max} = \left\lfloor \frac{2R_i}{R_r^+} \right\rfloor \tag{4.20}$$

$$\alpha \geq (h_{\max} + 2) \sum_{n \in C} r_n \tag{4.21}$$

It is to be noted that the value of α is constant for the path set consisting of shortest number of hops. Hence the equation 4.19 tries to find a set of shortest hops path set with minimal interference.

2. *Per-connection signal constraints:* The other approach to avoid the *Path Inflation* effect is to add a constraint which limits the number of hops taken by each path. Although the approach is elegant, this formulation would then result into a flavor of the *Constrained Shortest Path Problem* which is proved to be NP-hard in studies like [50]. The minimum number of hops needed to reach a destination can be calculated using *Breadth First Search(BFS)* algorithm. Let $h_{\min}^n$ be the minimum number of hops in the route between the source and destination of n^{th} connection. The sum of the $\hat{y}_i^n$ across all the nodes will give the number of nodes participating in the n^{th} connection, which will be equal to the $h + 1$ (h being the number of

hops) in the route. To restrict h to shortest number of hops, we have to add the constraints as given in Equation 4.22 where P is a constant termed as *Path Stretch factor*.

$$\sum_{i \in N} \hat{y}_i^n - 1 = \mathrm{P}(h_{\min}^n - 1) \quad \forall n \in C \text{ and } \mathrm{P} \geq 1 \tag{4.22}$$

The amount of *stretch* in the number of hops can be restricted by appropriately setting the value of P. *Path Stretch factor* is the ratio of the maximum allowable number of hops to the shortest hop count. If P = 1, then it forces the route to take the shortest number of hops $h_{\min}^n$. The value of P is a constant in this study, however, we would like to study the effect of adaptation of P in the future work. This can be done by either having a per-connection path stretch factor or the value can be implied by priority of the connection.

Even though the second approach is simpler than the first, it restricts the feasibility solution for traffic where the capacity can become the bottleneck. By enforcing the P strictly in the constraint in Equation 4.22, the algorithm may fail to find the path set when the required number of hops can be stretched because of the unavailability of the capacity. However, the former formulation will overcome this disadvantage by specifying the restriction on the number of hops in the objective function which is to be minimized. The latter approach also needs to run the shortest path algorithm (BFS) before the commencement of the optimization to figure out the shortest number of hops for each connection, $h_{\max}^n$.

4.5 Performance Evaluation and analysis

In this section, the performance of our formulation is compared with the existing routing and scheduling mechanisms. The CPLEX Linear Programming solver [27] was used to solve the LP formulation. The Qualnet simulator [105] was used to measure the performance of the proposed schemes under 802.11 protocol. We first study a grid topology of 6x6 and 8x8 nodes, and then evaluate the results of random deployment. The simulator was modified to use the Boolean Interference Model where the interference between two nodes is observed if the distance between them is lesser than a given threshold (as denoted by Γ in the model) to be consistent with the MCF

formulation. It bears repeating that the formulation is not specific to the Boolean model; in fact, we present some sample results with a signal to interference and noise ratio (SINR) model later. The IEEE 802.11 MAC protocol is used for all experiments.

To observe the behavior of the optimal routes, the solver results and the results from DSR are converted to static routes which are then used in the simulation. For each connection, the most commonly used route under DSR protocol is chosen and converted to a static route for use in the simulator. This approach is chosen to present the best possible performance obtained by DSR – always using the best path and ignoring dynamic effects and routing overhead.

4.5.1 Static connections in 6x6 Grid

A 6x6 grid network is studied with predefined connection patterns in order to demonstrate the characteristics of the routes given by the solver. The distance between the two adjacent nodes is set to 200m so that the a node can directly reach the immediate diagonal node. Figure 4.1 shows the path taken by various connections. The interference range(R_i) and the reception range(R_r) set in the solver is also shown for scaling of distances. The rate of all the connections are kept at the same value which was selected to ensure the presence of a feasible solution.

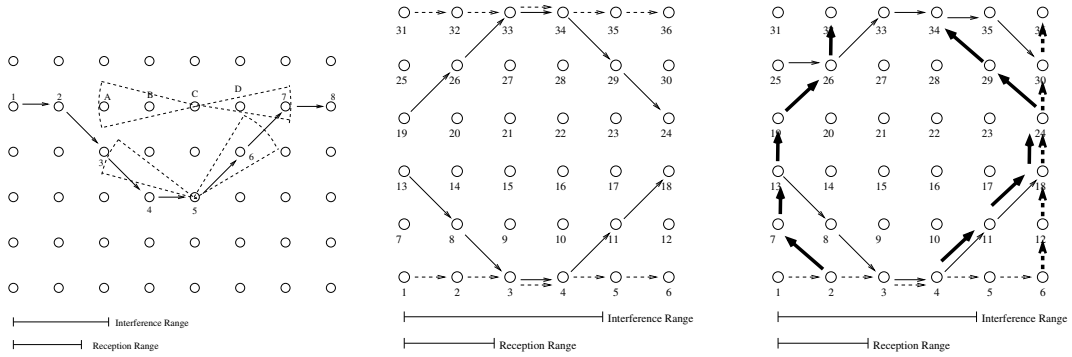

(a) 1 connection (b) 2 and 4 connections (c) 6 connections

Figure 4.1: Routes taken in in 6x6 Grid Topology

Self interference reduction A single connection from node 1 to node 8 is set up and the route taken is shown in Figure 4.1(a). In this scenario the reception range is set to 300m and interference

Metric \ Flows	2	4	6
End to End Delay	0.41	0.1	0.46
Throughput	2.44	1.17	1.24
Queue Drops	0.28	0	0.13

Table 4.1: Static connections in 6x6 Grid

range to 430m for the purpose of illustration. This is a 7 hop connection where the bottleneck node would be in the middle of the connection since it experiences interference from higher number of links. Let us compare two shortest routes, *[1-2-3-4-5-6-7-8]* and *[1-2-A-B-C-D-7-8]*. The LP formulation would lead to the former route. Node 5 and node C will be the bottleneck nodes for each of these connections respectively. The arcs drawn from the bottleneck nodes denote the interference range(R_i). The commitment period of node 5 would be flows across 4 links included in the sectors where as the commitment period of node C would be 5 links, thus leading the solver to take the former route. This depicts the reduction of self-interference by the proposed model.

The remaining scenarios use the standard interference range and reception range. We first describe the shape of the routes taken and then explain the simulation results. The solid lines in Figure 4.1(b) shows routes taken for two connections in a 6x6 grid. The interference is reduced by the separation at the middle of the connection. In Figure 4.1(b), it can be seen that two connections are coupled at each edge of the grid, thus leading to interference of two connections with each other. Even if one of the connections had passed through the middle of the topology, then there would be interference between three of the connections. The maximum separation can be seen in Figure 4.1(c) too.

The simulation results are for the 6x6 grid shown in the Table 4.1. The rates of the connections are adjusted such that when there are more connections, they each send at a lower rate. It can be seen that there is a significant improvement in the End to End delay, Queue drops and the throughput of the connection. The routes chosen by MCF formulation reduces the contention of the channel, thus leading to an increased success rate of packet transmission, helping nodes to transmit packets faster and reduce average queue size. On the other hand, if the contention success rate is lesser, then the packets accumulate in in the queue leading to packet drops. The decrease

Metric \ Flows	2	4	6
End to End Delay	0.069	0.24	0.58
Throughput	1.11	1.03	1.27
Queue Drops	0	0	0.32

Table 4.2: Static connections in 8x8 Grid

Metric \ Flows	4	6	8	10
End to End Delay	0.71	0.79	0.76	0.61
Throughput	1.11	1.02	1.02	1.07

Table 4.3: Random deployment

of end-to-end delay can also be attributed to the reduction in contention. Table 4.2 shows the ratio of the value obtained from standard routes to that of the MCF formulation in an 8x8 grid. Significant improvement can be observed in end to end delay and queue drops. Overall, the quality of the routing is significantly better than that obtained by DSR. However, the improvement in throughput is not as high as the 6x6 case. We conjecture that this is due to the longer routes that are present in this case. Longer number of hops have higher chances of packet losses, thus reducing the throughput of the connection. This motivates for the understanding of routing coupled with scheduling, which is presented later in Section 4.6.

4.5.2 Random deployment

Table 4.3 shows the results when 100 nodes were randomly deployed in a 1600m x 1600m area and different number of connections were randomly chosen. The end to end delay is considerably lower with the globally coordinated routes. Jitter and Queue drops also observed the same trend. However, the throughput gains are not very significant.

Deeper analysis of these results, has lead us to the following observations. Low level scheduling effects play an important role in defining the effect of interference. Specifically, for some geometric configurations of interfering nodes, 802.11 was not able to successfully arbitrate the medium. In the grid scenarios, these problematic configurations did not arise due to the regular deployment patterns. As a result, in the Section 4.6, we extend the model to take into account some scheduling

effects.

4.5.3 Path Stretch factor

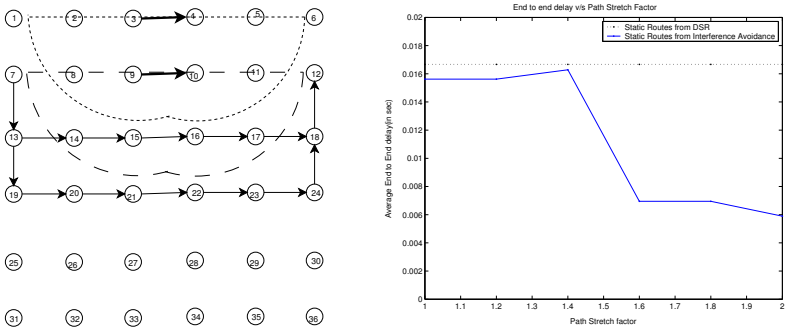

(a) Routes for 7-12 (b) End to End delay study

Figure 4.2: Path Stretch

Figure 4.2(a) shows a scenario where *Path Stretch* reduces contention. There are two one hop connections ($3-4$ and $9-10$) and a connection from $7-12$. The dotted semicircles show the interference area created by the two one-hop connections. The distance between the adjacent nodes of the grid is set such that the node can only reach horizontal or vertical neighbors but not the diagonal nodes. The shortest path from $7-12$ passes through the region which experiences the interference from both one-hop connections. A longer route *[7-13-14-15-16-17-12]* can avoid the interference from the connection *3-4* but not from *9-10*. Let us denote this route by *Path-1*. Further increasing the *Path Stretch Factor* would enable the route *[7-13-19-20-21-22-23-24-18-12]* which can avoid interference from both the one-hop connection. Let this route be denoted by *Path-2*.

A larger grid with a realistic interference range was constructed and the effect of the path stretch factor was observed in a similar scenario. The connection rate was adjusted such that there are no Queue drops. The end-to-end delay study in Figure 4.2(b) shows that when we increase the value of *Path Stretch Factor*, there is a significant decrease in the end-to-end delay. Even though the number of hops of the connection is increased, a reduced interference route would improve the end-to-end delay. Similar improvement was also observed in the jitter too.

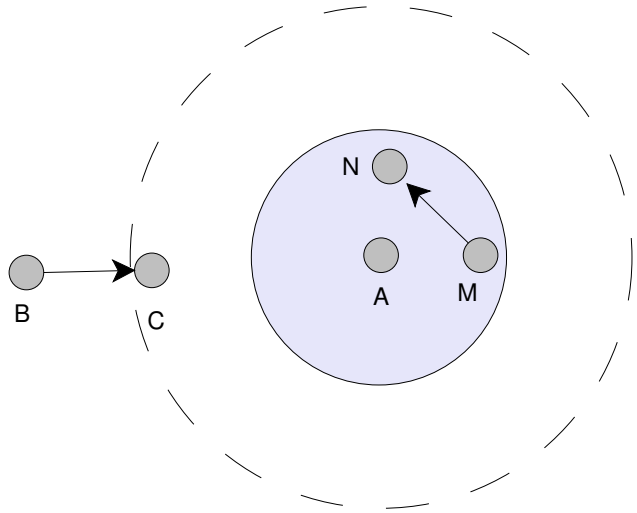

Figure 4.3: An example illustrating the effect of scheduling

4.6 Incorporating the Effect of Scheduling

In this section, we identify the drawbacks of a pure interference aware formulation under practical schedulers and propose an extention to the model to consider scheduling and interference issues. We henceforth refer to the formulation described in Section 4.3 as *Interference Aware (IA)* formulation.

4.6.1 Motivation

The goal of the IA formulation is to route the packets along a path with least interference. Tables 4.1, 4.2 and 4.3 show the results of the formulations. It can be seen that the throughput of the IA formulation is considerably greater than that of DSR for sparse traffic scenarios. However, as the traffic in the network increases, there is a decrease in the throughput gain. In sparse traffic scenarios, *non-interfering* regions are available for the optimizer to take advantage of. As the number of connections grow, it is harder to find completely *non-interfering* routes. In such cases, IA formulation chooses the path with the least interference.

Consider Figure 4.3 where there is an active link between nodes $B-C$ and $M-N$. The shaded circle represents the reception range and the dotted circle represents the interference range of an active node A. The commitment period of node A will include the sum of interference caused by connections $B-C$ and $M-N$. An optimal scheduler would prevent the packet drops by preventing

concurrent scheduling of the conflicting links. Under a practical scheduler like that of IEEE 802.11, the node A will not concurrently transmit the packet when link $M-N$ is active since A can sense the packets from $M-N$. However, node A will fail to avoid transmission when $B-C$ is active because of the *hidden-terminal effect*. This causes a collision at node C.

The IA formulation considers both $B-C$ and $M-N$ to cause interference at node A, and does not discriminate between the interference based on the impact it will have on operation. More specifically, interference where contending links can arbitrate the use of the medium is less harmful than that where they cannot (where packet collisions arise under a practical scheduler). As the number of connections increase, such scenarios become more common, causing higher packet collisions.

The IA formulation calculates the routes based on the commitment period of the nodes. Intuitively, under an ideal scheduler, the throughput of the link will only be a function of the *commitment period* of the nodes. However, in practical CSMA/CA based schedulers, packet collisions and timeouts arise, that degrade the overall throughput of the connection. For example, the channel may be sensed idle, at the source, but a collision occurs at the destination. Thus, the observed throughput will be a function of the available capacity as well as the scheduling interactions. The effect of scheduling on the throughput was demonstrated in Section 2.3.2.

4.6.2 Interference and Scheduling aware formulation

In this section, we address the issue of the formulating the interference aware routing by considering the practical scheduling issues. We henceforth call such a formulation as *Interference and Scheduling Aware(ISA)* formulation. A complete scheduling aware formulation will involve considering the intricate aspects of the scheduler protocol states. We approximate the scheduling characteristics at a higher level so that the complexity of the model is not increased.

Interference is observed at a node j from node i when $\Gamma_{ij} = 1$. The *Protocol model* [47] where the value of Γ_{ij} is set to 1 when the distance between the nodes i and j is lesser than the *Interference Range* was followed in the IA formulation. To account for the scheduling aspects in the ISA formulation, we define that a node i experiences an interference from node j if node j is

within the *Interference Range* but outside the *Reception Range*. Within the reception range, clean handshaking between the nodes makes the interference effect less harmful.

4.6.3 Evaluation of ISA Formulation

Figure 4.4 shows the evaluation of the ISA formulation against the IA formulation and the best routes found by DSR (referred as *Standard Routes*). Different connections with varying sending intervals were evaluated in a 6×6 grid topology. Figure 4.4(a) shows the throughput study. A throughput improvement of around 2x can be observed when the ISA and the IA routes are compared in the 4 connection scenario. While the throughput of the ISA is lesser than the IA routes for the 6 connection scenario, this effect was mainly due to the unfairness problem. In the IA routes, only a subset of the connections were capturing the channel while the others faced starvation, thus reducing the competing connections and increasing the overall throughput of the network. In order to measure the fairness of the flows, fairness index was calculated. The fairness index proposed by Jain et al. [64] is calculated and is as given in the Equation 4.23. The calculation of the fairness index deals with estimating the variance between the optimal throughput and the observed throughput. Since each connection has equal number of hops, we assume the optimal throughput for all the connections are equal. Under such an assumption, the fairness index is given by Equation 4.23 where x_i is the observed throughput of the i^{th} connection and n is the number of connections.

$$\text{Fairness Index} = \frac{\left(\sum x_i\right)^2}{n \sum x_i^2} \tag{4.23}$$

A fairness index of 1 indicates a perfectly fair system where each connection has the same throughput and an index of 0 denotes a unfair system. Figure 4.4(b) compares the fairness index with different routing schemes. It can be seen that the ISA routes are significantly fairer than the ISA routes at high traffic. This shows the the effect of packet collusions and timeouts on the throughput, thus motivating the need to account for scheduling at the routing layer. ISA routes reduce the packet drops across the connections, thus increasing the throughput of all connections, while the IA routes of certain connections does not account for the packet drops, thus may lead to starvation

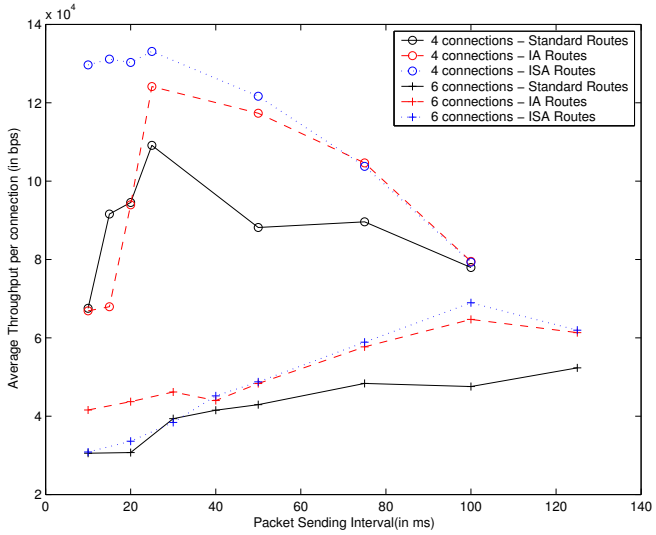

(a) Throughput study

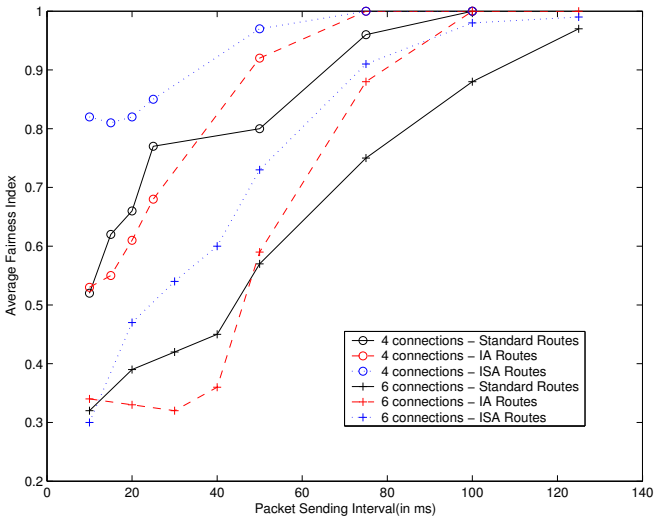

(b) Fairness study

Figure 4.4: Study of Interference and Scheduling Aware Routing

of a subset of the connections.

4.7 Conclusions

In this chapter we proposed a *node-based*, interference-sensitive, extensible multi-commodity flow formulation of the routing problem in multi-hop wireless networks. Multiple connection interaction were studied and *Path Separation Metrics* were abstracted. Approaches to control the *Path Stretch* and the significance of the *Commitment Period* and the *Bottle-neck node* were discussed and accounted to formulate a simple, yet effective, objective function. The extensibility of the model was shown by the ease of tuning the objective function for desired connection parameters. The results of the formulation in comparison to an existing routing protocol show promising improvement that can be achieved in connection health, despite the preliminary state of the model.

Extensions to the model by splitting the problem into sub-problems and removing the integer constraints would enable solving denser networks in lesser run-times. An extention of the model in this direction is proposed in Chapter 7.

The effect of scheduling is not completely integrated with the routing models in the literature. Existing routing models either assume the presence of perfect globally coordinated scheduling or ignore its effect. While scheduling models that characterize the practical CSMA protocols have been studied [16,18,40,41,118], this has not been accounted in routing models. A model to account for scheduling effects in routing decisions is discussed in Chapter 5.

The ultimate goal of this work is to develop distributed protocols that achieve more effective routing than pure greedy approaches. This is also a major thrust of our future research.

Chapter 5

Scheduling Aware Routing Model

Scheduling effects play a large role in determining link capacity. In Chapter 2.3 (see Figure 2.3(a)), we showed that under high interference, scheduling effects play a determining role in the observed capacity of a link. Thus, ignoring the effects of scheduling, as we have done so far, significantly compromises the quality of the routes that are derived by the framework.

This chapter models the scheduling interactions and incorporates them into the network-flow based routing model. We first formulate a light-weight scheduling model to account for capturing the detrimental MAC interactions. Based on this knowledge, the routing model excludes the links that have destructive relationships to calculate a scheduling aware routing configuration.

5.1 Introduction

Network Flow Models of Multi-Hop Wireless Networks have important applications. MHWNs, including mesh networks, ad hoc networks, and some sensor networks, are emerging as important components of an increasingly ubiquitous and wireless world. Network flow models of MHWNs have recently been developed to allow analysis of capacity and and optimization of routing [63, 77]; the disseratation also proposes two such models in the Chapters 4 and 7. Such models can be applied to analyze how far existing routing protocols, which are heuristic and greedy in nature, are from near optimal routing obtained with global knowledge and coordination among the connections. Further, they can be directly applied to traffic engineering and QoS for static

MHWNs. Moreover, the insight gained from these models can be used to better understand how to build effective protocols for more dynamic MHWNs.

However, existing models are limited, especially in how they model interference. While the initial efforts in this area make significant contributions, they make simplifying assumptions that limit their ability in finding effective solutions. Most important among the limitations is the approach to modeling interference, which does not take into account the effects that arise in a CSMA (Carrier Sense Multiple Access) MAC protocol. Instead, the existing models ignore the MAC effect or assume the presence of an omniscient scheduler. We show in Section 5.3 that MAC level interactions play an important, sometimes defining, role in determining link capacity, especially under high interference; ignoring their effect leads to inaccurate characterization of solution quality, which in turn produces inefficient solutions.

Detailed models of CSMA throughput may offer a solution; however, they are not suitable in this context. The problem of estimating throughput for CSMA networks is well researched problem [16, 18, 40, 41, 118]. Available models typically estimate the link throughputs for a given network configuration (including the routes). Thus, they may be suitable for our purpose: as the solver considers candidate solutions, each may be evaluated using the CSMA models. Unfortunately, they are often computationally expensive, making it difficult to use them as part of an iterative optimization process that evaluates candidate solutions to converge on near optimal routing configurations. In addition, many of the models use unrealistic simplifying assumptions. We discuss these models in more detail in Section 5.2.

The contribution of this study is a lightweight constructive model of the effect of scheduling on link quality, and its use to improve interference modeling in network flow models. The model, presented in Section 5.4 focuses only on the effect of scheduling. While we use a similar model of the network, the formulation is not iterative, allowing much faster solution time. Further, the model improves on the scheduling component of the CSMA models in a number of ways: it is link-based, rather than node-based; it uses Signal to Interference and Noise Ratio (SINR) physical model, rather than the simplified protocol model assumed by existing works [47]; and it does not use assumptions such as exponential distribution on packet transmission. The

integration of the scheduling model with a network flow formulation provides for the first time accurate accounting for the effect of interference in network flow models (Section 5.5). We show in Section 5.6 that the scheduling estimates are accurate, and the derived routes from the integrated model achieve large improvements in performance over the those from the model using aggregate interference metrics only. Finally, Section 5.7 presents concluding remarks.

5.2 Related work

In this section we overview related work, organized into two areas: (1) network flow models for MHWNs, and how our work improves on them; and (2) CSMA models of MHWNs and why they are not directly usable for improving network flow models.

5.2.1 Network Flow Models

Our work is motivated by recent efforts that use network flow models, extended to account for interference, to model the behavior of MHWNs [63,77,81]. Network flow models play an important role in wired networks in traffic engineering decisions [104]. These models specify the connectivity in the network, including the bandwidth of the links, and the connections in the network. The linear programming formulation is then solved against an objective function such as maximizing throughput, to obtain an effective routing configuration. The wireless models must account for the effect of interference on the wireless channel. The existing formulations do not account for the effect of scheduling on how contending links interfere. The primary contribution of this work is to improve this limitation, by incorporating more accurate characterization of link quality that takes into account the effect of scheduling.

The goal of the formulations by Jain [63] and Kodialam [77] is estimating the capacity of given scenarios. Further, they focus mostly on single connection scenarios. The formulation is node based whereas, in practice, the MAC level interactions occur at the granularity of links: two links with the same source exhibit different behavior. Finally, they use a physical model with a fixed interference range, which cannot account for the effect of capture. For these reasons, we extend our previously developed formulation which addresses these limitations [81]. It models a multiple-

connection network using a multi-commodity flow framework, and allows derivation of near optimal routes with regards to a user defined objective function. However, like the other formulations, this model uses aggregate metrics such as total interference power or expected channel busy time to model interference; it does not account for the effect of scheduling, which is the objective of the work in this study.

It is interesting to consider the relationship between traffic engineering via the network flow models and routing in the context of MHWN. The first generation of routing protocols in MHWNs used hop-count as the path quality metric. Hop count does not account for link quality, which can vary significantly due to the effect of interference as well as wireless propagation. Draves et al [30] compare various link quality metrics and conclude that expected number of retransmissions (ETX) [25] is the most effective measure in their experimental static network. ETX tracks transmission delivery ratio: packets are lost due to transmission errors or collisions. While there is indirect coordination between interfering connections, there is no explicit coordination; the network may oscillate between inefficient states. The problem of measuring the link quality dynamically is also complex (e.g., link quality varies with packet size and transmission rate). Moreover, the overhead for dynamically tracking the link and path quality has to be considered. For these reasons, experimentally, the advantage over hop based routing is modest.

5.2.2 CSMA Models of MHWNs

Modeling the operation of a CSMA based medium access protocol in a multi-hop wireless network is a classical problem (e.g., [16, 118]) and remains an area of active research (e.g., [18, 40, 41]). Existing models estimate the throughput of a network with a given routing topology –they cannot be used directly to derive routes. However, they could apply them as a fitness function to test solutions within an optimization problem that searches for effective routes. Unfortunately, the complexity of the existing models make them extremely computationally demanding, making the cost prohibitive. Thus, the goal of work is to come up with light-weight approach to account for the effect of scheduling.

Our approach builds on the classical model of the network introduced by Boorstyn et al [16]. In

this model, groups of senders (cliques) that can transmit concurrently are identified. A state model of the network is then constructed where each state represents the set of currently active senders. A transition from one state to another with one more sender can occur as a new transmission starts if the new sender belongs to a clique with the other senders in the current state. Similarly, a transition to a state with one less sender can occur if a sender finishes the current transmission. Balance equations on state transitions can be formulated, and an iterative solution used to estimate edge probability, and therefore the throughput obtained by each source. This iterative solution is the reason for the computational complexity of these models.

The early models use unrealistic assumptions such as perfect capture (no collisions), Poisson traffic, packets are discarded if the medium is busy, as well as others. They also model a generic CSMA protocol that is quite different from bi-directional protocols such as IEEE 802.11. Recent studies [18,40,41] improve many aspects of the original model and tailor them towards IEEE 802.11. These models predict the link quality by considering the available capacity of the links *and* the scheduling effects. However, the core of the approach remains an iterative solution of the balance equations. In addition, some assumptions on the interference and traffic remain.

Our work focuses on estimating the effect of scheduling on a given link assuming saturated traffic. The proposed model significantly reduces the complexity of the existing models by avoiding the iterative estimate of the state probability. Since we are not using the state probability to estimate throughput (we are using it to give weights to different cliques to estimate collision probability), a precise estimate is not critical. Moreover, the proposed model also improves on a number of limitations of the existing formulations with respect to scheduling. For example, it approaches the problem from a link-based view of interference, and uses a more accurate wireless propagation model. By considering interactions at both the source and destination, we are able to achieve a more accurate characterization of the effect of scheduling, especially in a two-way handshake protocols like IEEE 802.11. The more accurate propagation model allows accounting for capture and the effect of combined interference.

5.3 Motivation

It is well known that CSMA protocols such as IEEE 802.11 are prone to hidden terminal problems, depending on the relative location of contending links, leading to collisions [13, 42]. Transmissions are lost, and backoff values are increased, leading to significant underutilization of the available channel time. Since network flow formulations of MHWNs ignore these effects, they may overestimate the link quality. In this section, we use a simulation study to demonstrate this effect. We also show that the normalized efficiency (achieved throughput relative to ideal throughput) correlates with the percentage of collisions suffered by each link. This observation motivates the use of our approach, which estimates collision probability for each link, as a measure of the expected normalized efficiency for the link.

We simulate different sets of 144 uniformly distributed nodes with 25 arbitrarily chosen *one-hop* CBR connections. The aim of this experiment is to show how the performance achieved by these connections correlates with existing capacity metrics. Since the analysis targets MAC level interactions among interfering links, it does not require that the scenario be made up of multiple-hop connections–we are targeting link layer, rather than end-to-end phenomena.

Intuitively, under an ideal scheduler, the throughput of the link depends mainly on the available transmission time. For example, the channel may be sensed idle, at the source, but a collision occurs at the destination. Existing MHWN modeling studies (e.g., [63, 76, 81]) and many protocol efforts (e.g., [6]) use local estimates of interference to estimate capacity. Section 2.3.2 demonstrated the effect

5.4 Modeling Scheduling Effect in IEEE 802.11

In this section, we develop a lightweight model for estimating the effect of MAC scheduling on link quality by predicting the expected percentage of dropped packets. The network is represented as a graph $G(V, E)$ where V is the set of all the nodes and E is the set of active links. Let Θ_{ij} be a $n \times n$ matrix, representing the signal strength observed at node j for node i's transmission. This can be derived by geometric location of nodes or by experimental observations. Let T_{RX} represent the

Receiver sensitivity and T_{SINR} represent the SINR threshold above which a signal can be captured. W represents the Gaussian white noise.

We make the following assumptions: (1) Physical layer obeys the SINR model as explained in Section 2.2.1; (2) Transmission by the source is received instantaneously (zero propagation delay); and (3) The senders always have packets to send (saturated traffic). We assume saturation traffic for two reasons: (1) The impact of collisions is highest under high interference; and (2) the link busy time is estimated from the network flow formulation, and not from this component of the integrated model. The integrated formulation can give appropriate weight for the effect of scheduling depending on the actual degree of interference.

The proposed approach builds on the Boorstyn model [16] which was reviewed in Section 5.2. However, it differs from this work and others in literature [18, 40, 41] by considering a signal to interference and noise ratio (SINR) model, as opposed to the idealized protocol model where every source has a fixed interference range. As a result, our model takes into account effects such as capture, and cumulative interference from multiple transmitters.

We model the IEEE 802.11 protocol with RTS-CTS handshake to demonstrate the modeling approach. Although the use of RTS-CTS packets is optional, it represents the more challenging case to model. We believe the approach –identifying and modeling the occurrence of collisions– generalizes to other contention based medium access protocols. The problem is broken into the following parts: (1) Constructing the State Model via identification of the *Maximal Independent Contention Sets* (MICS); (2) Estimating the collision occurrence within each set; (3) Estimating the frequency of activation of each set; and (4) Combining the above estimates into a link quality estimate. In the remainder of this section, we discuss these steps in detail.

5.4.1 Constructing the State Model

This portion of the model is similar to the classical Boorstyn's Markov state model construction, with the exception that it is link-based rather than source-based. The first step in constructing the state model is to identify the set of edges that can be active concurrently, which we call Independent Contention Sets (ICS). A Maximal ICS (MICS) is an ICS to which no other edge can be added

without breaching independence of the sources (a maximal set of ICS).

Identifying all the MICS is an instance of the maximum clique graph problem which is known to be NP-hard. However, efficient approximate techniques exist for unit-disc graphs which arise in MHWNs [49]. We used an iterative heuristic [63] for finding independent sets. The states in the Markov model of the network consist of the power sets of the MICS.

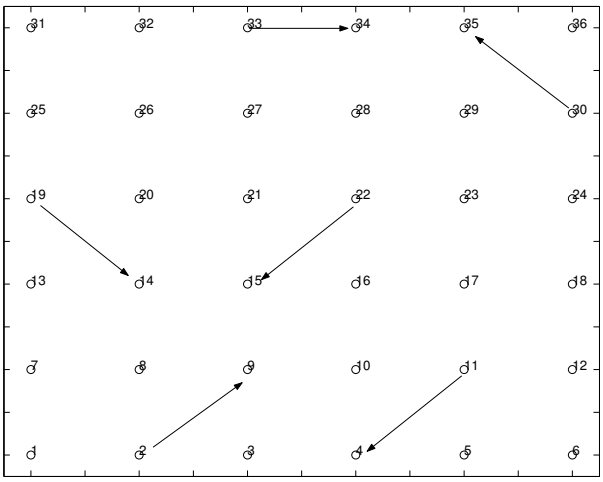

Figure 5.1: An example scenario

Figure 5.1 shows a scenario of 4 one-hop connections. The MICS diagram is shown in the same figure. Each node in the figure represents an active edge in the scenario. The hidden terminals that cause packet timeouts are shown by a directed arrow. For example, in the above figure links (A, B), (G, H) and (E, F) are in the same MICS (denoted by MICS-1); and, (G, H) is a hidden terminal for the link (E, F) in MICS-1.

5.4.2 Estimating Timeouts in each MICS

The saturation traffic assumption allows us to focus on the MICS states, rather than all the states in the model (eliminating, ICS that are not MICS). Collisions occur due to interactions within an MICS; transmissions across different MICS' are prevented by the protocol, with the exception of concurrent transmissions that arise due to two sources sensing the medium to be idle and transmitting concurrently. Truly concurrent collisions are a minor effect in randomized protocols (less than

3% of collisions in our experiments); moreover, such collisions cannot be prevented by the routing protocol, so they are immaterial for our purposes.

In this component, we consider each MICS separately and attempt to estimate the packet timeout percentage given the physical layer model. In an 802.11 RTS/CTS handshake, the source may perceive a packet collision when: (1) it does not receive a CTS from the destination (an RTS timeout); or (2) it fails to get an ACK for the DATA frame (an ACK timeout).

Identifying RTS Timeouts

An RTS timeout occurs for one of three reasons: (1) an RTS collision; (2) a receiver not responding to the RTS due to its physical or virtual carrier sensing being active; or (3) a CTS collision. In IEEE 802.11, CTS collisions are improbable since the channel at the sender is idle before the RTS, and because CTS gets priority over other transmissions by virtue of a shorter inter-frame separation period before transmission. Hence, we focus on the first two causes.

In a given MICS C, an *Unsafe Link* (s_1, d_1) for a link (s, d) is a link whose transmission at source (s_1) may create a busy channel at the receiver d (the first condition of Equation 5.1) or cause an RTS collision (the second condition). These two cases correspond to the two causes for RTS timeouts discussed above.

$$\mathrm{U}^{C}_{(s,d)} = \Big\{(s_1, d_1) \mid (s_1, d_1) \in C, \\ \Theta_{s_1 d} \geq \mathrm{T}_{RX} - W \text{ or } \frac{\Theta_{sd}}{\Theta_{s_1 d} + W} < \mathrm{T}_{SINR}\Big\} \tag{5.1}$$

Identifying ACK Timeouts

ACK timeouts, which are caused by collisions affecting DATA or ACK packets, are costly because they indicate the loss of the potentially long DATA packet. For the same reasons that CTS losses are improbable, ACK losses are also improbable. ACK timeouts are mostly due to DATA packet collisions.

The basis for modeling ACK timeouts is to determine the links (s_1, d_1) that can corrupt an ongoing DATA packet by a transmission from s_1 to d_1 (RTS or DATA packets) or from d_1 to

s_1 (CTS or ACK packets). DATA collisions due to interfering DATA packets are rare since such transmissions only happen after successful RTS-CTS exchange. The CTS and ACK transmission have to be considered separately as the CTS transmission happens after sensing that the channel is not busy (Clear Channel Assessment (CCA)), whereas the ACK transmission happens without a CCA.

We define a set of links in a MICS C that can corrupt the DATA transmission of the link (s, d) by initiating an RTS, CTS or ACK by $\mathrm{A}_C^{(s,d)}$. These set of links are derived in a fashion similar to derivation of the *Unsafe Edges*[1].

A DATA packet can also be dropped due to cumulative interference from multiple links (the longer duration of DATA packet transmission creates a higher possibility of such drops). We are able to detect this effect due to the SINR physical model we use; other models use a fixed interference range and cannot capture this effect [16, 40, 41].

5.4.3 Estimating the Probability of MICS Activation

In this step of the model, we need to estimate the frequency of activation of each MICS. From the previous step, we have a ranking of each link for each MICS it belongs to. Thus, we use the MICS probability to create a weighted average of the rating of each link across the MICS to which it belongs.

We use the saturation assumption to focus on MICS. Let m_C represent the probability that a MICS C is currently active. We observe experimentally that the relative MICS activation frequency correlates with the number of sources that belong to the MICS. The intuition is that with more contending sources, a MICS has a higher chance of one of the sources becoming active first and as a result, blocking MICS to which the active link does not belong from contention. Thus, we approximate the probability of the MICS activation by Equation 5.2. Informally, the amount of time a MICS will be active is proportional to the number of sources present in the MICS. However, with collisions and IEEE 802.11 backoff mechanism, the precise calculation of m_C is challenging. Refining

[1] A detailed derivation of the ACK timeout estimate and related metrics is omitted due to space; it can be found in the following technical report [80].

this probability estimate is an area of future refinement of the model discussed in Section 5.4.5.

$$m_C = \frac{|C|}{\sum_{C' \in \mathrm{M}} |C'|} \tag{5.2}$$

5.4.4 Quantifying Link Quality

In this paragraph, we use the estimates developed in the previous sections to quantify the susceptibility of the links to RTS timeouts and ACK timeouts.

RTS Timeout Metric

Recall from Section 5.4.2 that the *Unsafe links* cause RTS timeouts by two primary events: an RTS collision or a busy channel at the receiver. It can be seen that both these events are mainly caused by the DATA transmission from an unsafe link (we ignore the effect of smaller sized RTS/CTS/ACK packets). If the unsafe link has not yet started its DATA transmission, then an RTS timeout will not occur. Also, a larger number of unsafe links will result in higher chances of RTS timeout. Hence, the above two conditions – the ordering of the link transmissions and the number of unsafe links – need to be accounted for calculating RTS timeout metric.

We define $p_u(k)$ to be the probability that at least one of the k unsafe links of the given link (s, d) will initiate transmission before (s, d). It can be shown that $p_u(k) = \frac{1}{k+1} \sum_{i=1}^{k} (-1)^{(i-1)} \binom{k}{i}$ (please refer to technical report [80] for derivation).

The probability of an RTS Timeout for the link (s, d) in a MICS C is the conditional probability of the unsafe links transmitting before the given link ($p_u(|\mathrm{U}^C_{(s,d)}|)$), given that the MICS C is active (Note that m_C is the probability of occurrence of MICS C). The RTS Timeout metric of a link (s, d) is the sum of such conditional probabilities over all the MICS C that the link belongs (Equation 5.3)

$$\mathcal{R}_{(s,d)} = \sum_{C \in \mathrm{M}, (\mathrm{s,d}) \in \mathrm{C}} p_u(|\mathrm{U}^C_{(s,d)}|) m_C \tag{5.3}$$

ACK Timeout Metric

An estimate for the amount of ACK Timeouts is obtained by accounting for the links that corrupt DATA packet by RTS, CTS and ACK. ACK Timeouts due to cumulative interference is also accounted by estimating the interference by multiple links of the same MICS. Let $\nu_C^{(s,d)}$ be the probability that the interference from the links of the MICS C corrupts the DATA packet. We calculate the $\nu_C^{(s,d)}$ based on observing the cumulative noise from the sources of the MICS (not shown due to space; please refer to the technical report [80]).

The fraction of ACK timeouts depend upon the probability of the link (s, d) winning the contention (represented by $w_{(s,d)}$). This can be directly derived by considering the set of all MICS that (s, d) belongs. Equation 5.4 represents the rating that a link (s, d) is susceptible to an ACK timeout considering the above factors.

$$\mathcal{D}_{(s,d)} = \frac{1}{w_{(s,d)}} \sum_{\forall C \in \mathrm{M}} \left(m_C \; p(|\mathrm{A}_C^{(s,d)}|) + \nu_C^{(s,d)} \right) \tag{5.4}$$

We henceforth refer to the timeout ratings ($\mathcal{R}$ and $\mathcal{D}$) as *Interaction based Link Rating (IBLR)* metrics. IBLR metrics along with the interaction vectors (U and A) will be used in the routing model to identify and constrain destructive link interference.

5.4.5 Discussion

A limitation of the current formulation is that we do not account for the effect of timeouts due to the virtual carrier sense being set at the receiver (around 17% of observed timeouts were due to this effect). Modeling this effect requires estimating: (1) Packet capture ability of the node under a given MICS (which cannot be assumed to be a constant "reception threshold" as done in Protocol Model of interference); (2) Distinguishing the timeouts due to "False VCS" where an RTS packet turns on the VCS at a node and fails to followup with the DATA packet (due to RTS timeout). This effect is referred as "Gagged Node Situation" in [33]. A deeper study of VCS related effects is an area of extension of the model. We also note that for cases when RTS/CTS is not enabled,

this effect is not present, and more accurate modeling of the quality is possible.

Precise formulation of probability of occurrence of a MICS (m_C) is a challenging problem due to the dynamic nature of MICS activation which depends on several factors.We are pursuing a more accurate constructive model of MICS probabilities based on the probability of link activation. However, a more accurate model is more complex; the current approximate solution allows faster searching of the optimization space.

5.5 Scheduling-aware Routing Formulation

Algorithm 4 Algorithm for SAR

1: **while** iterationCount ≤MAX_ITER **AND** constraintsAdded = true **AND** *Interference metric* is acceptable **do**
2: Calculate routes by Network Flow (*Netflow routes*)
3: Calculate *Interference metric* for ALL the routes
4: Evaluate the routes by IBLR metric
5: Calculate *Link quality metric* link qualities considering routing behavior
6: constraintsAdded = Check for mutual excluding of conflicting links and add constraints
7: *CIM* = Weighted measure of *Interference metric* and *Link quality metric*
8: **if** *Netflow routes* is the best route seen **then**
9: *best_routes* = Update the best routes
10: **end if**
11: **end while**
12: **return** *best_routes*

In this section, we integrate the scheduling model into our previously developed multi-commodity network flow formulation [81]. Algorithm 4 briefly explains how the integrated framework works. We use the network flow model to provide an initial interference aware routing configuration, which we refer to as *Interference-Aware Routes* (IAR). The scheduling component evaluates these routes and finds poor quality links, and the links which cause them to have collisions (line 5 in Algorithm 4). This information is fed back into the network flow model in the form of additional constraints, allowing the solver to avoid using conflicting links (line 6 in Algorithm 4). The updated network flow problem is solved to obtain another candidate configuration (*Netflow routes*) and the procedure is repeated.

At each iteration, the overall quality of this routing configuration *Configuration Interaction Metric (CIM)* is computed. CIM serves as the fitness function of each configuration, which can

	$\mathcal{R}$	Interference Level	Busy Time	SINR
R	0.819	-0.121	0.655	-0.059
ρ	0.872	0.183	0.529	-0.404

Table 5.1: Correlation of RTS Timeouts

	$\mathcal{D}$	Interference Level	Busy Time	SINR
R	0.916	-0.071	0.262	-0.061
ρ	0.899	0.110	0.320	-0.558

Table 5.2: Correlation of ACK Timeouts

be compared against other routing configurations. To compute CIM, the route quality obtained from the network flow optimization problem are combined updated with the scheduling derived link quality metric to obtain the overall quality. In addition, since drops at links closer to the destination are more costly than drops closer to the source, we bias the link quality to attempt to select more stable links as we get closer to the destination.

The iterative routing and link quality estimation process terminates when either no constraints can be added (since all the links have the IBLR rating lesser than a given threshold) or when the quality of the interference based metrics alone drops below a certain threshold (currently we use 20%) of the initial IAR routes. The configuration with the best CIM is chosen to derive the **Scheduling-Aware Routes (SAR)**.

5.6 Experimental Evaluation

We use the QualNet simulator [105], which is a commercial simulator with state of the art physical propagation and MAC models. We use the *SINR Threshold* propagation model and 2Mbps data rate. The transmission power and receiver sensitivity is set to 24.5 dB and -73 dB respectively and the standard IEEE 802.11 MAC parameters are used.

The first experiment evaluates the success of IBLR metrics in estimating timeouts. We use a scenario with random placement of 144 nodes in a 1600m×1600m area with 25 one-hop connections. We use 10 different scenarios for a total of 250 active links.

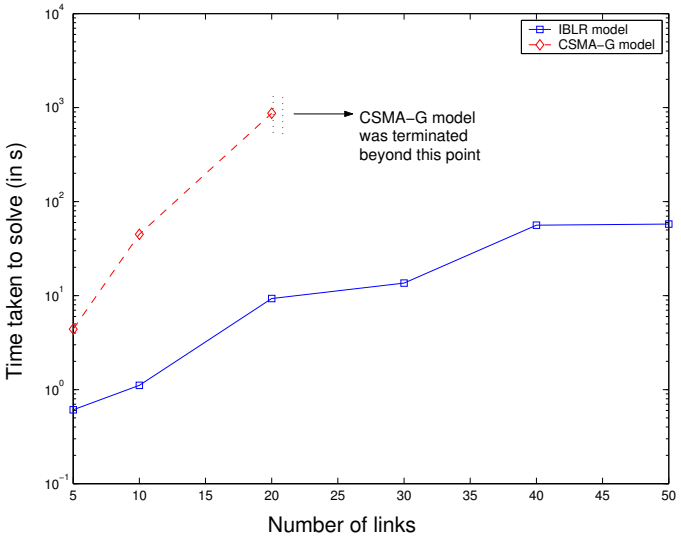

Figure 5.2: Timing comparison

Tables 5.1 and 5.2 use correlation (R) and Spearman's Rank Coefficient (ρ) to measure how successfully different interference metrics predict timeouts.[2] We evaluate the IBLR RTS Timeout ($\mathcal{R}$) and ACK Timeout ($\mathcal{D}$) along with the aggregate metrics in Tables 5.1 and 5.2. *Interference Level* was computed by measuring the interference at the destination of each link by all the active sources. The *Busy Time* is calculated as the amount of time the destination of a link was busy due to interfering traffic (measured in simulation). The ratio of the signal strength to the cumulative interference by all the other sources was used to calculate *SINR* metric. There is a strong correlation between IBLR and simulation result while the aggregate interference metrics which are used in existing models [63, 77, 81], correlate poorly; they cannot predict the effect of scheduling.

The argument against using using existing accurate CSMA models for estimating the impact of scheduling is their high run-time. Figure 5.2 compares the time taken to evaluate a given network by the IBLR formulation and a recent accurate CSMA throughput model proposed by Garetto et al [41] (*CSMA-G*). CSMA-G estimates the expected throughput of each link using an iterative numerical process. As a result, its runtime grows very quickly with the size of the problem (note

[2] ρ is used to measure the ranking order correlation which is especially helpful in the absence of a linear relationship. R and ρ can take any real values between -1 and 1. A value of 1 indicates a perfect correlation and a value of 0 indicates independence of the two values. Negative values indicate inverse relationship.

that the y-axis is log-scale). CSMA-G model was terminated if it failed to complete within 2 hours. In contrast, IBLR computation is lightweight, making it suitable for use in a network flow optimization framework.

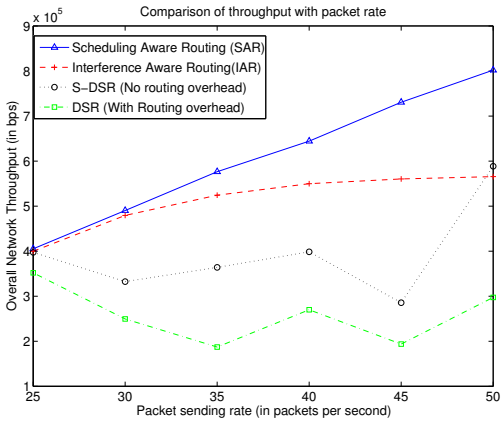

(a) Throughput

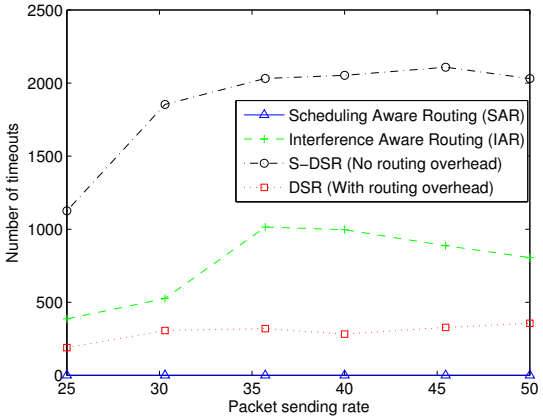

(b) Timeouts

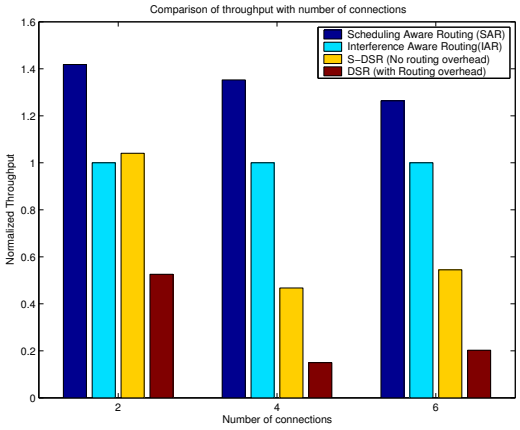

(c) Effect of multiple connections

Figure 5.3: Study of connection parameters v/s packet sending rate in a Grid topology

In the next experiment, we evaluate the effectiveness of scheduling aware routes (SAR) obtained using the approach proposed in this study. First, we compare SAR against the routes obtained by a conventional routing protocol (DSR [65]). Since SAR uses static routes, to provide a fair comparison that eliminates routing overhead and dynamic effects such as false disconnections [125], we allowed DSR to use static routes (selecting the most commonly used route found by DSR). We refer to such routes as *S-DSR*. The need for a scheduling metric in conjunction with standard interference

metric is shown by comparing SAR with an Interference-only-aware routes(IAR).

We first demonstrate the effectiveness of SAR in a 10×10 grid topology. The width of the grid is 1000m and the transmission range is around 390m. Two connections are placed on the opposite edges of the grid. Figure 5.3(a) compares the average throughput of the connection for varying packet sending rates. The scheduling effects play a less important role under lower traffic as concurrent transmission between unsafe links is less likely. Under high packet sending rates, it can be observed that the throughput of the scheduling aware scheme is significantly higher than the other schemes. The average throughput of the S-DSR is lesser than the IAR and SAR routes. The throughput of the DSR and S-DSR fluctuates widely over different seeds. In around 30% of the cases, the best routes from S-DSR performed better than the IAR routes. DSR treats packet drops (after 4 ACK timeouts, or 7 total timeouts for the same packet) as an indication of broken path and switches to another path. Thus, the most used path in S-DSR are likely to have relatively few timeouts which will allow them to be used for a long time without packet drops.

In this regular setting, SAR found routes with no destructive scheduling interactions, leading to zero packet timeouts (Figure 5.3(b)). An improvement of around 50% was observed in end-to-end delay. Next, we analyze the effect of cross connection interference. The number of connections in the above grid topology is increased, thus increasing the number of competing links. Although SAR cannot find a configuration with perfect scheduling, it chooses the configurations with low scheduling conflicts while maintaining interference separated routes. The normalized throughput is shown in the Figure 5.3(c).

We now examine the performance of these schemes in 10 random scenarios with 64 nodes placed in 1000m×1000m area. Six connections were randomly selected. Figure 5.4 shows the throughput improvement of SAR over other protocols (normalized with respect to IAR throughput). An improvement of 33% over IAR and a greater improvement over the DSR protocol under high loads was observed. Notable improvements in other metrics like end to end delay and packet drops were also observed. Detailed results is available in the technical report [80].

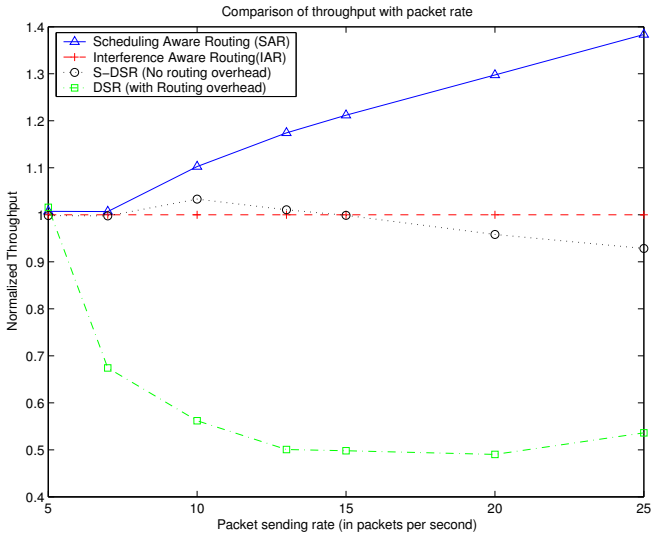

Figure 5.4: Throughput study in random scenarios

5.7 Concluding Remarks

Aggregate metrics of link capacity such as channel busy time do not account for the effect of scheduling. It is known that in CSMA networks, scheduling plays a critical role in how interference is manifested. Thus, it is desirable to avoid links that experience mutually destructive interaction. We used this observation to develop a methodology for rating link quality based on their interactions with other links. We show that these estimates correlate strongly with packet drops. We integrate the developed model in a network flow formulation of traffic engineering in static MHWNs. We show that capturing the scheduling effects leads to considerable improvement in performance of the derived routes.

In our future work, we wish to explore the refinement of the *Configuration Interaction Metric (CIM)*. Formulating an accurate CIM have to address many challenging issues. Routing packets over a connection introduces pipelining effect where the links towards the destination carry lesser traffic than the links towards the source. Expressing the traffic-loss that occurs when a packet travels towards the destination due to the scheduling effects is an interesting area of future work.

Another area of future work is to calculate the CIM based on the observed busy time at the source. It was shown in Figure 2.3(a) that the impact of scheduling is minimized when nodes

observe smaller fraction of the busy times. This occurs in scenarios with under-saturated traffic and also due to the above pipelining effect.

Even with proposed approximations, the results indicate significant improvement over traditional interference aware schemes. If these results can transition to realistic environments, they have important implications for mesh network traffic engineering and provisioning. Further, identifying the nature of collisions that influence the quality of the links provides a starting point for distributed algorithms that capture these interactions in a distributed environment.

Chapter 6

Routing Real-time Traffic

In this chapter, we formulate the real-time routing problem in static multi-hop wireless networks as an optimization problem, whose solution is the optimal routes relative to an end-to-end delay based objective. The contribution of this chapter is to change the objectives of the optimization problem from those based on throughput to ones based on delay. Formulating the problem requires estimating the relationship between delay and interference.

The problem is formulated as a mixed integer linear program. The variance of the delay with respect to the aggregate interference measures is empirically studied and a linear approximation is proposed; although more detailed estimates using, for example, queueing theory are possibly, we are not sure whether the structure of the problem remains convex. We show that this formulation yields routes that significantly outperform the best routes obtained by OLSR. Finally, we discuss the applications of such a model both in terms of capacity analysis, on-line algorithms for static scenarios, and extensions to allow the development of distributed protocols that solve the optimization problem.

6.1 Introduction

Real-time traffic is common in MHWNs as real-time events are detected and relayed, or as users access multimedia content on the move. Supporting real-time traffic is significantly more difficult than in wired networks because of the time-varying properties of the wireless channel and the

complex and unpredictable nature of interference among nearby nodes [42].

Existing real-time solutions use local heuristics to estimate link quality or to differentiate traffic based on real-time deadlines(e.g., [53,85]). While such distributed protocols are directly deployable in MHWNs, they use a greedy routing strategies that do not coordinate among competing flows. As a result, they may be unable to find an optimal (or even efficient) configuration for the routes in the network. In this chapter, we formulate the real-time routing problem as an optimization problem whose solution is the routing configuration that optimizes a delay based objective. As such, we are better able to judge the ability of the network to support the required traffic given its deadlines.

While the basic model is centralized, it provides valuable insight into the available capacity of the network and the shape of optimal routes, which can then be used to guide the construction of distributed protocols. It can be also be directly applied as on-line tool for providing QoS guarantees, admission control, or for guiding provisioning decisions for real-time traffic in static MHWNs. Finally, its been shown that such formulations, for example in the context of TCP congestion control, can lead directly to distributed protocols (using the decomposition based approaches) [22].

6.2 Model Formulation

In this section, we describe the classic MCF problem formulation and extend it to account for interference. We develop a heuristic approach to estimate the delay from the level of interference experienced by a link. We the delay estimates then to specify an objective function to minimize the end-to-end delay of the connections in the network. Finally, we discuss how this delay minimization problem can be extended to support real-time traffic.

Assumptions and Notations: This model uses the same the notations as used in the IAR model (Chapter 4). In this paragraph, we briefly recall them for completeness. An MHWN is represented as a graph $G(N, E)$ where N is a set of wireless nodes. E denotes a set of all the edges (i, j) such that node i is able to transmit to node j. Let Γ_{ij} be the coupling (or gain matrix) which indicates how a node i interferes with node j. For simplicity, we assume a two-disk model of interference, where node i can transmit/interfere to/with a node j if its within a reception/interference range;

thus Γ_{ij} is a boolean matrix where an element Γ_{ij} is 1 if node i interferes with node j. Future extensions will explore more realistic interference models, which can be readily expressed in the framework. Let (s_n, d_n, r_n) denote source, destination and the rate of the n^{th} connection. The rate of connection, r_n, is the number of bits to be sent per unit time. Let C be the set of connections and let U be the capacity of the wireless channel. Let x_{ij}^n represent the flow that the edge (i, j) is carrying for the n^{th} connection.

Flow formulation: We start with the classical MCF constraints [7], which specify traffic sources and destinations, as well as edge capacity (we dont present these constraints for space considerations). The formulation is capable of providing a multiple routes for a given connection. However, many applications require a single route from source to destination to reduce the routing protocol overhead and to avoid the multi-path routing side-effects (like packet re-ordering). Hence, we introduce a new constraint to force the use of a single-route for each connection (Equation 6.1). The variable y_{ij}^n is a boolean variable which is set to 1 if the edge carries the traffic for the n^{th} connection and 0 otherwise. Under such conditions, the problem transforms into a integer MCF problem.

$$x_{ij}^n = r_n \cdot y_{ij}^n \quad \forall n \in C, \forall (i,j) \in E \tag{6.1}$$

The key difference in the wireless problem is the impact of interference. Specifically, in the wired problem, the link capacity is constant, and one has only to worry about which flows use what links. In wireless networks, nearby sources interfere and the capacity of an edge in the network graph is a complex function of traffic at other edges. Furthermore, many forms of interference arise (e.g., interference from a hidden node, vs. interference from a node close enough for the MAC protocol to avoid collisions).

Modeling Interference: Capturing the effect of interference faithfully under a realistic physical and MAC protocol is a challenging problem. Precise estimation of interference, even under a simple physical model, requires accounting for detailed scheduling intricacies of the MAC pro-

tocol like IEEE 802.11, which is extremely complex [42]. Computing the sets of edges that are concurrently active under a given MAC protocol is an instance of "Maximal independent sets" graph theory problem, which is NP-hard for general graphs. Moreover, the scheduling effects are a function of the routing configuration (which determines which edges are active), and have to be re-evaluated for every candidate routing configuration. Thus, we target simplified models of interference to reduce the complexity of the solution.

We now describe an approximation model to capture interference. A link (i, j) has interference from a link (a, b) if: (1) the sources interfere with each other, i.e $\Gamma_{ai} = 1$; or (2) the destination of the link can be interfered by another source, i.e. $\Gamma_{aj} = 1$. Hence, the amount of "busy time" an edge (i, j) experiences due to interference is given by Equation 6.2.

$$I_{ij} = \sum_{n \in C, (a,b) \in E, \Gamma_{ai}=1 \vee \Gamma_{aj}=1} x_{ab}^{n} \quad \forall (i, j) \in E \tag{6.2}$$

The total amount of traffic carried by an edge (i, j) is represented as *Signal* ($S_{ij} = \sum_{n \in C} x_{ij}^{n}$). Thus, the channel as viewed from a link (i, j) is busy for the duration of its transmissions in addition to the duration of interference from nearby links (that is, $S_{ij} + I_{ij}$); we call this quantity the *commitment period* of link (i, j) (denoted by $\mathcal{A}_{ij}$). For feasibility, the commitment period should be less than the capacity of the wireless channel (U). For the edges which do not carry any traffic (passive edges), the commitment periods are immaterial for the routing objective. Thus $\mathcal{A}_{ij}$ is $S_{ij} + I_{ij}$ for active edges, and zero for passive ones.

Before formulating the objective function, we seek to establish the relationship between the commitment period and delay. We assume that all flows are equally important to simplify the presentation. However, direct extensions to differentiate flows based on their respective deadlines are possible. The commitment period of an edge approximates the amount of delay over an edge since it represents the channel reservation at the link.

In order to verify this, we simulated 100 random scenarios in a 1000x1000 MHWN with 2 Mbps capacity. We varied the number of one-hop connections in the network to alter the amount of

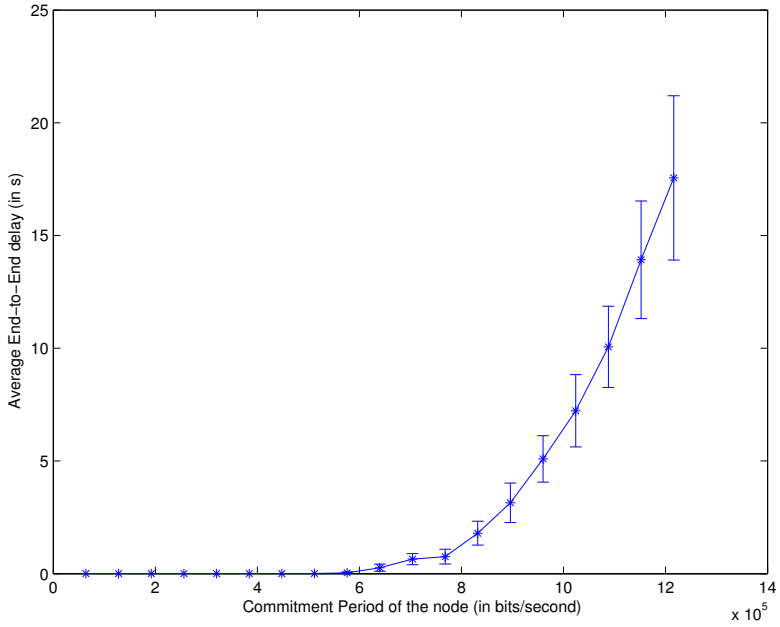

Figure 6.1: Variation of End-to-End delay with Commitment Period

traffic on the channel. The commitment periods of different active edges and the end-to-end delay of the packet as observed in simulation are plotted in Figure 6.1. It can be seen that the average delay almost monotonically increases with the calculated commitment period, which suggests that commitment period can be used as an approximation for the end-to-end delay. The delay is very small (orders of transmission time of the packet) for commitment periods until 30% of the capacity, after which the delay grows acutely (approximately an exponential curve).

The threshold point at which there is a sharp growth in the delay is also a function of the packet sending rate and the number of interferers. Capturing such variances would require precise characterization of the interference with respect these parameters. An additional problem is to represent them as a linear/convex equation in an optimization problem. However, the approximately monotonic increase in the delay with commitment period can be assumed for simplification and we use this relationship for formulating the objective function. In the future work, we want to explore the use of Gallager's formulation [38, 122] for minimum delay routing in MHWNs.

Objective function:

The total delay of a connection over all the hops can be represented as a the sum of the commitment periods.

$$\text{Delay for Connection } n = \sum_{(i,j)\in E} \mathcal{A}_{ij}^{n}$$

Minimizing the delays for all the connections will convert the formulation to a multi-objective function, which is harder to solve than a single objective function. Hence, we convert the objective function to minimize the sum of delays of all the connections (Equation 6.3).

$$\text{Minimize} \sum_{n\in C,(i,j)\in E} \mathcal{A}_{ij}^{n} \tag{6.3}$$

A real-time routing model can be directly extended from the above delay-sensitive routing formulation. The real-time delay deadlines for each connection can be mapped back to the respective commitment period deadlines by means of the empirical function shown in the Figure 6.1. Hard-real time deadlines can be added by constraining the delay on each connection to its commitment period deadlines. For soft-real time guarantees, a dual-optimization problem can be formed to account for the difference between the expected delay and the deadline. We wish to pursue this direction in our future work.

6.3 Simulation Results

In this section, we the evaluate the developed model against OLSR, an optimized and widely used routing protocol for ad hoc networks [24]. The Linear Programming formulation for the model was solved using the CPLEX solver [27]; the model instance is derived automatically from the scenario file (which changes the number of nodes and edges, the sources and destinations, as well as the Interference matrix Γ). The Qualnet simulator [105] was used to measure the performance of the proposed schemes under the IEEE 802.11 protocol.

We first demonstrate the shape of delay optimized routes using representative scenarios. We consider a 6x6 grid topology. CBR connections resembling VoIP G.711 codec (160 byte packets at

20MS interval) is simulated [87]. Each scenario is run for 20 random seeds and the 95% confidence interval is shown. In order to provide a fairer comparison that eliminates the dynamic routing overheads and route flapping from OLSR, we extract the set of *most used* route that was discovered by OLSR for each connection and use it under static routing. Such routes are referred as *Max used OLSR routes*.

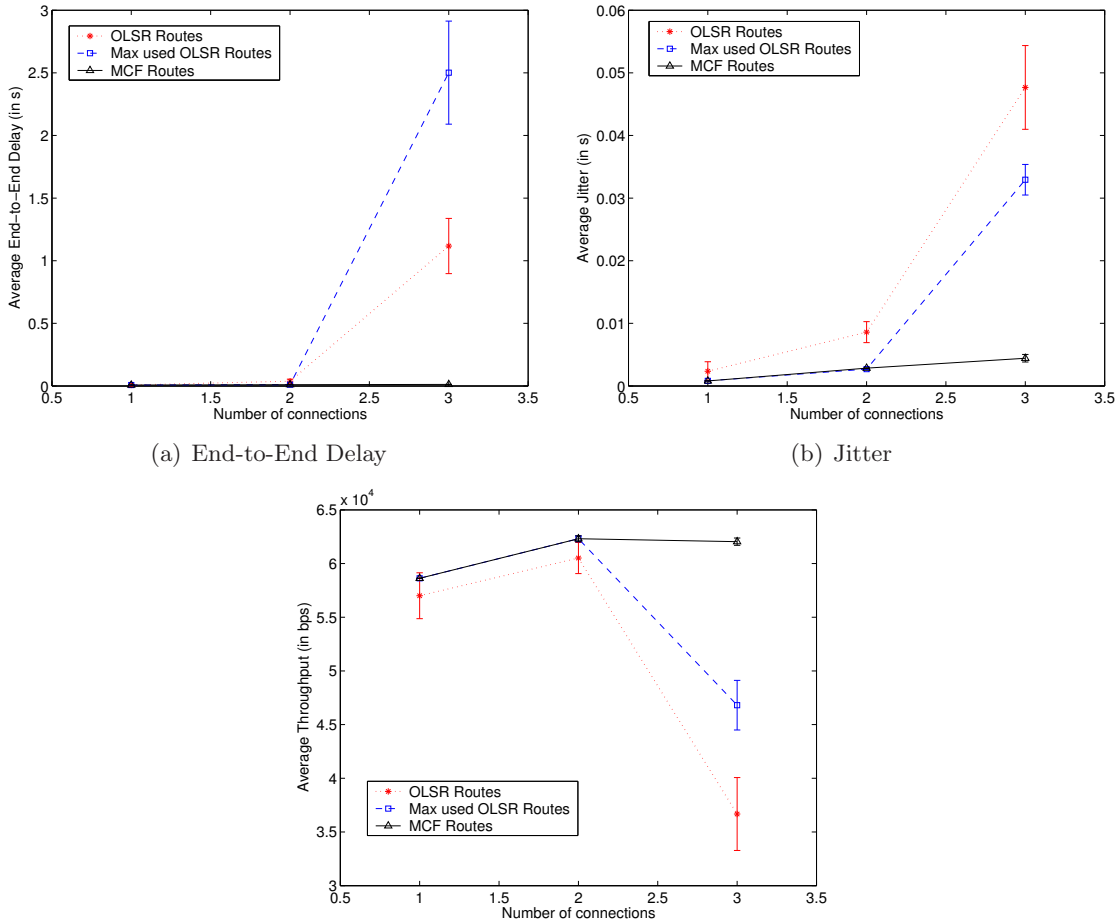

(a) End-to-End Delay

(b) Jitter

(c) Throughput

Figure 6.2: CBR traffic – Grid scenario

In this first study, the connections are separated such that the source and destinations are 5 hops away from each other. We increase the traffic (and therefore interference and delay) by adding more connections. Figure 6.2 compares the end to end delay, jitter and throughput, achieved by the formulation to those of OLSR. It can be seen that the all the protocols perform equally well

under a lightly loaded network. As the number of connections increases above 3, we see that the formulation routes (MCF routes) outperform the other two in all the performance metrics. The exponential increase of delay due to slight variations in commitment periods is pronounced in 3 connection scenario where orders of magnitude difference in end-to-end delay is observed between the *Max used OLSR routes* and the MCF routes. Since OLSR does not account for interference, it is unable to route the connections effectively under high load.

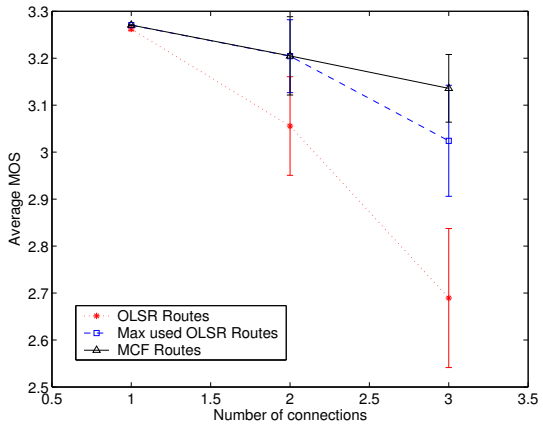

(a) MOS

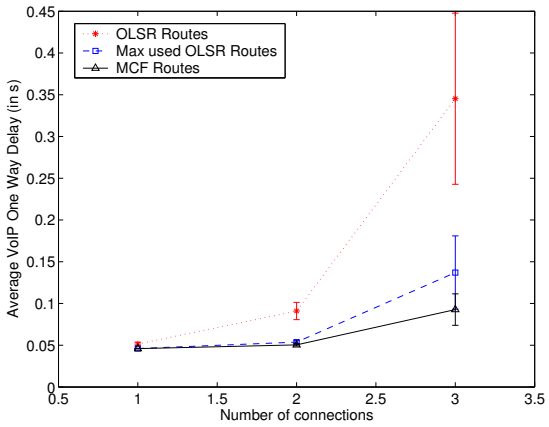

(b) VoIP Delay

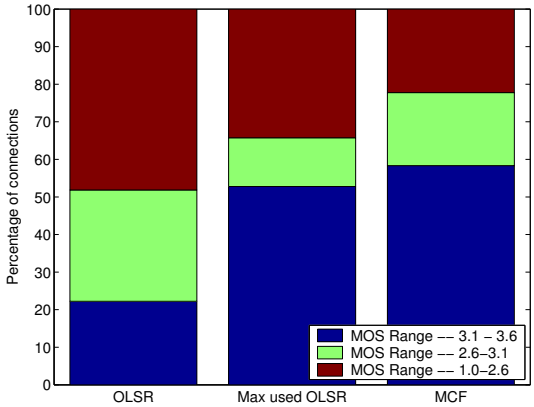

(c) Percentages of connections in each MOS Category

Figure 6.3: Performance for VoIP traffic

The second study compares the performance of the MCF routes under real-time traffic in a random scenarios in a $1000 \times 1000m^2$ area. VoIP traffic with G.711 codec is used. 20 random scenarios were simulated under such a traffic and the Mean Opinion Scores (MOS) and End-to-

End delay were measured as the number of connections were altered. MOS scores for VoIP traffic measure the user satisfaction and ranges from from 1 (worst) to 5 (best). Figure 6.3(a) and Figure 6.3(b) present the average MOS and one-way delay respectively. Figure 6.3(c) categorizes the MOS score according to VoIP categories; A MOS value of 3.6 and above is generally considered as acceptable limits for a satisfactory call [87]. It can be seen that the MCF routes out-perform the OLSR routes significantly both in terms of MOS (it has the largest population of high quality connections) and delay. Especially in the higher interference regions, MCF is able to find low delay routes.

6.4 Conclusions and Future Work

This chapter formulates the delay-sensitive routing problem in MHWNs (whereas the previous chapters focused on the throughput problem). To formulate the objective function, we characterize delay behavior in the presence of interference using simulation. Extensions of the model for real-time routing are discussed. Simulations show that large improvements in end-to-end delay and jitter over OLSR are obtained.

The scheme is centralized, but can be used for on-line optimization in static networks where it would not have to be invoked frequently. However, similar formulations have resulted in distributed protocols that essentially solve the optimization problem [22]. This is a topic of future work.

Chapter 7

A Decomposition based Routing Model

In this chapter, we analyze and algorithmically refine the MCF formulation proposed in Chapter 4. The goal of this work is two fold: (1) first, lowering the complexity of the problem via decomposition extends the range of applications and scale of network that can be managed by this approach; and (2) decomposition has been applied in similar contexts as a means to develop distributed protocols.

7.1 Introduction

Chapter 3 discussed the importance of Globally-Coordinated routing in MHWN and, as a contribution of the dissertation, Chapter 4 proposed an extensible network flow based model (the MCF model) to calculate such routes. Several efforts for modeling MHWNs for analysis and optimization of specific networks have been undertaken [63,76,81]. These models are largely network flow based, and take into account interference. This line of research is extremely promising for a number of reasons, including: (1) it provides practical limits for performance of specific MHWN networks, allowing more effective provisioning and design of these networks; (2) similarly, the developed models can be used to guide traffic engineering decisions to achieve effective usage of the available network resources; and (3) it provides understanding of the shape of effective solutions, and insight into

what makes them effective, to aid in the design of protocols that converge to such solutions.

The developed models are network flow based expressed as a Mixed Integer Linear Programming (MILP) problem [113], which is then solved relative to an objective function such as maximizing throughput. MILP problems are NP-hard [43]. The MHWN problem is especially difficult because of the large number of constraints that result from mutual interference on the wireless channel among nearby nodes. To make the model more realistic, the effect of scheduling and the channel can be taken into consideration, further increasing the complexity of the problem. Thus, while the approach is promising, it is critically limited by the computational complexity, which grows exponentially with the size of the network and the number of edges. This limitation restricts the utility of the approach to small networks, and for off-line analysis.

In this chapter, we explore efficient solutions to the MILP formulation of MHWNs, taking advantage of domain knowledge to reduce complexity. As a result, the developed approach can be used to significantly scale the size of the problems that can be studied, while maintaining the ability to obtain effective solutions.

The chapter first analyzes the complexity of a previously proposed MCF model in Chapter 4 and then applies domain-specific heuristics as well as decomposition to simplify it into a model that can be solved in polynomial time. The lower complexity allows scaling the size of networks that can be studied. The notations and conventions used for describing MCF formulation are the same as the ones proposed in Chapter 4.

Decomposition judiciously breaks the problem into smaller sub-problems, in our case, each subproblem attempts to route an individual connection. The sub-problems are then coordinated using a master problem to take into account interference across connections. We analyze the run-time complexity of the two models and show that large reductions in run-time are achieved (up to 3 orders of magnitude in the scenarios we study); this gap is likely to increase as the models scale due to the much lower asymptotic complexity of the proposed formulation. Further, the quality of the routes obtained compares favorably with those obtained from the full model.

7.2 Complexity Analysis of the MCF Model

Even though the *MCF model* provides interference separated routes, the high complexity due to multiple integer variables and large number of constraints makes the model inefficient to solve for scenarios with moderate number of nodes and connections. We study the complexity of the MCF model under two categories: (1) size of the model; and (2) integer programming complexity.

Size of the model: The number of variables in the model gives an estimate of the dimension of the space to be searched. In a network of n nodes, m edges and c connections, Table 7.1 shows the number of constraints, variables and assignments in the MCF model to evaluate the objective in Equation 4.19. The number of variables in the formulation is $O(mc)$ [1]. Even if we assume that linear program is non-integer (we discuss integer programming complexity in the next case), such a polynomial time variable scalability can make the formulation inefficient. For example, the solving time for one well-known Karmarkar's algorithm [98] is a polynomial function of the number of variables and the solving time for the Simplex algorithm *generally* grows linearly as the number of variables [2]. The number of constraints in the MCF model will also be order of $O(mc)$. As the size of the problem is scaled, optimization of such complex multi-commodity problem is generally not feasible in a single-shot. Rather, often the problem is broken into smaller sub-problems that can be solved efficiently and coordinated to achieve an effective overall solution. However, the choice of these subproblems and their coordination requires domain-specific understanding. This chapter presents a decomposition approach targetted to the multi-hop wireless network.

Integer Programming:

MCF formulation with mixed integer linear programming (MILP) is an NP-hard problem. However, the same problem without integer variables can be solved in polynomial time. Two sets of integer variables, $y_{i,j}^n$ and $\hat{y}_i^n$, are present in the MCF model. The boolean variable $y_{i,j}^n$ denotes that if an edge (i,j) carries traffic for the n^{th} connection and is necessary to restrict the routing formulation to result in a single path route as given in the Equation 4.5. The boolean variable $\hat{y}_i^n$ indicates if the node i carries traffic for the n^{th} connection and is used to calculate the maximum

[1] In the worst-case, the number of edges m is $O(n^2)$ in wireless networks

[2] The worst case time complexity of Simplex algorithm is an exponential function of the number of variables. However, it is efficient in most of the practical cases

Variables and assignments	Equation	Number
Flow Variable (x_{ij}^c)	-	mc
Interference (I_i) Assignment	Equation 4.8	n
Signal Assignment (S_i)	Equation 4.6	n
Inequality Assignments	**Equation**	**Number**
Assignment for $\hat{y}_i^c$ (*Integer variable*)	-	$3nc$
Assignment for $\hat{\mathrm{A}}_i^c$	-	$5nc$
Assignment for $\hat{\mathrm{S}}_i^c$	-	$6nc$
Assignment for $\max(\hat{\mathrm{A}}_i^c)$	-	nc
Constraints	**Equation**	**Number**
Rate Bounds Constraints	Equation 4.2	$2mc$
Bundle Constraints	Equation 4.3	$2mc$
Flow Constraints	Equation 4.4	$2nc$
Integer flow constraint	Equation 4.5	mc

Table 7.1: Complexity of MCF Model

commitment period $\hat{\mathrm{I}}_i$. Generic integer programming algorithms first reduce such MILP problems into non-integer LP by relaxation techniques [97], calculate the integer polytope for the feasible region and judiciously use branch-and-bound techniques to solve the problem. All the integer points in the feasible region has to be processed by the branch-and-bound algorithm to guarantee optimality of the solution (or infeasibility). However, the number of integer variables in the MCF formulation is $O(mc)$ and using a generic branch-and-bound technique of such high dimensions is not practical. This provides the motivation for eliminating the integer variables by applying MHWN domain specific heuristics.

7.3 A Decomposition based Formulation

In this section, we describe a simplified model to efficiently obtain the near-optimal solutions by *decomposition* [7]. The main idea for the classical decomposition approach is to identify subproblems that can be solved efficiently. A *Master Problem* then coordinates the subproblems, updating their inputs in response to other subproblems and iteratively moving towards a near-optimal solution.

Let $G(N, E)$ be the graph representation for the network as per the MCF model formulation in Section 4. We elect to decompose the problem by considering each flow separately, reducing the problem to multiple single-commodity problems (which are polynomially solvable). The route

for each connection is found irrespective of the other connections' route. The routes are then coordinated as follows. Each node is assigned a weight by the master problem based on the amount of interference created by the node upon other connections. Upon solving a subproblem, these weights are re-adjusted based on the new solution and the subproblems are re-evaluated. Convergence is detected when none of the subproblems can observe a change in the optimality. Of course, the solution can converge to a local minimum, and the globally optimal solution may be missed. We do not explore measures to attempt to get out of local minima in this study; in our experience the resulting solutions are effective even without this step. In addition, the solution may take too long to converge due to interactions like route oscillations between the sub-problems. We address this challenge by limiting the number of iterations allowed, and accepting the best solution available at that stage. Most scenarios converge very quickly. Finally, we develop solutions to remove the integer constraints from the sub-problems, turning them into simpler non-integer linear programming problems.

7.3.1 Formulation of the subproblem

The problem is decomposed into c sub-problems where the k^{th} subproblem attempts to route the k^{th} connection ($1 \leq k \leq c$). The rate bounds (Equation 4.2), bundle constraints (Equation 4.3) and the flow constraints (Equation 4.4) for the k^{th} subproblem are set similar to those of the MCF model, but accounting only for the k^{th} connection.

Let the flow on edge (i, j) for k^{th} connection be denoted by $x_{k,ij}$. Let U be the upper bound of the capacity that can be carried by each $x_{k,ij}$. We relax the upper bound assumption on the sum of capacities carried by the edge for all the connections. This can be included as a part of master problem. However, the optimal route set computation to reduce total interference is calculated assuming infinite capacity. Let r_k denote the rate of the connection k and let b_i^k be the demand at node i for connection k which can be computed by a formula similar to Equation 4.1.

The *Signal* carried by a node i for the k^{th} connection ($S_{k,i}$) is assigned as the sum of in-flows and out-flows to node i.

The cost of using a node in a route depends on the amount of cross-interference it creates, which

is computed by the master problem. Let $w_{k,i}$ (a constant assigned by the master problem) be the weight for node i while solving the k^{th} subproblem. The objective function of the subproblem is given in Equation 7.1.

$$\text{Minimize} \sum_{i \in N} w_{k,i} S_{k,i} \tag{7.1}$$

Each subproblem becomes an MILP minimum-cost flow problem [7]. The effective linear program to solve the k^{th} subproblem is shown in Equation 7.2.

$$\begin{aligned} \text{Minimize} \sum_{i \in N} w_{k,i} S_{k,i} \text{ subject to} \\ 0 \leq x_{k,ij} \leq U, \forall (i,j) \in E \\ 0 \leq S_{k,i} \leq \infty, \forall i \in N, \forall k \in C \\ 0 \leq x_{k,ij} \leq r_k, \forall (i,j) \in E, \forall k \in C \\ b_i^k = \sum_{(i,j) \in E} x_{ij}^k - \sum_{(j,i) \in E} x_{ji}^k, \forall k \in C, \forall i \in N \\ S_{k,i} = \left(\sum_{(i,j) \in E} x_{k,ij} \right) + \left(\sum_{(j,i) \in E} x_{k,ji} \right) \end{aligned} \tag{7.2}$$

The subproblem given in Equation 7.2 can be solved by highly efficient shortest-path algorithms, like Dijkstra's algorithm, further improving the efficiency of the solution.

7.3.2 The Master Problem

The master problem updates the node weights w_i reflecting the cross-connection interference and ensures the convergence of the solution by forcing the sub-problems to choose routes which have the least effect on other connections. As a result, the overall solution moves towards an effective solution with respect to the global objective function (minimizing interference while controlling

path stretch).

Computing node weights: If a node i is part of the k^{th} connection, then the weight of node i should be proportional to the amount of interference added to the other connections. We consider node i to interfere with a connection k, if node i interferes with its bottleneck node(s). The bottleneck nodes affect many connection performance metrics like the throughput and end-to-end delay.

Consider the assignment of node weights to the k^{th} sub-problem. Denote the bottleneck commitment period of connection m by $\hat{\text{A}}^{m}_{max}$. The objective is to reduce the overall maximum commitment periods of the connections ($\sum_{m \in C} \hat{\text{A}}^{m}_{\text{max}}$). The weight assigned to node i should reflect the fraction of increase in commitment periods of the connections except k (since we relax the self-interference constraints for computational reasons) caused by the node i if it participates in the k^{th} connection. We now briefly explain the procedure for computing the weights.

The amount of interference added by i depends on the normalized signal $S_{k,i}$ in the k^{th} sub-problem. $S_{k,i}$ is a constant which is r_k for the source/destination and $2r_k$ for the intermediate nodes, where r_k is the rate of connection k. Let j be an active node in a connection m, such that $k \neq m$. The amount of interference contributed at node j by choosing node i (if i and j interfere) is $S_{k,i}$. If the added interference makes j the bottleneck link of connection m, then the weight w_i should reflect the amount of interference added to j. Let the commitment period of such node j for connection m be denoted by $\ddot{A}_m$ and let i interfere with bottleneck nodes of n connections. If i is chosen, the bottleneck commitment period increases to $nS_{k,i} + \sum_{m \in C, m \neq k} \ddot{A}_m$. The normalized increase in total bottleneck commitment periods of the connections is the ratio of the above factors, given by w_i in Equation 7.3. The weight is set 1 if $\sum_{m \in C, m \neq k} \hat{\text{A}}^{m}_{\text{max}}$ else 0.

$$w_i = \frac{nS_{k,i} + \sum_{m \in C, m \neq k} \ddot{A}_m}{\sum_{m \in C, m \neq k} \hat{\text{A}}^{m}_{\text{max}}} \tag{7.3}$$

Convergence of the solution: A connection is considered solved if it repeats a solution for a preset number of times. The overall problem is considered to be solved when all the sub-problems

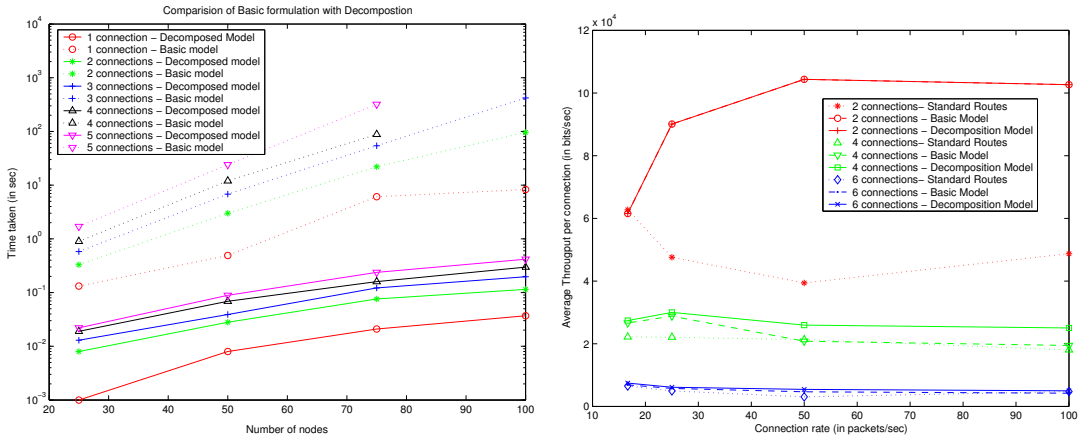

(a) Runtime study (b) Throughput study

Figure 7.1: Comparing MCF Model and Decomposition

are solved. Certain interactions, like oscillations between a set of connections, can slow down or prevent the convergence of the solution. We observe such interactions and apply heuristics, like storing previous routes, to detect oscillations and reduce their effect. The detailed explanation is not given in the abstract due to space constraints.

7.4 Performance Evaluation

Runtime analysis was conducted by varying nodes and connections in a random network scenario. Each point represents the average of ten different networks with uniformly distributed nodes and connected pairs. The models were run on a 2 GHz Intel Pentium 4, with 512 kB RAM. It can be seen (Figure 7.1(a) that the decomposed problem is orders of magnitude faster to solve than the MCF model (please note that the y-axis is in log-scale). For example, an improvement of over 1000 *times* is seen at larger node and connection scenarios. Since the MCF formulation is NP-hard, while the decomposed formulation polynomial, this advantage increases as the size of the problem scales.

Figure 7.1(b) compares the quality of the solution (in terms of throughput) obtained by a standard routing protocol[3], MCF formulation and the decomposed formulation for a 6×6 grid.

[3]Standard routes are the most frequently observed routes on DSR protocol in QualNet simulator. Such routes

Clearly, decomposition does not degrade the quality of the routes when compared to the MCF formulation. Extended analysis of other metrics and scenarios is omitted due to space constraints.

The scalability of the decomposed model is analyzed for larger networks. The network parameters were varied to study the different break-down points of the model. The runtime of the model was divided into the time consumed by the subproblem and the master problem. Figure 7.2 shows the split time taken by the decomposition model. It can be seen that the solution time of the subproblem grows with the size of the network. This is due to min-cost flow problem with a large number of edges in the network. The evaluation of the shortest-path algorithms to replace the subproblem formulation is an area of future work. Figure 7.2(d) shows the convergence histogram of the formulation. A very small number of experiments (about 2.4%) resulted in maximum number of iterations, while most of the iterations converged within 6 iterations of the sub-problems.

7.5 Concluding Remarks

Interference aware network flow models for MHWNs are promising for analysis and optimization of these networks. However, the computational complexity of these models prevents their use in large scale realistic scenarios. In this study, we presented approaches for reducing the computational complexity of the of the Multi-commodity flow based Mixed Integer Linear Programming (MILP) problem via domain specific heuristics as well as multi-level decomposition. The resulting formulation was shown to be several orders of magnitude more efficient than the basic formulation, while being able to maintain efficient solutions.

were converted into static routes to eliminate the overhead of the routing protocol and provide a fairer comparison.

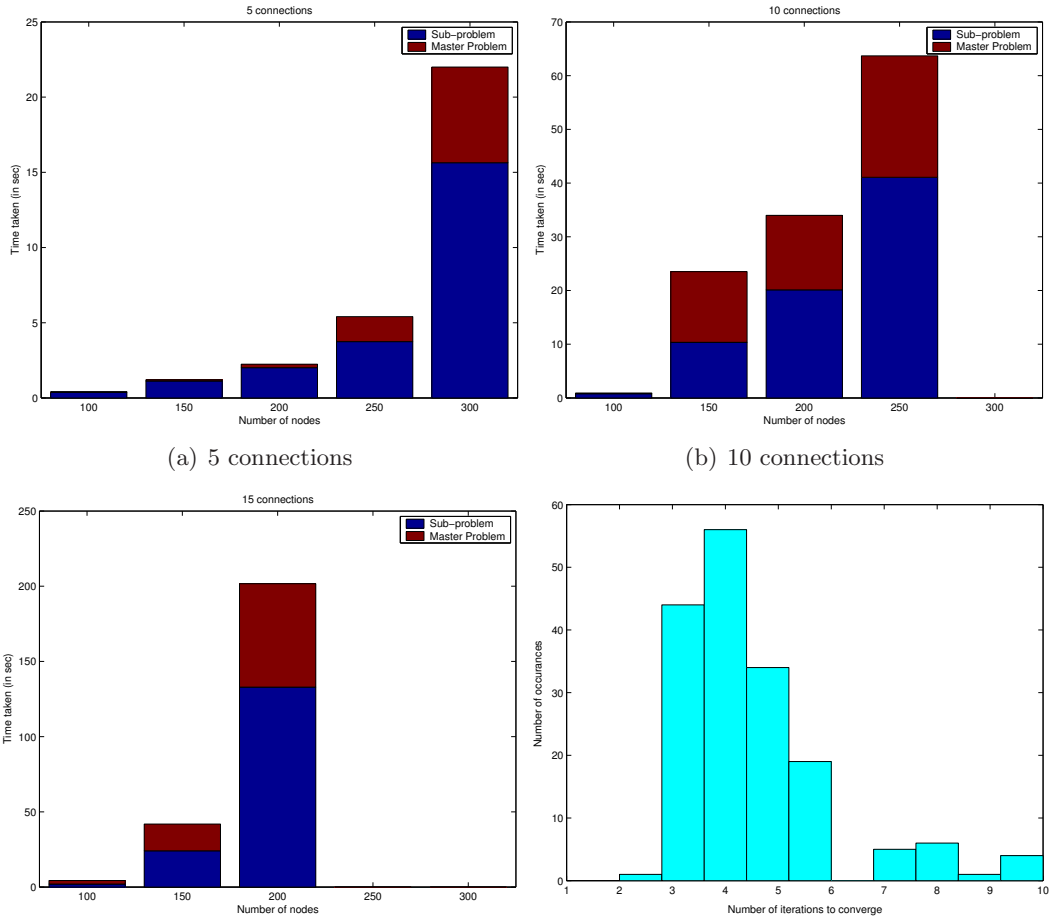

(a) 5 connections

(b) 10 connections

(c) 15 connections

(d) Convergence Study

Figure 7.2: Timing analysis and convergence study

Chapter 8

Contention-fairness Model in CSMA networks

The next three chapters refine the models developed so far in a number of ways to analyze some important and complex phenomena that arise in MHWNs. Scheduling interactions have a defining effect on the performance of the MHWNs.

We saw in Chapter 5 that the behavior of a MHWN can be described using Independent Contention Sets (ICS, and Maximal ICS under saturation traffic) that represent the sets of links that can transmit concurrently per the MAC protocol rules. A challenge in that framework is to estimate the probability of occurrence of the different MICS; we have thusfar heuristically estimated this probability as a function of the number of links in the MICS. In this chapter, we present initial models for deriving the MICS probabilities under saturation traffic and in the absence of collisions. Our future work will target extending the model to relax these two assumptions (saturation traffic and no collisions).

In addition to helping in understanding the MICS probabilities for reasons of planning traffic, the MICS probabilities directly influence the degree of fairness achieved in the competition between links. In this chapter, we discuss the problem from the fairness perspective, but the goals of the model are equally applicable to the original problem.

The CSMA scheduling policy introduces several fairness issues in multi-hop wireless networks.

Such fairness factors have a significant influence on the performance of the network [84, 125]. We analyze a fundamental form of unfairness in CSMA scheduling even in the absence of hidden terminals. The unfairness stems due to insufficient channel contention experienced by certain nodes and we refer this property as *Contention fairness*. Contention fairness model is proposed to estimate the throughput and is validated by simulations. Based on the insights gained from analysis and model, we propose and evaluate a distributed scheme that reduces the effect of unfairness due to contention. Simulation results show that average fairness improvements of approximately 25% with an acceptable overall network throughput degradation.

8.1 Introduction

Because of the complex and asymmetric nature of the wireless channel, achieving fairness among a set of competing links is one of the challenging problems in MHWNs [84, 125]. Fairness issues in IEEE 802.11 arise due to several reasons, namely (1) The location of the nodes cause different edges to suffer higher contention levels than others. Note that this is not simply a function of the number of contending neighbors, but a complex competition at the level of MICS. We term the unfairness resulting from such unfair contention as "Contention fairness"; and (2) *Hidden-terminals* [119], where a node experiences packet collision due to simultaneous transmission by two unsynchronized sources. Hidden terminals can cause excessive backoffs, leading to unfairness, and also have important implications on MICS transitions.

In this chapter, we analyze the contention fairness in MHWNs under CSMA, and without accounting for the effect of hidden terminals (which remains an area for future extension of the model). The fundamental behavior of CSMA scheduling in MHWNs, even in the absence of collision avoidance (CA) schemes, create acute fairness concerns. Sophisticated protocols have been proposed to avoid hidden-terminals [37]. However, even under such protocols, contention fairness cannot be guaranteed due to the unique pattern of competition for the channel. Existing studies in the analysis and modeling of CSMA networks have identified this effect.

We study the root causes of contention fairness and develop a constructive model to characterize this effect. In this study, the pattern of interaction and the dynamic changes in the channel states

are analyzed when the links compete under a CSMA protocol. We propose a throughput model to capture contention pattern and verify the accuracy through simulation. We assume no packet collisions since the focus of the study is to characterize contention fairness in the absence of hidden terminals. While this assumption reduces the direct applicability of the model in realistic scenarios, we believe that the proposed model and insights are essential steps towards a precise understanding of the dynamism of CSMA in MHWNs and, therefore, the design of fair protocols.

The remainder of the chapter is organized as follows. Related work is described in Section 8.2. We describe the framework for analysis using an example to illustrate the effect of contention fairness in Section 8.3. Section 8.4 proposes a model to estimate the link throughput by capturing the contention fairness and validates it. Based on the insights gained from the model and analysis, we propose and evaluate a distributed protocol to account for contention fairness in Section 8.5. The chapter is concluded and the future work is discussed in Section 8.6.

8.2 Related work

The problem of fairness in single-hop wireless networks with IEEE 802.11 is widely studied [11, 12, 55]. However, the fairness problem in a multi-hop setting represents a significantly different and more complicated problem. There exists some work in fairness in multi-hop wireless networks [41, 88, 94, 123]. However, the existing work does not separate out the causes of unfairness or present a constructive analysis for the problem; rather, most works simply identify the problem and explore heuristics for it. In the following, we summarize some of the most important related work.

A simple and typical contention based problem that is present in multi-hop network is termed as "Flow in the middle"(FIM), where the one link is starved due to due to the activity of two if its neighboring links. Garetto et al. [41], Wang et al. [123] and Chaudet et al. [21] analyze the FIM problem. In this study, we generalize the FIM problem for multi-hop wireless networks under the proposed framework and quantify the effect of starvation.

Several works analyze fairness with *with hidden terminals* under the assumption of traffic arrivals governed by a Poisson process [41, 88, 123]. Li et al. [84] study the effect of short-term unfairness due to hidden terminals. Several works [11–13, 52, 55, 78, 84, 88] have observed and analyzed the

effect of backoff contention window for fairness under their respective framework and assumptions. While a certain set of work [52,78] does not observe 802.11 semantics for backoff, another category is specifically tuned for single-hop networks [11,12,55]. Under multi-hop networks, most of the analysis study the effect of altering backoff for providing *fairness under hidden terminals* scenario [84].

Various distributed protocols, both in single-hop [11,12,55] and multi-hop wireless networks [13, 29,61,68], achieve fairness among the contending nodes by dynamic tuning of the backoff contention window parameter. Natkaniec et al. [96] argue by experimental results that adjusting backoff based on number of contending stations in single-hop networks can increase the throughput. In this paragraph, we highlight the applicability of such fairness schemes to solve "contention fairness". The *proportional fairness* [11] and *distributed fair scheduling* [120] are effective in single-hop networks. These fairness schemes are insufficient in multi-hop wireless networks. Heusse et al. [54] show that the 802.11 network inherently observes *Max-min fairness* [59], thus leading to starvation of some nodes.

The MACAW protocol [13] proposes Multiplicative Increase/Linear Decrease (MILD) backoff algorithm after listening to neighboring transmission's contention window. However, this algorithm was designed to attain fairness in the presence of collisions in a single-hop wireless networks. The study proposes identical backoff values for all neighboring nodes. In contrast, we argue that adopting a single strategy of setting identical backoff windows will increase contention unfairness in multi-hop wireless networks and propose a protocol that sets varying backoff windows based on the contention observed at the neighbors. Nandagopal et al. [94] propose a protocol that uses probabilistic contention and backoff to attain various kinds of fairness metrics. While the above study considers adapting contention probability, we propose a scheme that works purely on an adaptive backoff mechanism. Other studies [1,29] suggest to decrease the backoff congestion window slowly after successful transmission. While such schemes help to attain fairness under hidden terminals, the focus of the paper is to understand contention fairness and the analysis indicates that such an approach will not solve contention fairness effectively.

Yi et al. [131] and Rao et al. [107] assume a layer 2 protocol for throttling MAC transmissions. Gambiroza et al. [39] studies fairness of TCP if an ideal input rate is computed. These studies rely

on exchanging the "contention information" in the neighborhood. Intuitively, the need for fairness scheme is imperative under saturation traffic with starved stations. We quantify the feasibility of exchanging such information (which forms the basis for such protocols) and systematically evaluate the role of the backoff contention window in this aspect.

8.3 Background Information and Example

In this section, we develop the framework for analysis of CSMA/CA protocols and provide a motivating example to illustrate the effect of contention fairness in MHWNs. An outline of the framework for capturing the interactions in CSMA protocols is described in Section 8.3.1, while an example is presented in Section 8.3.2.

8.3.1 Capturing the interactions in CSMA/CA protocols

Consider a multi-hop wireless network where N denotes the set of wireless nodes. Each wireless node is capable of *sensing the channel*. The strength of the signal sensed at a node is termed as "Receiver Signal Strength Indicator (RSSI)" and the process of sensing the channel is called "Clear Channel Assessment (CCA)". The channel is said to be "idle" if the RSSI is greater than a *Receiver Sensitivity* threshold (T_{RX}). Let $\mathcal{N}(i)$ be the set of neighbors for node i. Node j is a neighbor of i if it can sense the signal from i. Formally stated, $\mathcal{N}(i) = \{j \mid S_{ji} \geq \mathrm{T}_{RX}\}$ where S_{ji} is the strength of node i's signal at node j.

We first model the basic mode of IEEE 802.11. Let L be a set of one-hop links denoted by source and receiver quintuple $\langle s_i, r_i, l_i, \mathrm{CW}_i \rangle$ where s_i, r_i, l_i and CW_i are the source, receiver, packet length and the source node's $\mathrm{CW}_{\min}$. We also denote the link by a tuple $\langle s_i, r_i \rangle$ for simplicity. Since the ACK packet is very small in size with respect to the DATA packet, we assume a model with instantaneous ACK. Under such an assumption a set of links can be active at the same time when each source cannot sense the transmission of other sources (otherwise the CSMA protocol prevents transmission). A group of such links whose sources' can transmit together denotes a *independent set* of links. It is to be noted that even though we consider L one-hop links, the links compete in a multi-hop fashion.

Recall that a "Conflict Graph", as described in Section 3.3, does not capture the temporal relationships between the transmissions of the links and, hence, cannot be used to represent the channel states. The maximum number of independent set of links that can concurrently transmit is represented by *Maximal Independent Contention Set* (MICS). One type of interactions that cannot represented by MICS is packet collisions due to co-ordinated sources [41]. This happens when two sources which are in sensing range of each other, transmit at the same chosen slot. However, it is observed in studies [41, 79] that such interactions constitute a minority of the packet collisions. We do not consider the packet collision due to co-ordinated sources in this study. In order to capture the interactions, we assume that the physical layer is according to the *Signal-To-Interference-Noise Ratio (SINR)* Model and the traffic at the sources are saturated.

An independent set based approach for modeling CSMA protocol is not the primary contribution of the study. Existing research studies [16, 41, 123] have developed an independent set based Continuous Time Markov Chain model for calculating the link throughput. The studies assume scheduling of packets for each link observes a Poisson Point Processes and thereby derive the parameters for throughput. However, the scheduling points are not Poisson point processes in saturated traffic since the packet is scheduled over the channel based on the channel activity and the backoff process. In this chapter, a significant part of the study is devoted to capture the detailed scheduling behavior and transition rates between a pair of concurrently active MICS. We then use the computed rates, instead of parameter of the assumed Poisson point process, in a Continuous Markov chain to predict the throughput of the links.

8.3.2 Contention Fairness – An example

We now describe the contention in a multi-hop wireless network (MHWNs) through a simple but common example. We use this example to motivate the importance of contention fairness, demonstrate the model construction and evaluate the effectiveness of the proposed adaptive scheme.

Contention for channel in MHWNs differ significantly from single-hop wireless networks where each node is able to sense the transmission of the other nodes. Thus, the channel state observed at each node is the same. Under a homogeneous network, where each node has the same MAC

level parameters, the hidden-terminals are absent in single-hop wireless network. Packet collisions arise when two or more sources start transmitting at the same chosen slot. Such interaction under the backoff semantics of 802.11 is characterized by the model proposed by Bianchi et al. [14]. The fairness of a link in such network depends upon the parameters like the transmission rate, packet length, CW, etc. Imposing a simplified assumption that all the nodes have the same parameters, traffic is saturated and probability of simultaneous transmissions is negligible, each source has an equal probability to win an idle slot. However, even under such simplified assumption the behavior in a MHWN is drastically different.

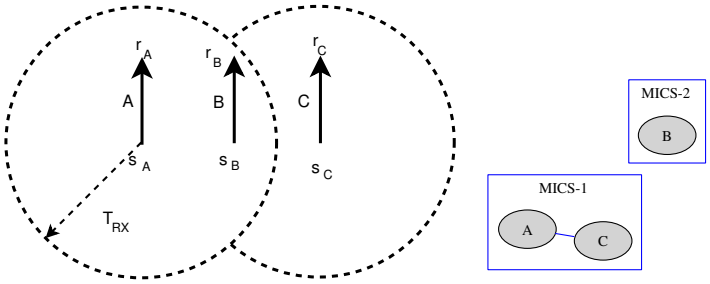

(a) FIM scenario

(b) MICS representation of FIM

Figure 8.1: Flow in the Middle scenario

Consider the "Flow-in-the-Middle (FIM)" scenario which demonstrates the contention unfairness in MHWNs. The scenario is shown in Figure 8.1(a) where link A, B and C compete for the channel. Link A and Link C can transmit concurrently while source s_B can transmit when neither link A nor link C is active (because of the busy channel from link A and/or link C). The MICS representation of the FIM is shown in Figure 8.1(b). While there is no hidden terminal in the above scenario, link B faces an acute starvation due to constant busy channel by link A or link C. Generalizing this property, we refer *Contention Fairness* to quantify the amount of starvation that a node experiences due to contention for idle channel. While previous studies have concentrated on measuring the impact of hidden terminals on fairness [41,84,88,123], we believe that contention fairness is a more basic case of fairness. In fact, the effect of hidden terminal can be measured after quantifying the contention effectiveness of the link that experiences hidden terminal and the hidden terminal node itself. This scenario has been analyzed in past studies [41, 123] by assuming that

the transmission of the nodes observe a Poisson process. The contribution of the study is to derive the necessary distributions to relax the above assumption and to generalize the contention fairness in MHWNs. While the above framework is capable capturing hidden terminal interactions, we analyze scenarios with no hidden terminals for modeling contention fairness. We intend to extend the model for measuring hidden-terminals in the future.

8.4 Throughput model

In this section, we analyze the contention fairness in a multi-hop wireless network (MHWNs) and propose a throughput computation model to capture the contention experienced by the nodes.

Assumptions We consider a multi-hop wireless network with no hidden terminals and several single-hop links. Without loss of generality, we use IEEE 802.11 protocol under *basic mode* as a representative CSMA/CA protocol. The basic mode of IEEE 802.11 is more widely used (a default setting in a majority of the wireless network cards). This is not a significant assumption since no hidden terminals are considered and very few collisions occur. Instead, we assume that the source node of the link i picks an exponentially distributed waiting time, henceforth called as *backoff period*, Y_n^i where $n = 1, 2, 3, \ldots$ denotes the n^{th} backoff value chosen. It is to be noted that under the scenarios without hidden terminals, the IEEE 802.11 chooses a backoff window of the from of a uniform discrete distribution between $0, CW_{\min}$, while we choose an exponential backoff window with mean $\frac{CW_{\min}}{2}$. The expectation values of the above distributions are equal.

$$Y_n^i \sim \exp(\beta_i) \tag{8.1}$$

After the backoff is decremented, the node transmits the packet over the channel. The packet sizes of link i is denoted by Z_n^i where $n = 1, 2, 3, \ldots$.

$$Z_n^i \sim \exp(\tau_i) \tag{8.2}$$

The p.d.f and the c.d.f. of Y is represented by f_Y and F_Y, respectively. Similarly the p.d.f and c.d.f for Z is represented by f_Z and F_Z.

The notations used in the model is shown in Table 8.1. While an exponential distribution is assumed for backoff period in the model derivation, we show the model matches the simulation results even when uniform discrete distribution is chosen for backoff interval. The simulations results also demonstrate a close match even with the constant packet length, which is primarily used CBR connections, though we have assumed an exponential packet length distribution.

8.4.1 A Continuous-time Markov chain model

Let $M = \{M_1, M_2, \ldots M_n\}$ be the set of possible MICS for the given network scenario. The channel state can be represented by the links that are concurrently transmitting at a given point of time. Under our assumption of saturated sources, an active MICS is a good candidate to represent the channel state. As we observe the changes in the channel state over time, we see transitions from one active MICS to another. A transition from MICS M_a to MICS M_b will occur when the links in the MICS M_a that are not present in MICS M_b (i.e. links in the *difference set* $M_a - M_b$) are idle and the links in the set $M_b - M_a$ become active. The difference of two MICS is represented by $C_{ab} = M_a - M_b$. It can be seen that the transition between two MICS is largely dependent upon the current active MICS. Hence, we represent the different states of the channel by active MICS. A Continuous-time Markov chain is defined with a state space M, each state representing the state of the channel that is currently active i.e. the active MICS. Let λ_{ab} be the rate of transition between two MICS M_a and M_b. If we assume λ_{ab} to be exponentially distributed, then the long term probability of staying at a MICS a (represented as P_a) can be calculated by solving the balance equations as shown in Equation 8.3.

$$P_a \sum_{b \in M, b \neq a} \lambda_{ab} = \sum_{b \neq a} P_b \lambda_{ba} \qquad \forall a \in M \tag{8.3}$$

$$\sum_{a \in M} P_a = 1 \tag{8.4}$$

After the computation of λ_{ab}, the throughput of a link i (denoted by T_i) by Equation 8.5. The

Notation	Description
	Conventions
i, j, k	Variables for denoting links
a, b, c	Variables for denoting MICS
	Constants
M_a	A Maximal Independent Contention Set
M	The set of all possible MICS, $M = \{M_1, M_2, \ldots, M_n\}$
C_{ab}	The difference set $M_a - M_b$
DIFS	Duration of DIFS period (in slots)
s_t	Duration of a single slot time
	Packet length representations
l	Denotes packet length.
t	Time to transmit a packet of length l
ε_i	Efficiency factor for transmission of expected packet length of l_i with an expected backoff time of $\frac{1}{\beta_i}$ slots and standard MAC overheads like SIFS and DIFS.
	Random variables
Y_n^i	Exponential i.i.d. random variable indicating the backoff time chosen by the source of link i. $Y_n^i \sim exp(\beta_i)$
Z_n^i	Exponential i.i.d. random variable indicating the time required to transmit a packet for link i. $Z_n^i \sim exp(\tau_i)$
X_n^i	Random variable indicating the time required to wait for backoff and transmit the packet for a link i. $X_n^i = Y_n^i + Z_n^i$
	MICS related notations
P_a	Long term probability of remaining in MICS M_a
λ_{ab}	Expected rate of transition from MICS M_a to MICS M_b
C_{ab}	Difference set between MICS M_a and M_b, $C_{ab} = M_a - M_b$
	Channel idle time related notations
$g_i(t)$	The probability that the link is going to be idle at time t given that the link has started transmitting at 0 and has been active ever since.
$p_{\mathrm{LI}i}$	The long term probability that link i will be idle
$p_{\mathrm{LS}i}$	The long term probability that link i *becomes idle* at this timeslot
$p_{\mathrm{ci}}(I)$	The probability that channel *becomes idle* at this timeslot (none of the independent links in set I is transmitting).
$G(I)$	Random variable denoting the minimum of exponential random variables Y_n^i $\forall i \in I, n = 1, 2, 3, \ldots$ and $G(I) \sim \exp({\mu_g}^I)$
$\chi(i, I)$	Probability that the link i wins channel contention conditioned that a the set of independent links I have become idle. All the links in I interfere with link i.

Table 8.1: Contention Fairness: Notation description

fraction of time available for a link i is given by the sum of all long term probabilities of MICS to which i belongs. The throughput is computed by determining the the efficiency factor of the link (ε_i). The efficiency factor of a link is the ratio of the time required to transmit the data payload to the time required for completing one successful transmission with the overhead. The overhead consists of the time required for decrementing the average backoff duration, DIFS, physical layer and MAC layer headers and the ACK assuming no interference from any other links.

$$T_i = B\varepsilon_i \sum_{a \in M, i \in M_a} P_a \tag{8.5}$$

where B represents the bandwidth of the channel.

The unknowns to compute the throughput from Equation 8.5 are ε_i and λ_{ab}. While the link overhead can be determined by the expected value of backoff and other MAC specific details, computation of λ_{ab} is challenging. The next section describes the model to compute the λ_{ab}.

8.4.2 Computation of transition rates

We briefly describe the transmission process of a node while using the IEEE 802.11 protocol. Then we estimate the 'contention' experienced by a source node due to interfering links. Under such a contention, we calculate the fraction of the time the source node successfully captures the channel to transmit the packet. In order to capture the time share received by a link and its interfering links, it is more intuitive to view the contention at a MICS level. We calculate the contention experienced by the link and then compute the transition rates.

Contention at a node due to active MICS Before transmitting a packet, the source node starts decrementing the backoff periods only after its finds a contiguous channel gap for the period of DIFS. If the channel becomes busy, then it re-waits till a contiguous DIFS period is observed. If a gap of DIFS period is observed, the node decrements its backoff until the it reaches zero, upon which the node transmits the packet. If the channel becomes busy, it will freeze the backoff time and will restart the process by waiting until a contiguous gap of DIFS is observed.

We now explain the transition from a MICS point of view. Consider the transition between the

only two MICS M_a and M_b. At channel idle times, the links start the backoff procedure and the links that win the channel first is going to determine the transition between M_a and M_b. Hence, the competition to decrement the backoff between the links of M_a and M_b is going to determine the transition from MICS M_a to M_b. A transmission from any link $i \in C_{ba}$ will increase the chances of transition from M_a to M_b.

From the above discussion, it is apparent that the calculation of the channel idle periods at a source node, specifically the contiguous idle periods that allows the node to decrement the backoff, is a primary parameter in computing the transition rates between the MICS. Henceforth, the term *channel gap for a link* i is used to indicate the contiguous time that the channel is observed idle at the source of the link i. We first derive the probability that the channel will be idle for a single link. Later the channel gap distribution as seen by a link i due to interference from a set of links $I(i)$ is computed. Finally, we derive the various probabilities required for computing the rate of transition λ_{ab}.

Channel idle times for a single link

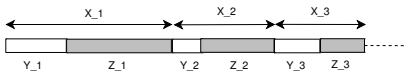

Figure 8.2: Alternating Renewal Process

In this paragraph, we derive the channel idle time distribution of a single link and compute the related variables. When the link is transmitting continuously over the channel, we represent the backoff time and transmission time as an *Alternating Renewal Process* [69] as shown in Figure 8.2. Let Y_n^i denote the backoff time chosen at before the n^{th} transmission and Z_n^i represent the packet transmission time for the n^{th} transmission by the source node of link i. $\{Y_n^i\}$ are i.i.d random variables with p.d.f. and c.d.f as f_Y and F_Y. $\{Z_n^i\}$ are i.i.d random variables with p.d.f. and c.d.f as f_Z and F_Z. Let $X_n^i = Y_n^i + Z_n^i$ and let f_x and F_x denote the p.d.f and c.d.f of X_n^i. $\{X_n^i\}$ represents the time taken to finish one cycle of backoff and transmission. In this derivation, the notations X_n, Y_n and Z_n are used to represent X_n^i, Y_n^i and Z_n^i, respectively. Let $N = \{N(t), t \geq 0\}$ be the renewal process with interarrival times $\{X_n\}$, where $N(t)$ represent the counting process

that denotes the number of transmissions in the time $(0, t]$. Let $M(t)$ represent the *renewal function* where $M(t) = E[N(t)]$ and $m(t)$ be the *renewal density*.

Interarrival times of the renewal process We first derive f_x, F_x, $m(t)$ and $M(t)$. X_n is the sum of two exponential variables Y and Z.

$$\begin{aligned} f_x(t) &= \int_{-\infty}^{\infty} f_Y(t-z) f_Z(z) dz \\ &= \int_0^t \beta e^{\beta(t-z))} \tau e^{-\tau z} dz \\ &= \beta\tau e^{\beta t} \int_0^t e^{(\beta-\tau)z} dz \\ &= \beta\tau e^{\beta t} \frac{1}{\beta-\tau} \left[e^{(\beta-\tau)t} - 1\right] \\ f_x(t) &= \frac{\beta\tau}{\beta-\tau} \left(e^{-\tau t} - e^{-\beta t}\right) \end{aligned} \tag{8.6}$$

Let the $f_x^e(s)$, $m^e(s)$ and $M^e(s)$ represent the laplace transforms of $f_x(t)$, $m(t)$ and $M(t)$. Then,

$$f_x^e(s) = \frac{\beta\tau}{(s+\beta)(s+\tau)} \tag{8.7}$$

$$\begin{aligned} m^e(s) &= \frac{f_x^e(s)}{1 - f_x^e(s)} \\ &= \frac{\beta\tau}{s(s+\beta)(s+\tau)} \end{aligned} \tag{8.8}$$

Hence,

$$m(t) = \frac{\beta\tau(e^{-(\beta+\tau)t} - 1)}{\beta+\tau} \tag{8.9}$$

$$\begin{aligned} M^e(s) &= \frac{m^e(s)}{s} \\ &= \frac{\beta\tau}{s^2(s+\beta)(s+\tau)} \end{aligned} \tag{8.10}$$

Hence,

$$M(t) = \frac{\beta\tau(\beta t + \tau t - 1 + e^{-(\beta+\tau)t})}{\beta+\tau} \tag{8.11}$$

Let $I(t)$ denote an indicator function with value 0 if the channel is idle and a value of 1 if the channel is busy. The *renewal-type equation* $g(t)$ is the probability that the channel is idle, i.e. $g(t) = P(I(t) = 0)$

$$g(t|X_1 = x) = \begin{cases} P(Y_1 > t|X_1 > t), & \text{if } x > t \\ g(t-x), & \text{if } x \leq t \end{cases} \tag{8.12}$$

We now derive the expression for $g(t)$.

$$g(t) = \int_t^\infty P(Y_1 > t|X_1 > t) f_x(x)dx + \int_0^t g(t-x) f_x(x)dx$$

Let the first term of the above equation be denoted as $h(t)$. Then

$$\begin{aligned} h(t) &= \int_t^\infty P(Y_1 > t|X_1 > t) f_x(x)dx \\ &= \int_t^\infty \frac{P(Y_1 > t, X_1 > t)}{P(X_1 > t)} f_x(x)dx \\ &= \int_t^\infty \frac{P(Y_1 > t)}{P(X_1 > t)} f_x(x)dx \\ &= \frac{P(Y_1 > t)}{P(X_1 > t)} \int_t^\infty f_x(x)dx \\ &= \frac{P(Y_1 > t)}{P(X_1 > t)} P(X_1 > t) \\ &= P(Y_1 > t) \\ &= 1 - F_y(t) \\ h(t) &= e^{-\beta t} \end{aligned} \tag{8.13}$$

$$\tag{8.14}$$

Applying the *Key Renewal Theorem*:

$$g(t) = h(t) + \int_0^t h(t-x)m(x)dx \tag{8.15}$$

$$\tag{8.16}$$

Using the result of Equation 8.13 and Equation 8.9 in Equation 8.15:

$$\begin{aligned}
g(t) &= e^{-\beta t} + \int_0^t e^{-\beta(t-x)}\Big(- \frac{\beta\tau}{\beta+\tau}(e^{-(\beta+\tau)x} - 1)\Big)dx \\
&= e^{-\beta t} - \frac{\beta\tau}{\beta+\tau}\int_0^t \Big(e^{-\beta(t-x)-(\beta+\tau)x} - e^{-\beta(t-x)}\Big)dx \\
&= e^{-\beta t} - \frac{\beta\tau}{\beta+\tau}\int_0^t \Big(e^{-\beta t-\tau x} - e^{-\beta(t-x)}\Big)dx \\
&= e^{-\beta t} - \frac{\beta\tau}{\beta+\tau}e^{-\beta t}\int_0^t \Big(e^{-\tau x} - e^{\beta x}\Big)dx \\
&= e^{-\beta t} - \frac{\beta\tau}{\beta+\tau}e^{-\beta t}\Big[\frac{1}{\tau}(e^{-\tau t} - 1) - \frac{1}{\beta}(e^{\beta t} - 1)\Big] \\
&= e^{-\beta t}\Big[1 - \frac{\beta\tau}{\beta+\tau}[\frac{1}{\tau}(e^{-\tau t} - 1) - \frac{1}{\beta}(e^{\beta t} - 1)]\Big] \\
g(t) &= \frac{\tau + \beta e^{-(\tau+\beta)t}}{\beta+\tau}
\end{aligned} \tag{8.17}$$

We now compute the asymptotic value of $g(t)$, which is of interest while estimating the long term probability that the link is idle.

$$\begin{aligned}
\lim_{t\to\infty} g(t) &= \frac{1}{t}\int_0^t g(u)du \\
&= \frac{E[Y_1]}{E[X_1]} \\
&= \frac{E[Y_1]}{E[Y_1] + E[Z_1]} \\
&= \frac{\frac{1}{\beta}}{\frac{1}{\beta} + \frac{1}{\tau}} \\
\lim_{t\to\infty} g(t) &= \frac{\tau}{\beta+\tau}
\end{aligned} \tag{8.18}$$

This completes the derivation of channel idle times for a single link.

Calculating idle probabilities for a set of links

In this section, we calculate the probability that the set of independent non-interfering links becomes idle in a given timeslot (p_{ci}). In a scenario where a link i experiences interference from a set of neighboring links $I(i)$, link i *first* sees an idle slot when none of the links in $I(i)$ are active. Calculating the probability that the channel *first becomes* idle for link i is useful determining when the link i may trigger the procedure to decrement DIFS and possibly, decrement the backoff later.

Let p_{LS_i} be the probability that source of the link i will start transmitting the packet at a given timeslot. This corresponds to one slot for each renewal cycle. Hence,

$$\begin{aligned} p_{\text{LS}i} &= \frac{1}{E[X(i)]} \\ &= \frac{1}{E[Y(i)] + E[Z(i)]} \\ &= \frac{1}{\frac{1}{\beta_i} + \frac{1}{\tau_i}} \\ p_{\text{LS}i} &= \frac{\beta_i \tau_i}{\beta_i + \tau_i} \end{aligned} \tag{8.19}$$

Similarly, the probability that the a link i is idle is denoted by $p_{\text{LI}i}$. This probability is equal to $\lim_{t\to\infty} g(t)$ that was given in Equation 8.18.

$$\begin{aligned} p_{\text{LI}i} &= \frac{E[Y(i)]}{E[X(i)]} \\ p_{\text{LI}i} &= \frac{\tau}{\beta + \tau} \end{aligned} \tag{8.20}$$

With the aid of $p_{\text{LS}i}$ and $p_{\text{LI}i}$ values for all the links in L, we now calculate the probability that the channel *first becomes idle* (denoted by $p_{\text{ci}}(L)$).

$$\begin{aligned} p_{\text{ci}}(L) &= P(\text{One of the Link } i \text{ starts, everyone else in } L \text{ is idle}) \\ &\quad - P(\text{Two links start, everyone else is idle}) \\ &\quad + P(\text{Three links start, everyone else is idle}) - \ldots \end{aligned} \tag{8.21}$$

Using these values for all the links in L, we can calculate the value of $p_{\text{ci}}(L)$. An example for estimating one of the terms in Equation 8.21 is given below.

$$P(\text{One of the Link } i \text{ starts, everyone else in } L \text{ is idle}) \quad = \quad \sum_{i \in L} \left(p_{\text{LS}i} \prod_{j \in L, j \neq i} p_{\text{LI}j} \right)$$

Channel gap distribution from a set of interfering links

In the previous section, we calculated the probability that the channel first appears idle for a given link. The source node has to transmits a packet only when the channel has been idle for a certain amount of time. In this section, we find the probability of distribution of these contiguous channel idle times that determine the transmission time for the source node. The channel gap lengths when a set of independent links are transmitting is first computed.

Competing exponential random variables Consider a set of independent links I. Each link k chooses a backoff period from an exponential distribution with parameter (β_k). Owing to the memoryless property of the exponential distribution, the probability that the link k will be idle for a time t is the same irrespective of the when k started its backoff procedure. The length of the *collective channel gap* (G), where all the links in I are inactive, is determined by a competing exponential random variables. Hence, the collective channel gap is exponentially distributed with the parameter ${\mu_g}^I = \sum_{k \in I} \beta$. Hence,

$$G(I) \sim \exp({\mu_g}^I) \quad \text{where} \quad {\mu_g}^I = \sum_{k \in I} \beta \tag{8.22}$$

Hence, the expected value of the collective channel gap is given by:

$$E[G(I)] = \frac{1}{{\mu_g}^I} \tag{8.23}$$

Collective Channel Gap for a link i due to independent links $I(i)$ The collective channel gap for a given link i when the set of independent links $I(i)$ that block its transmission is derived in this paragraph. The distribution of this parameter is necessary for computing the channel gaps

as seen by the source node of link i. Using this information, we can calculate the expected time that is required to decrement the backoff of link i and, possibly, transmit the packet. Given that link i has just observed a channel gap after the set of independent links $I(i)$ are idle, the length of the collective channel gap of the set $I(i)$ is given by the distribution similar to Equation 8.22. We denote this variable by $G(i, I(i))$.

Probability that the link transmits given that a channel gap is observed In this paragraph, we compute the probability that a link i transmits after successfully decrementing its backoff conditioned that a channel gap is observed. This probability is denoted by $\chi(i, I(i))$ where $I(i)$ is the set of independent links that interfere with i. Link i chooses a backoff period from an exponential distribution with parameter β_i (Equation 8.1). The channel gap length is given by the random variable G. The probability that the link i transmits is equivalent to the probability that the backoff value of link i (denoted by random variable Y) is lesser than the gap length G (Equation 8.22). We represent the density and c.d.f of Y (and G) by F_y and f_y (and F_g, f_g).

$$\begin{aligned}
\chi\big(i, I(i)\big) &= P(Y < G) \\
&= \int_0^\infty P(Y < t | G = t) dt \\
&= \int_0^\infty P(Y < t) P(G = t) dt \\
&= \int_0^\infty F_y(t) f_g(t) dt \\
&= \int_0^\infty (1 - e^{-\beta_i t}) {\mu_g}^{I(i)} e^{-{\mu_g}^{I(i)} t} dt \\
\chi\big(i, I(i)\big) &= \frac{\beta_i}{{\mu_g}^{I(i)} + \beta_i} \qquad (8.24)
\end{aligned}$$

Probability that the gap is greater than DIFS As explained earlier, the procedure to decrement the backoff is started only after the channel is observed idle for DIFS duration. The default values of backoff parameters chosen under IEEE 802.11 with $CW_{\min} = 31$ slots. The probability of a channel gap being greater than DIFS for a link i drops to significantly low value when multiple independent links of I have to be idle. In the FIM scenario, with the expected backoff length of 15.5 slots, a packet size of 1024 bytes and 2 Mbps channel, the probability that

the channel gap at link B is lesser than DIFS, conditioned that link A and link C are idle, is as high as 30%. This indicates that a significant number of channel gaps observed are not even sufficient to start the backoff procedure, consequently leading to severe contention unfairness. Hence, using the expected value of the channel gap length from the distribution of $G(I)$ predicts excess throughput for the link i assuming greater channel gap. The probability that the length of the channel gap is greater than DIFS (denoted by $p_D(G(I))$) can be directly obtained from the distribution of $G(I)$.

$$p_D\big(G(I)\big) = e^{-\mu_g{}^I \,\mathrm{DIFS}} \tag{8.25}$$

8.4.3 Computing the expected wait time until link i starts decrementing backoff

Consider a link i that is waiting to transmit a packet after a successful backoff procedure while the independent links $I(i)$ are transmitting. The backoff counter is decremented only after the channel is idle for DIFS slots. The paragraph computes the expected value of the time(in number of slots) that the node has to wait in order to *start decrementing its backoff*. If p_{ci} represents the probability that the links in $I(i)$ are inactive and p_D denotes the probability that the channel gap is greater than DIFS, then:

$$E[\text{wait time to start decrementing BO}] = \frac{1}{p_D \; p_{\mathrm{ci}}} \tag{8.26}$$

Backoff durations to enable transition Consider the transition between the two MICS M_a and M_b. At channel idle times, the links start the backoff procedure and the links that win the channel first is going to determine the transition between M_a and M_b. Hence, the competition to decrement the backoff between the links of M_a and M_b is going to determine the transition from MICS M_a to M_b. A transmission from any link $i \in C_{ba}$ will increase the chances of transition from M_a to M_b. Until now, we had computed the channel gaps that were seen by a link in MICS M_b. We now approximate the expected backoff value that the nodes in MICS M_b have to decrement to enable the transition.

An accurate estimation of the transition parameters using all the possible permutations of link transmissions is complex. We, hence, approximate the parameters for transition from MICS M_a to

M_b by considering the the links in the difference set C_{ba}.

Since the backoff periods of all the links are chosen from an exponential distribution (with respective parameters as given in Equation 8.1), the backoff period for any of the links from MICS M_b to win the channel can be considered as competing exponential random variables (Equation 8.22). We denote $G(C_{ba})$ as a random variable representing the backoff length to be decremented till a transition is observed from the MICS M_a to M_b.

8.4.4 Computing the expected time required for transition between MICS

A transition from MICS M_a to MICS M_b occurs only when the links that in the set $C_{ab} = M_a - M_b$ stop transmitting and the links in $C_{ba} = M_b - M_a$ starts transmitting. Using the above derivations of link idle time, channel idle time and probabilities of the link transmitting, we derive the expected time that a transition occurs between MICS M_a and MICS M_b.

In order to compute the expected time for transmition from M_a to M_b, we compute the following for all the links $i \in M_b$:

- $I(i) = \{k | k \in M_a, \text{k interferes with i}\}$: Set of links in the difference set C_{ba} that prohibits transmission of link i.
- $p_{\text{ci}}(i)$: The probability that the channel is idle at a given time slot since none of the links in $I(i)$ is transmitting.
- $p_{\text{DIFS}}(i)$: Probability that the channel gap is greater than DIFS
- $E[G(i, I(i))]$: Expected value of the gap length from the set of competing links $I(i)$
- E[wait time to start decrementing BO]: Expected value of the wait time to start decrementing the backoff

We approximate the overall expected values of wait time and channel gap length for all the links in C_{ba} and assume an exponential distribution with parameter $\alpha_1 = \frac{1}{E[G]}$ where G denotes the averaged channel gap length as observed by links in the set C_{ba}. The average wait time to start decrementing backoff by links in C_{ba} is represented as $E[W]$.

We then compute the the backoff period distribution ($G[C_{ab}]$ as given by Equation 8.22) that prohibits a transition from M_a to M_b. Let α_2 denote the parameter for this exponential distribution. The probability of transition from M_a to M_b conditioned that the links in C_{ba} has become idle is:

$$P(\text{Transition from } M_a \text{ to } M_b) = \frac{\alpha_2}{\alpha_1 + \alpha_2} \tag{8.27}$$

Based on the values of $E[W]$ and Equation 8.27, we now compute the expected time for transition from M_a to M_b .

$$E[\text{Time required for transition from } M_a \text{ to } M_b] = \frac{E[\text{wait time to decrement BO}]}{P(\text{Transition from } M_a \text{ to } M_b)} \tag{8.28}$$

The rate of transition from M_a to M_b, denoted by λ_{ab}, is given by Equation 8.29

$$\lambda_{ab} = \frac{1}{E[\text{Time required for transition from } M_a \text{ to } M_b]} \tag{8.29}$$

This completes the derivation of expected transition rates from one MICS to the other and hence the throughput model.

8.4.5 Example

The model is demonstrated through the "Flow in the Middle" example. Consider the FIM scenario as given in Figure 8.1(a). The parameters for the exponential distribution for the backoff (packet lengths) of the link A,B and C are given by β_A, β_B and β_C (τ_A, τ_B and τ_C) respectively. MICS $M_1 = \{A, C\}$ consists of links A, C and MICS $M_2 = \{B\}$ consists of link B. The set of all MICS $M = \{M_1, M_2\}$.

We now consider the derivation of parameters that is required for the transition from MICS M_1 to M_2, which is the more difficult and the interesting case. We first calculate the probability that link A, C will be idle at a given time t ($g_i(t)$ for each link) by using the Equation 8.17. The graph of $g_A(t)$ is shown by a blue line in Figure 8.3 with $\beta = \frac{2}{31}$ and $\tau = \frac{1}{241.75}$ which corresponds to the expected value of backoff duration under value of IEEE 802.11 (with $CW_{min} = 31$) and a packet

size of 1024 bytes. The red line in Figure 8.3 indicates $g_C(t)$ with different β and τ.

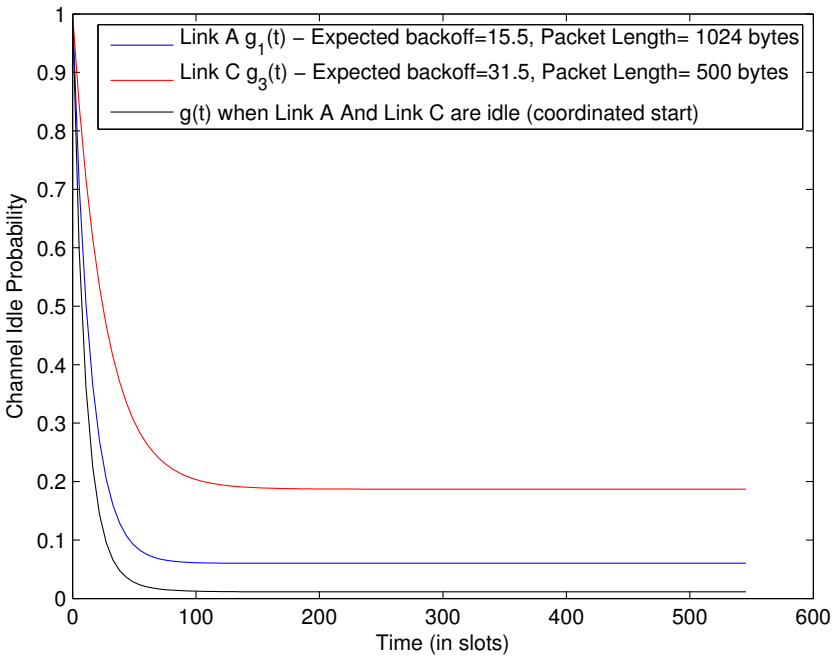

Figure 8.3: Idle channel probabilities

The probabilities $p_{\text{LI}i}$ and $p_{\text{LS}i}$ are calculated for links A and C by Equations 8.19 and 8.20. The probability that the channel is observed idle at link B at a given time slot depends upon link A and link C and occurs when both the links A and C are idle. This value ($p_{\text{ci}}(\{A, C\})$) is calculated by computing the probability that either link A is idle and link C becomes idle during this slot or vice-versa (Equation 8.21). The channel gap at B conditioned that the channel becomes idle at a given slot (denoted by $G(\{A, C\})$) can be calculated by the gap distribution in Equation 8.22. Link B is going to decrement its backoff only when the channel gap observed is greater than DIFS slots. The probability of B finding the channel gap period greater than DIFS, denoted by $p_D(G(\{A, C\}))$, is calculated by Equation 8.25. Having determined $p_{\text{ci}}(\{A, C\})$ and $p_D(G(\{A, C\}))$, we can determine the expected time to wait till the source of link B starts decrementing the backoff (E[wait time to start decrementing BO]) from Equation 8.26.

The next step is to calculate the probability with which link B is going to transmit conditioned that the channel has become idle which is denoted by $\chi(B, \{A, C\})$ by Equation 8.24. The overall

expected rate of transition from MICS M_1 to MICS M_2 (λ_{12}) is then calculated by Equation 8.29.

The expected rate of transition from MICS M_2 to MICS M_1 (λ_{21}) is similarly calculated and the limiting probabilities for occurrence of MICS M_1 and M_2 (denoted by P_1, P_2) are computed by solving Equation 8.3. Finally, throughput of the three links are computed by Equation 8.5.

8.4.6 Model Validation

The results of verifying the accuracy of the model in simple topologies is discussed in this section. A detailed investigation of the effectiveness of the model for the FIM problem is first studied and the random scenarios are later verified with simulations.

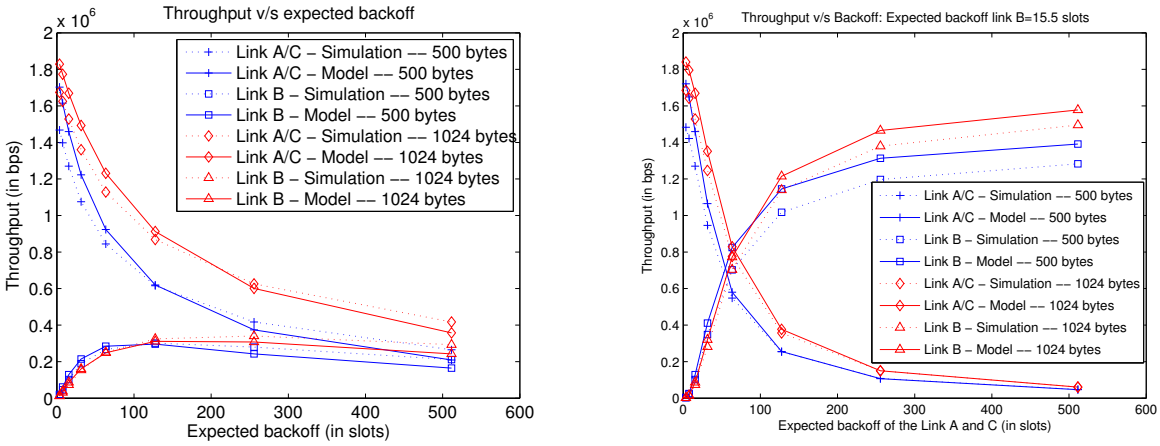

(a) All nodes with equal backoff window

(b) Vary the backoff of Link A and C

Figure 8.4: FIM: Comparison with simulation

Analysis of FIM In this paragraph, we validate the model in the FIM scenario. We first set the same β values for all the links and validate the model. We then alter the β to observe the starvation effect in the FIM scenario.

Figure 8.4(a) shows the FIM scenario where the packet sizes are varied. We plot the fraction of the throughput of the middle link (link B) as we vary the β of the links. It can be seen that there is acute starvation of link B during lower β due to the unavailability of channel idle times to observe DIFS and decrement the backoff. Fairness is achieved at very high backoff values at the

cost of severe throughput degradation. This demonstrates that fair contention cannot be ensured in multi-hop wireless networks by uniformly altering the value of backoff window.

In order to capture the effect of heterogeneous backoffs, we observe the throughput and fairness levels by varying the backoff window of Link A and Link C. This allows different channel idle times to be seen by link B. Figure 8.4(b) shows the fraction of the throughput at link B. As we vary the backoff window of the link A and link C, we see that the channel share of the link B increases drastically. It can be seen that the model predicts the throughput of the links with a good accuracy and, more importantly, demonstrates that the judicious choice of backoff values at each node can attain overall network fairness. This motivates the development of a "Contention-aware Adaptive Backoff Scheme (CABS)", which we describe in Section 8.5, that alters the backoff window appropriately to attain contention fairness while maintaining an acceptable overall throughput degradation.

Random scenarios Random scenarios were chosen such that there were no collisions (Or minimal collisions due to "co-ordinated source problem"). Two types of simulations were conducted: (1) A MAC with exponential backoff length and exponential packet size; and (2) Default IEEE 802.11 with CBR traffic. Figure 8.5 shows that the model accurately captures the throughput. The figure also conveys that the assumption of exponential backoff length and exponential packet size does not differ largely from the IEEE 802.11 MAC and CBR traffic (while long term throughputs are compared).

8.5 Contention-aware Adaptive Backoff Scheme (CABS)

In this section, the insights gained from the analysis and modeling of contention fairness is used to develop a distributed mechanism for altering $CW_{\min}$ to overcome unfairness. Henceforth, we refer to this adaptive backoff mechanism as "Contention-aware Adaptive Backoff Scheme" (CABS).

Contention unfairness primarily occurs in MHWNs when the source node observes a continuous busy channel due to the overlapping transmission by a set of independent links. In the FIM example, source node of link B has constant busy channel due to the overlapping transmissions from links

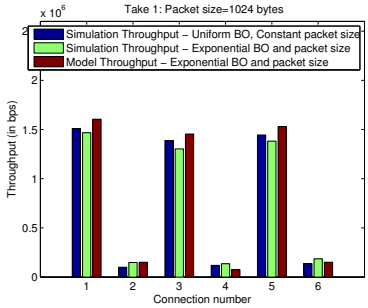

(a) Scenario 1

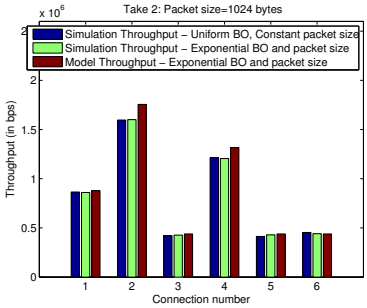

(b) Scenario 2

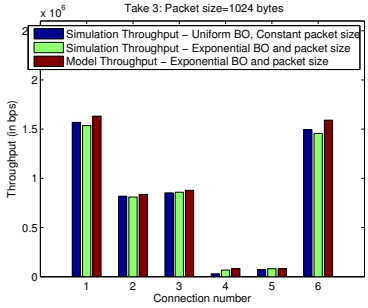

(c) Scenario 3

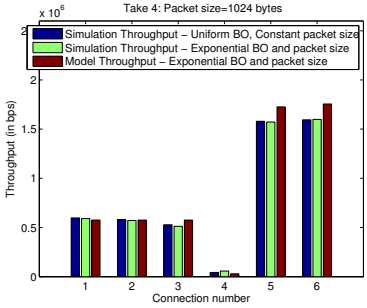

(d) Scenario 4

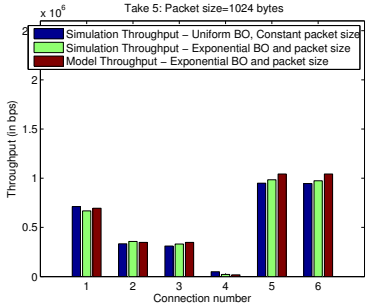

(e) Scenario 5

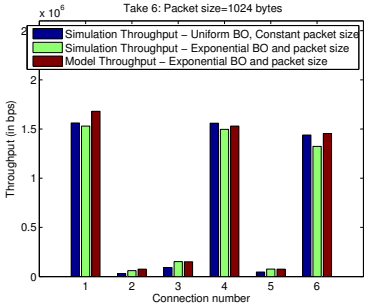

(f) Scenario 6

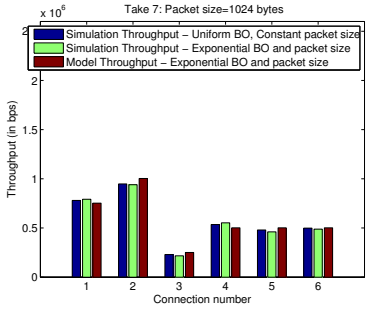

(g) Scenario 7

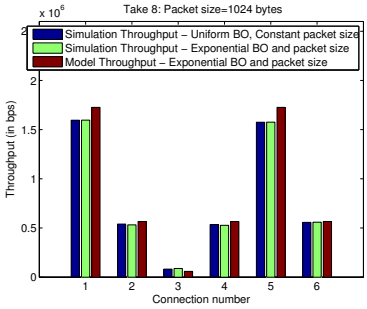

(h) Scenario 8

Figure 8.5: Throughput comparison in random scenario

$\{A, C\}$ transmit. The probability that link A and link C is idle reduces to the product $p_{\mathrm{LI}A}\ p_{\mathrm{LI}C}$. We propose a completely distributed approach to increase the chances of channel idle time as seen by a weak links (e.g. link B) and, hence, avoid unfairness.

8.5.1 CABS algorithm

The main idea of CABS is to observe the channel busy times at the neighbors and modify the $CW_{\min}$ at the source nodes accordingly. For example, in the FIM scenario, the links A and C overhear the contention observed at link B and suitably increase their $CW_{\min}$ to avoid unfairness for link B. We propose a contention aware adaptive backoff mechanism that adapts the $CW_{\min}$ based on the contention experienced by the neighbors.

As observed in the analysis of contention fairness, the link that experiences unfairness is characterized by a extended channel busy times due to the overlapping transmissions of the neighboring independent links. Hence, information about the average waiting time to successfully schedule one packet represents the contention experienced by the node. The time line is divided into equally spaced *epochs*. During each epoch, the contention metric ($C(X)$) of node X, such as the average wait times for one transmission $\bar{W}$ at every source node. Approximately once in every epoch, the contention information $C(X)$ is piggybacked with the packet. In addition to $C(X)$, the node also includes its current $CW_{\min}$ in the packet. Promiscuous mode is enabled at all the nodes in order to overhear neighbor's contention period. Another approach can be explicit transmission of contention broadcast information by the source nodes. However, this approach incurs added overhead of MAC/Physical layer headers for the small size of the contention information. Moreover, the conjested sources rarely capture the channel and contending for broadcast packet will be expensive.

Upon receiving the contention information from the neighbors, it updates a the neighbors contention information and, if necessary, adaptively alters its backoff window $CW_{\min}$. Each node maintains a "Contention Information Table" where it maintains the following information about its neighbor: (1) Neighbor address (X) (2) contention information $C(X)$; (3) The $CW_{\min}$; and (4) Time last updated. In order to support the network dynamism, each neighbor entry is purged if the contention information is not updated for a certain period of time.

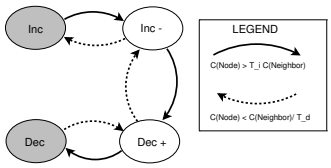

Figure 8.6: States of a node in CABS

Algorithm 5 shows the procedure to update $CW_{\min}$. The node additively increments/decrements the $CW_{\min}$ in constant steps (S_i/S_d). In order to avoid the oscillation between frequent incrementing and decrementing, the node observes the certain rules. Each node maintains the *state* which signifies its current alteration procedure. The four states of the node is represented in Figure 8.6. The node increments (or decrements) the backoff window only when it is in the pure increment "*Inc*" (or pure decrement, "*Dec*") state. Transition from *Inc* to *Dec* happens only through the transient states *Inc*− and *Dec*+ as shown in the Figure 8.6. The thresholds $T_i, T_d > 1$ (set to 1.3 in our simulations) limit also prevent oscillations when the contention information of the neighbors are similar. Also, the $CW_{\min}$ is incremented only if the neighbor's $CW_{\min}$ is lesser than the nodes $CW_{\min}$. A higher $CW_{\min}$ of the neighbor may also signify a neighbor who is waiting for other starved neighbors and not a starved neighbor. Similar approach is taken for decrementing $CW_{\min}$.

Algorithm 5 CABS: Backoff adaptation algorithm

Require: Node X promiscuously receives a packet from node Y
  {// S_i/S_d = *The increment/decrement step – number of slots to increment/decrement*}
  {// T_i/T_d = *The threshold factor for incrementing/decrementing* $CW_{\min}$. $T_i, T_d > 1$}
  {// *state* = *The current state of the node. state* $\in \{Dec, Dec^+, Inc^-, Inc\}$}
  {// $CW_{\min}(N)$ *The* $CW_{\min}$ *of node* N}
  {// $C(N)$ *The contention metric of node* N.}
  Extract $CW_{\min}(Y)$, $C(Y)$ from the received packet and update neighbor contention table
  if $C(X) > T_d C(Y)$ **then**
    {// *Decrement* $CW_{\min}(X)$ *to compete more aggressively, if necessary*}
    Decrement *state*
    Additively decrement $CW_{\min}$ by step S_d, if *state* = *Dec*
  else if Y is the most contended neighbor AND $C(X) > T_i C(Y)$ **then**
    {// *Increment* $CW_{\min}(X)$ *to compete less aggressively, if necessary*}
    Increment *state*
    Additively increment $CW_{\min}$ by step S_i, if *state* = *Inc*
  end if

8.5.2 Simulation Validation

In this section, we evaluate the effectiveness of the protocol by simulation. We use the QualNet simulator [105] with default parameters and alter the backoff procedure according to the CABS. We first analyze the FIM example and then evaluate the random scenarios.

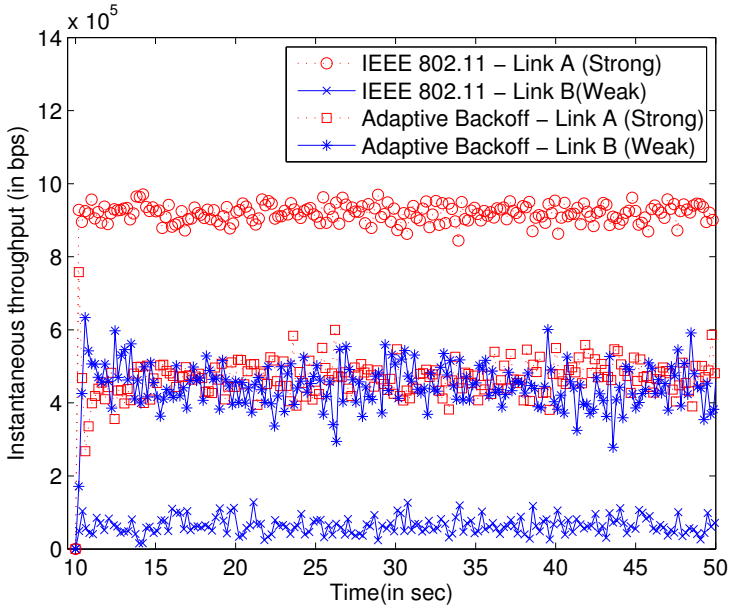

Figure 8.7: Instantaneous Throughputs

FIM scenario In the FIM scenario, the weak link (link B) suffers severe unfairness under the default backoff mechanism due to constant busy channel from the stronger links (Links A and C). Figure 8.7 compares the proposed CABS with the default backoff mechanism of IEEE 802.11 with a saturated CBR traffic packet with 200 bytes packets. Link B obtains only about 6% of link A/C's throughput. The figure also demonstrates that the CABS attains superior long term fairness for the links. However, regulating the short term fairness in FIM scenario is challenging since ensuring sufficient channel gaps to link B (in the presence of the overlapping transmissions from Link A/C) at a short intervals. TDMA based slotted access schemes can ensure such short term fairness. However, efficient slot assignment in a multi-hop wireless networks, with possibly varying packet sizes, incurs additional overhead and the objective of the CABS was to demonstrate

fairness properties in a pure CSMA scheduling

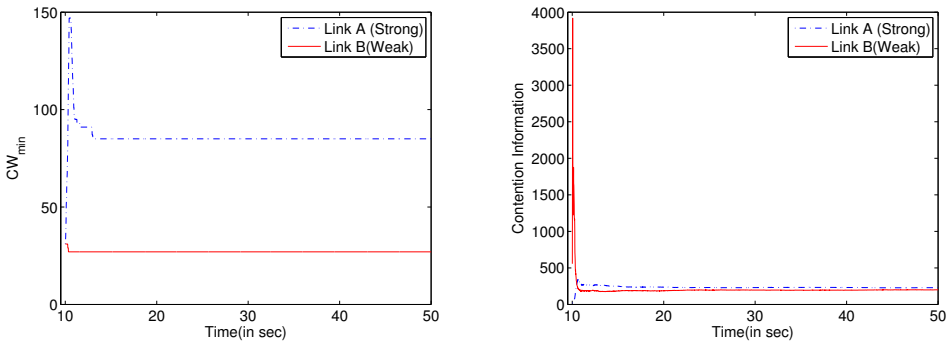

(a) Backoff values (b) Contention information

Figure 8.8: Analysis of CABS for FIM scenario

Figure 8.7 also shows the convergence and stability of the protocol. Figure 8.8(a) demonstrates the adaptation of the backoff windows and Figure 8.8(b) shows the contention information $C(X)$ of the links A and B. The contention information used for the protocol was a function of $\bar{W}$ and the average number of channel gaps that was observed ($\bar{nG}$) for one successful channel transmission.

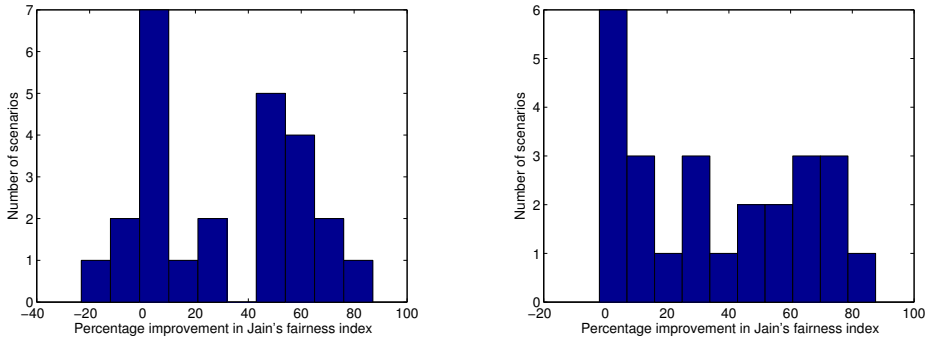

(a) 5 connections (b) 6 connections

Figure 8.9: Random Scenario: Analysis of fairness in CABS

General scenarios This section describes the results of random scenarios with varying number of one-hop connections. We compare the fairness of the connections using Jain's fairness index [64]. The fairness index $f(x_1, x_2, \ldots, x_n)$ for n connections with throughputs $(x_1, x_2, \ldots, x_n)$ is defined by Equation 8.30. This index maps the fairness of the flows to a number between 0 and 1, 0 being

unfair and 1 being completely fair.

$$f(x_1, x_2, \ldots, x_n) = \frac{\left(\sum_{i=1}^{n} x_i\right)^2}{n \sum_{i=1}^{n} x_i^2} \tag{8.30}$$

25 random scenarios of 5 and 6 one-hop connections were simulated and the fairness index is measured. The histograms in Figure 8.9 plots the histogram of the percentage improvement of fairness in the proposed protocol over the standard IEEE 802.11. It can be seen that improvement of upto 80% is achieved using the proposed CABS. While achieving fairness reduces the overall network throughput, the results indicate that an average improvement of the fairness was approximately 25% and average throughput degradation was only 15%. The histograms in Figure 8.9 also show a significant number of scenarios with no improvement. However, it can be seen that large fairness benefits can be achieved if the scenarios starve due to contention fairness. The investigation into the individual scenarios reveal that the a high order of fairness improvement can be achieved when: (1) A link is present only in the lower order MICS (MICS with lesser number of links). (2) Transition to certain MICS is only possible when multiple independent links are idle. Both of these properties are present in the FIM and have been accounted in the model.

Metric \ Flows	4	5	6
Fairness	1.22	1.24	1.3
Throughput	0.9	0.86	0.83

Table 8.2: Performance study of CABS: Ratio of performance metric in CABS to IEEE 802.11

Table 8.2 summarizes the performance of the CABS by varying the number of one-hop flows in the network. The mean of fairness index for a given scenario and the mean throughput per connection are evaluated. The ratio between the CABS and the IEEE 802.11 is shown in the Table 8.2. It can be seen that around 25% improvement is seen in the fairness levels

Discussion While the simulation demonstrates the feasibility of achieving fairness through simple protocols, the protocol can be enhanced by: (1) Tuning the various parmeters to their optimal values which may be scenario specific; (2) Choice of different $CW_{\min}$ update schemes like Multiplicative Increase/Linear decrease(MILD); and (3) A hybrid approach that uses a slotted approach and

CABS. By adapting $CW_{\min}$ at every slot boundary, the competition during the slots can be biased towards the unfair nodes such that short term fairness is achieved. (4) In the current scheme, the dissemination of the contention information is not reliably transmitted to all the interfering sources. While some interfering sources fail to capture the contention information packet due to low signal strength, others sources experience a packet collision due to neighboring transmissions. While reliable delivery can be attained using additional control channels, delivering the information over a single channel will increase the utility of such the protocol in the general wireless network. Moreover, disseminating the information to all the interfering neighbors within the the small durations of channel gaps is challenging. We wish to pursue the evaluation of such schemes in the future.

8.6 Conclusions and Future work

In this chapter, we analyzed the fairness issues due to the inherent nature of CSMA contention. We proposed a framework to capture such contention fairness and estimate the throughput. We proposed an accurate and constructive throughput estimation model that accounts for contention fairness. The novelty of the model, apart from a detailed derivation, is its generality to enable varying parameters like packet sizes and $CW_{\min}$. Enhancing the model to account for unsaturated traffic, where fairness plays a less important role, is a part of the immediate future work. The insights gained from analysis and model was used to propose a *contention-aware adaptive backoff scheme*. This backoff adaptation mechanism converged to provide fair access to starving links without an acceptable throughput degradation.

Incorporating such starvation due to contention into the routing models proposed in Chapter 5 would enable a more accurate estimation of the scheduling properties in a routing model. This is a part of the future work. The observations and the analysis of the proposed model can be applied for designing a distributed MAC protocol to account for contention fairness. This is another study that we wish to pursue.

Chapter 9

Throughput Estimation Model for Two-flows

Characterizing the impact of interference remains a primary challenge in MHWNs in general and in this work in particular. Incorporating the effect of scheduling takes an important step in improving the interference estimate; however, deep understanding of how interference occurs remains an important and relatively open problem. In this chapter, we model from first principles the behavior of two interfering one hop links in isolation. We believe that such an analysis represents an important first step in understanding the effect of interference.

Existing studies reveal that the two links interact in numerous ways based on the interference relationship between the links and interactions with similar behavior has been grouped into different categories. In this chapter, we develop a throughput estimation model for various categories of interactions that have been identified in MHWNs.

9.1 Introduction

In Multi-Hop Wireless Networks (MHWNs) that use Carrier Sense Multiple Access (CSMA), interference is manifested in different modes of operation, which can lead to poor performance and short term or long term unfairness. Complex interactions occur between interfering links based on

the relative location of the senders and receivers (more accurately the state of the channels among them). These interactions play an important role in determining performance, and give rise to long or short term unfairness. Understanding these interactions is critical for understanding and characterizing behavior in MHWNs and for designing effective protocols for them.

Existing studies have analyzed and classified different behaviors that arise between two interfering links that use the IEEE 802.11 protocol [42,110]. Understanding and characterizing interactions at this level using formal techniques is a promising first step towards an understanding of the effect of interference from first principles, and in designing protocols that more effectively account for it.

More recently, the study by Razak et al. [108] has identified and analyzed additional interactions that occur under a more advanced model of interference (*Two Disc* interference model). The probability of occurrence of interactions and the nature of interaction has also been studied. The contribution discussed in this chapter is a part of combined effort to characterize the throughput of two-flows under a Two-disc model of interference [108]. The chapter proposes throughput estimation models for all the five categories identified in the paper [108] and verifies them with the simulation.

9.2 Related work and Background

In this section, we first summarize the interactions that was identified in a *One disc model* of interference [42] and then briefly discuss the interactions that were studied by Razak et al. [108] under a *Two Disc model* of interference.

9.2.1 Interactions in One disc interference model

Garetto et al [42] categorize the two-flow interactions using a *one disc model* where the transmission radius is equal to the interference radius. The two links are represented by S_1D_1 and S_2D_2 where S_i represents the sources and D_i represents the destinations. In a two flow scenario, two senders S_1 and S_2 communicate with two receivers D_1 and D_2 respectively. There exist four secondary (or cross-flow) channels that lead to the different modes of interactions; these are S_1S_2 S_1D_2, S_2D_1 and D_1D_2. The nodes for each secondary link can be either in range or out of range, leading to 2^4 different scenarios corresponding to the different combinations of states that each of the four

secondary links can be in. The 16 scenarios can be reduced to 13 by eliminating the dual scenarios (mirror scenarios that are identical by relabelling the connections). They compute the occurrence probability of each of the scenarios conditioned on a fixed distance between the primary senders and receivers. More interestingly, they recognize that the individual scenarios can be grouped into three basic categories described below.

- **Sender-Connected (SC):** This category includes all scenarios where the two senders are in range. Thus, CSMA prevents senders from concurrent transmission, and no collisions other those arising when the two senders start transmission at the same time will occur. Such collisions are unavoidable, and their probability is low due to the randomization of the backoff period.

- **Asymmetric Incomplete State (AIS):** In the remaining scenarios the senders are not connected (Incomplete State). A distinguishing attribute is whether the state of the S_1D_2 and S_2D_1 links are identical (Symmetric) or different (Asymmetric). In Asymmetric Incomplete State, only one of the senders interferes with the other destination and only one the flows experiences collisions.

- **Symmetric Incomplete State (SIS):** In this category, the senders are not connected. However, either both the senders can interfere with the other destination, or they cannot. In these scenarios, short term unfairness may arise, but no bias exists to lead to long term unfairness.

9.2.2 Interactions in Two disc interference model

We now briefly discuss the categories of interactions between two-flows under a Two-disk model of interference [108]. We assume the IEEE 802.11 basic mode (without RTS/CTS), which is the default mode in most of the IEEE 802.11 network cards.

In order to enable communication on the link, the source and destination of the flow have to be within communication range. The possible relations between the four secondary flows (S_1S_2, S_1D_2, D_1S_2 and D_1D_2) are: (1) in communication range; (2) in interference range, but not in

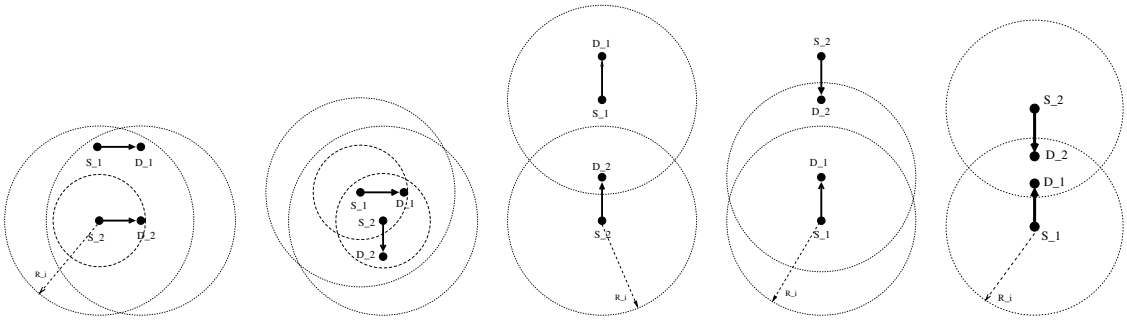

(a) SCSI (b) SCAI (c) AIS (d) IDIS (e) SIS

Figure 9.1: Sample scenarios in each category

communication range; (3) out of range. Based on these relationships between the secondary flows, the interactions can be classified into five types:

- **Senders Connected Symmetric Interference (SCSI):** SCSI represents sender connected scenarios where there is *symmetric* interference between opposite source and destination. For example, if link S_1D_2 is in interference range then D_1S_2 is also in interference range. Figure 9.1(a) shows a sample SCSI scenario. Flows in this group share the medium fairly due to symmetry.

- **Senders Connected Asymmetric Interference (SCAI):** In SCAI: (1) the senders are within communication range of each other; (2) One sender and the opposite receiver (belonging to the other flow) are in interference range (e.g., $S_1D_2 \leq R_i$ in Figure 9.1(b)); and (3) The other sender and receiver are not in interference range of each other.

  Figure 9.1(b) shows a SCAI scenario where S_1 and D_2 are in interference, but not in communication, range. Under IEEE 802.11, S_1 can sense the channel busy when D_2 sends an ACK to S_2, but cannot decode the packet. It perceives such a busy signal as an ongoing transmission. In order to avoid a possible collision, S_1 waits for the channel to be idle for an EIFS period (a significantly larger period than the standard DIFS inter-frame separation) to ensure completion of the ongoing transaction. S_2 receives the ACK from D_1 and waits for DIFS before decrementing its backoff. As a result, S_2 wins the channel again and long term unfairness occurs.

- **Asymmetric Incomplete State (AIS):** This category is identical to the AIS category in the original classification. Specifically, (1) the senders are out of interference range (incomplete state); (2) One source and the opposite receiver are in interference range; and (3) The second source and its opposite receiver are out of range. Figure 9.1(c) shows a sample AIS scenario. Many of the packets sent to D_2 are lost because of interference from S_1, while D_1 receives all packets from S_1 successfully.

- **Interfering Destinations Incomplete State (IDIS):** This category is a absent in the *one disc* interference and was identified by Razak et al. [108] under the Two disc interference model. This group includes scenarios where all the secondary links are out of range except the two destinations. Figure 9.1(d) shows one such scenario. Since both the sources are out of range (not sender connected), they transmit packets simultaneously. The destination that receives its packet sends an ACK, thus causing a collision for the ongoing packet transmission at the other destination. This causes short term unfairness for each link. IDIS is a *Sender Unconnected*, *Symmetric* and *Incomplete state* scenario that experiences drops due to ACK packets.

- **Symmetric Incomplete State (SIS):** The senders are out of range and both sets of opposite source and destination are within communication or interference range. Figure 9.1(e) shows a scenario with SIS. Since the two senders are out of range, they can transmit simultaneously. Since each destination can be interfered by the opposite source, there is a packet drop at both the destination. This will cause significant throughput degradation for both links.

9.3 Throughput model for two-flows

In this section, we propose a model for the computation of throughput for the proposed categories. We derive the throughput model under a homogeneous network where the all the nodes have the same MAC level parameters. The channel capacity is denoted by C. The minimum and maximum backoff window is represented by $\mathrm{CW}_{\min}$ and $\mathrm{CW}_{\max}$, respectively. The packet loss probability given that the link transmitted a packet (conditional collision probability [14]) is represented by

p. The probability that a source node starts transmission during an idle slot is denoted by τ. Bianchi [14] derived the expression for τ under Binary Exponential Backoff (BEB) as a function of p (Equation 9.1).

$$\tau = \frac{2q(1-p^{m+1})}{q(1-p^{m+1}) + \mathrm{CW}_{\min}[1-p-p(2p)^{m'}(1+p^{m-m'}q)]} \tag{9.1}$$

where $q = 1-2p$, m is maximum number of retries and m' is the number of stages to reach $\mathrm{CW}_{\max}$ ($m' \leq m$). The p and τ for the link i is denoted by p_i and τ_i respectively. Bianchi's model accounts for the probability of transmission in a given slot based on the binary exponential backoff model.

We make the following assumptions: (1) The traffic on both the links is saturated. Under less than saturated assumptions, the interactions will play a less important role. It should be possible to extend the model to account for different packet assumptions; and (2) The nodes use the basic mode of IEEE 802.11 (without RTS/CTS), which is becoming the default mode in the network cards due to its superior performance in a majority of the scenarios. Extension of the model by relaxing the above assumptions is an area of future work.

For the SCSI, where the links have a fair-share of the channel without the hidden terminals, the throughput can be directly estimated using techniques similar to Single-hop wireless network (for example, Bianchi's model [14]). We briefly show the derivation of the model for the four other categories.

9.3.1 SCAI formulation

Under SCAI category, the sources are within interference range of each other and hence the transmission from the sources will not overlap. However, the EIFS effect causes one of the links (which we refer to as the 'weaker link') to wait for longer times before decrementing the backoff, thus causing throughput degradation.

Let τ_1 (τ_2) be the probability that the source of the weaker (stronger) link transmits the data packet, conditioned on the channel being idle. Since the links share a common channel, the probability of winning the channel for transmission by the weaker and the stronger link are in the ratio $\tau_1 : \tau_2$. Both the links suffer no hidden terminals ($p = 0$ for both links). Hence, the throughput

of the link i is given by the Equation 9.2. l_i and o_i denotes the time required to transmit the data payload and the overhead per transmission, respectively. The overhead includes the time to transmit the physical and MAC layer headers and the propagation delay along with the average backoff duration to transmit one packet ($\frac{CW_{\min}}{2}$).

$$T_i = C\frac{\tau_i}{\tau_1 + \tau_2} \cdot \frac{l_i}{l_i + o_i} \tag{9.2}$$

The second part of Equation 9.2 denotes the fraction of the transmission time that is used to send the payload. The stronger link always transmits with the same probability *when the channel is idle*. Hence, τ_2 can be calculated by equation 9.1. The only variable to be computed is τ_1 to determine the throughput of both the links.

Since we are interested in calculating the *transmission probability conditioned on the channel being idle*, we ignore the time during which the channel is busy. An idle slot can be in one of the backoff/EIFS states (a countable state space). And, the weak link will transmit when the backoff counter is zero (a subset of the state space). Hence, we use a discrete time Markov chain to calculate the probability of transmission at an idle slot (τ_1).

We refer to the source of the weaker link as *the node* in this derivation for clarity purpose. Under an idle slot, the node may be decrementing its backoff or experiencing an EIFS wait period. We also assume that the DIFS period (which is realistically around $50\mu s$) is zero since it is greatly lesser than the EIFS period (around $380\mu s$). Simulation validation shows that this approximation is reasonable.

In order to compute the state space, we observe that the source may be decrementing its backoff or experiencing an EIFS wait period during an idle slot. The i^{th} backoff stage is denoted by $B(i)$ where $0 \geq i \geq \text{CW}_{\min}$. We represent the EIFS duration by M slots where slot j represents the number of slots left for completion of the EIFS duration. $E(i,j)$ denotes the j^{th} EIFS slot during the i^{th} backoff stage and $0 \geq j \geq M$. $B(i)$ and $E(i,j)$ are the states of the chain. The chain is represented in Figure 9.2. In this figure, the variable τ_2 is represented as t.

The channel becomes busy for the weaker link when the stronger link starts transmitting during

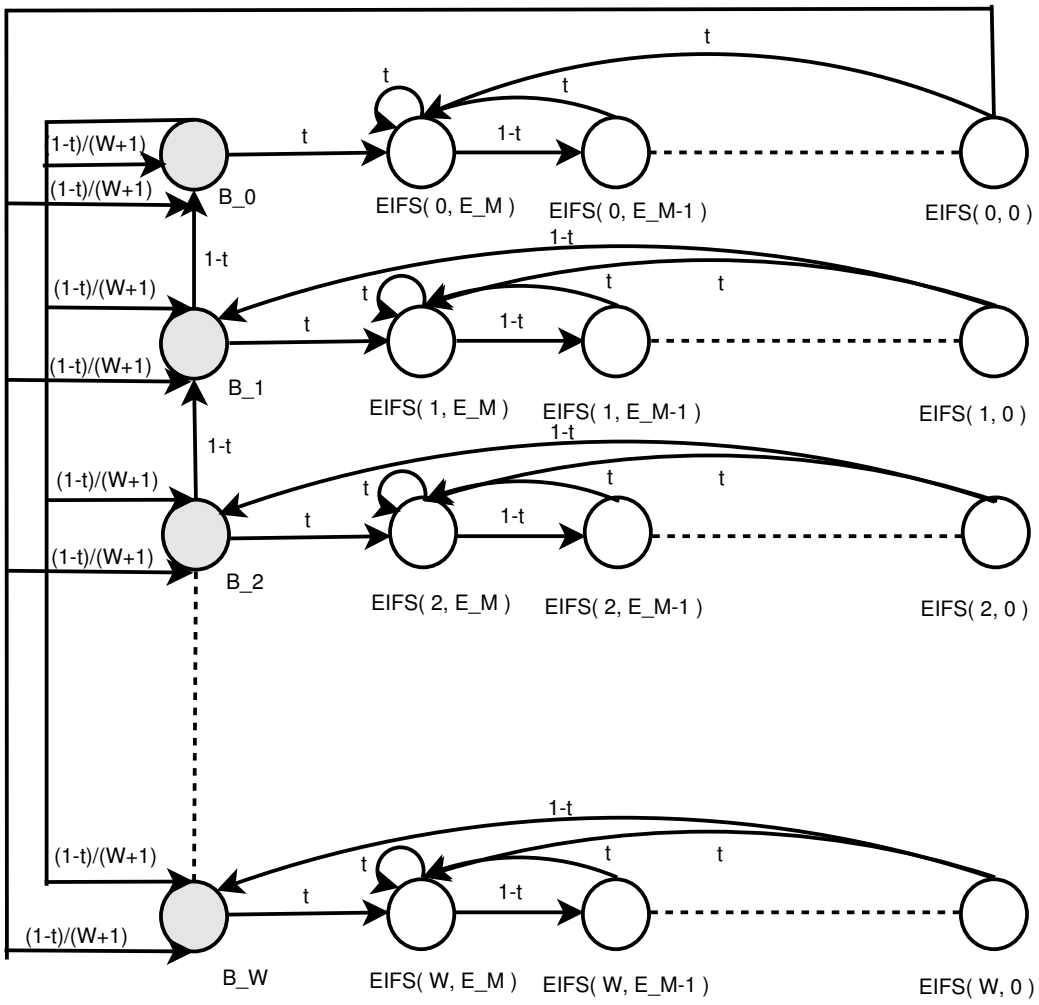

Figure 9.2: Markov chain for EIFS calculation

an idle slot (τ_2). The value of τ_1 is dependent upon τ_2 since the weaker link experiences greater EIFS related backoffs when τ_2 is higher. However, τ_2 is independent of τ_1. The transition probabilities between the states are represented in Table 9.1 and are calculated based on the following set of rules.

During the backoff period, a node will move from backoff stage $B(i)$ to backoff state $B(i-1)$ when the channel is sensed idle at the end of a slot (Rule 1). If the channel is sensed busy, it will freeze the backoff and start its EIFS (at state $E(i, M)$) once the channel becomes idle again (Rule 2). While in EIFS, the node will decrement the number of EIFS slots to wait if the channel

Rule	From	To	Probability
1	B(i), $i \neq 0$	B(i-1)	$1 - \tau_2$
2	B(i)	E(i,M)	τ_2
3	E(i,j), $j \neq 0$	E(i,j-1)	$1 - \tau_2$
4	E(i,j)	E(i,M)	τ_2
5	E(i,0), $i \neq 0$	B(i)	$1 - \tau_2$
6	B(0)	B(i)	$\frac{1-\tau_2}{\mathrm{CW}_{\min}+1}$
7	E(0,0)	B(i)	$\frac{1-\tau_2}{\mathrm{CW}_{\min}+1}$

Table 9.1: Transition probabilities

is sensed idle (Rule 3). If the channel becomes busy during an EIFS, the node will resume EIFS from the start when the channel is sensed idle again, hence moving to the state $E(i, M)$ (Rule 4). When the backoff stage reaches 0 (stage B(0)), the node will transmit the packet and then choose a uniform random backoff from $[0, \mathrm{CW}_{\min}]$ upon the successful completion of DIFS(Rule 6). Similar explanations can be provided for the other rules.

The node starts transmitting the packet only when the channel is idle at the slot boundary when: (1) the backoff counter is zero (state $B(0)$); or (2) The EIFS period is completed and backoff counter is zero (state $EIFS(0,0)$). Hence, the probability with which the node starts transmitting a packet at an idle time slot (τ_1) is given by Equation 9.3.

$$\tau_1 = (1 - \tau_2)(\Pi_{B(0)} + \Pi_{EIFS(0,0)}) \tag{9.3}$$

where Π are the limiting probabilities of the above chain.

Figure 9.3 validates the model by comparing it with simulation (with standard MAC parameters). The simulation was conducted using the QualNet simulator, which implements a detailed model of IEEE802.11 [105]. Packet size was varied from 200 bytes to 1024 bytes. Since the links compete with a ratio $\tau_1 : \tau_2$, a constant ratio of the throughput between the weak and the strong link can also be seen (24% according to the simulations and 32% according to the model). The comparison between the model and the simulation the indicates that the assumptions of the model (especially the discrete EIFS slots and independence of τ_1) are reasonable.

We now model the categories with hidden terminals (AIS, SIS and IDIS). The models include

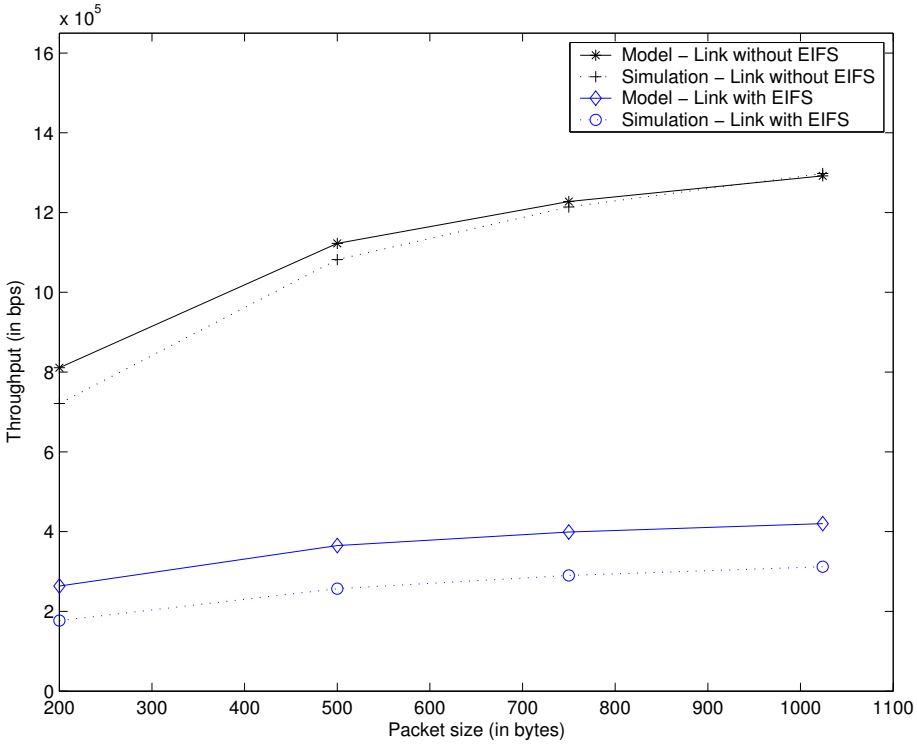

Figure 9.3: Throughput study for EIFS effect

the impact of the backoff mechanisms in a manner that allows different strategies to be evaluated. We first derive a general throughput estimation model and discuss the effect of hidden terminals with respect to this model.

9.3.2 General Hidden Terminal Scenario

In this section, we derive a generic model to compute the *long-term* throughput of the links under hidden terminals using *Renewal Reward Process*. We then specialize this model to account for the different interaction cases. Figure 9.4 shows the abstraction of the events observed at a source between two successful packet transmissions.

Modeling long-term throughput as a Renewal Reward process

Consider the process of a source transmitting a packets. Let t_s and t_u represent the constant packet transmission durations for a successful and unsuccessful attempt, respectively. The source waits

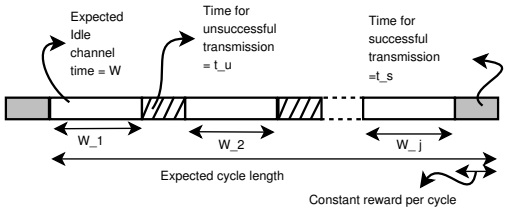

Figure 9.4: Packet transmission attempts

for a certain amount of time when the channel is idle (to decrement its backoff) and transmits the packet. The probability that a link starts transmitting at an idle slot is denoted by τ (conditional transmission probability) [14]. The packet may be successfully transmitted or may lead to a collision. Let p represent the packet loss probability given that the link transmitted a packet (conditional collision probability [14]). Let W_i be the random variable denoting the wait times before the source transmits the packet. Let U_j be the number of attempts before successfully transmitting a packet. We assume the following (1) W_i are iid random variables; (2) The transmission initiation (transmit or not transmit in a given timeslot) and its result (success or collision) are Bernoulli trials; (3) W and U are independent. Under these assumptions, the long-term expected value of W is given by Equation 9.4. The expected value of U is given by Equation 9.5.

$$E[W] = \frac{1}{\tau} \tag{9.4}$$

$$E[U] = \frac{1}{1-p} \tag{9.5}$$

Consider the process where a source waits for a certain amount of time (W_i) and transmits a packet. Consider a renewal process which constitutes of each cycle ending with a successful transmission. Figure 9.4 shows one such cycle. Let $W_1, W_2, \ldots, W_i$ denote the wait times before each transmission and let $U_j = u$ represent the number of attempts before a successful transmission in one such cycle. We now find the expected value of the time required to complete one cycle (one

successful transmission) given that $U_j = u$. We note that $U_j \geq 1$.

$$\begin{aligned} E[\text{cycle length}|U_j = u] = & \quad E\Big[\big(\sum_{i=1}^{u}(W_i + t_u)\big) - t_u + t_s\Big] \\ = & \quad \Big(\sum_{i=1}^{u}(E[W_i] + t_u)\Big) - t_u + t_s \\ = & \quad u(E[W_i] + t_u) - t_u + t_s \end{aligned}$$

Now, the expected value of the cycle length is given by:

$$\begin{aligned} E[\text{cycle length}] = & \quad E\big[E[\text{cycle length}|U_j = u]\big] \\ = & \quad E[u](E[W_i] + t_u) - t_u + t_s \quad \text{(since } W \text{ and } U \text{ are independent)} \end{aligned}$$

We now apply the renewal-reward theory to predict the long-term throughput. The expected reward per cycle is the number of payload bits transmitted in one cycle which is equal to Ct_s. Hence, the long-term throughput is given by Equation 9.6.

$$T_i = \frac{\text{Expected reward per cycle}}{E[\text{cycle length}]} \tag{9.6}$$

$$= \frac{Ct_s}{n_u(t_w+t_u)-t_u+t_s} \tag{9.7}$$

where $n_u = E[U]$ and $t_w = E[W]$ as given by Equations 9.4 and 9.5. The variables that need to be computed are p and τ, which vary based on the type of hidden terminal. The time required to transmit the DATA packet for link i is represented as l_i. We assume that both the links have the same data packet size.

9.3.3 AIS formulation

Recall that in AIS, a source of one link can cause collision at the destination of the other, but not vice versa. Figure 9.5 shows this case where a transmission from S_1 can cause a collision at D_2. The transmission of S_2D_2 will succeed only during the idle periods of the link S_1D_1. This can lead

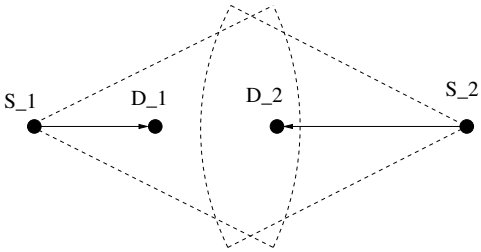

Figure 9.5: Hidden Terminals in AIS

to severe long term unfairness for S_2D_2.

We explain the derivation with respect to the scenario in Figure 9.5. The estimates for link S_1D_1 is straight forward since the link does not experience any hidden terminals. Hence, the value of $p_1 = 0$ and the value of $\tau_1 = \frac{2}{\mathrm{CW}_{\min}}$.

Let p_2 and τ_2 represent the p and τ for link S_2. The link S_2D_2 can transmit only when S_1D_1 is not active, otherwise the transmission from S_1 will cause a packet collision at D_2. Let p_2 be the probability that the packet transmitted by S_2 will result in a collision conditioned on S_2 transmitting a packet. Let τ_2 be the probability that link S_2 starts transmitting at an idle slot.

Deriving p_2:

We first derive the success probability $(1 - p_2)$ of link S_2D_2. The packet transmission of S_2D_2 is successful only if the complete packet of S_2D_2 is transmitted when S_1 is inactive. A single slot of overlap between S_1D_1 and S_2D_2 can cause a packet collision at D_1. Let i be the congestion window (CW) chosen by the link S_1D_1. The link S_2D_2 can be successful only if the complete transaction of S_1D_1 lies within that duration of i slots. For example, as shown in Figure 9.6, let S_1D_1 choose a backoff of $i = 10$ slots and let $l_2 = 7$ slots. A transmission of S_2D_2 will succeed only if the 7 slots of transmission lie within the 10 slots when S_1D_1 is idle. As seen from the Figure 9.6, there are 4 possible arrangements of a successful transmissions out of 10 possible ways.

Generalizing this *arrangement* of l_2 slots in i slots of idle period, it can be shown that there are $(i - l_2 + 1)$ ways of placing a successful transmission from S_2D_2. Let $p'_2(i)$ be the probability that the transmission from link S_2D_2 succeeds given that S_1D_1 has chosen a backoff window of i. Equation 9.8 gives $p'_2(i)$ based on the number of successful *arrangements* of the transmission.

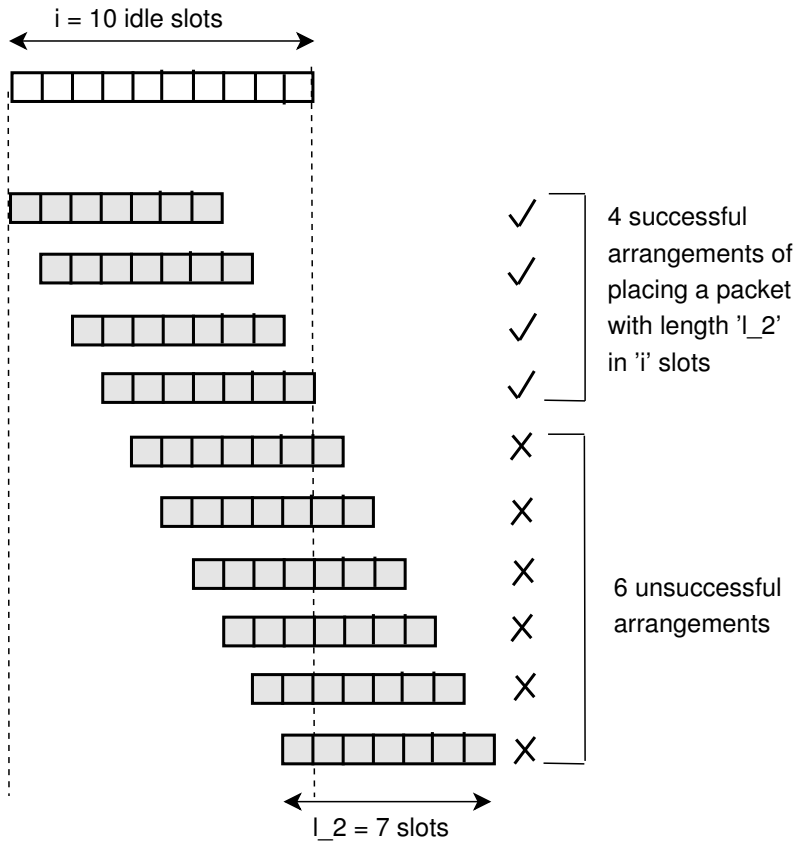

Figure 9.6: Packet success in AIS. i represents the CW chosen by S_1D_1 and l_2 denotes the packet length of the link S_2D_2

$$\bar{p}_2(i) = \begin{cases} 0, & if\ i < l_2 \\ \frac{(i-l_2+1)}{i}, & otherwise. \end{cases} \tag{9.8}$$

Since the probability of choosing i from $[0, \mathrm{CW}_{\min 1}]$ is $\frac{1}{\mathrm{CW}_{\min 1}+1}$ it can be shown that:

$$p_2 = 1 - \frac{\sum_{i=0}^{\mathrm{CW}_{\min 1}} \bar{p}_2(i)}{\mathrm{CW}_{\min 1} + 1} \tag{9.9}$$

Under the BEB scheme, the value of τ_2 can be calculated by Equation 9.1. We also model

AIS throughput under a simple scheme where backoff window is always chosen from 0 to CW_{min} irrespective of the collision of the transmitted packet (which we refer henceforth as *No backoff* mechanism), $\tau = \frac{CW_{min}}{2}$. The comparison of BEB model with this model helps to identify the effectiveness of BEB.

This completes the calculation of all the variables (p's and τ's) for throughput estimation of the links.

We now compare the effectiveness of AIS throughput formulation. Under standard MAC parameters (with $CW_{min} = 31$), the link with the hidden terminal cannot successfully transmit (even relatively smaller packets) between the idle time of the other link (because CW_{min} is only 31 slots). Hence, we vary the CW_{min} of the links and validate the model for varying CW_{min} and packet sizes.

As seen in Figure 9.7(b), the prediction by the model matches closely with the simulations. It can be seen that the starving link S_2D_2 gets a fair throughput only when CW_{min} is very high. Exponential backoff at S_2 will reduce the frequency of transmission of link S_2D_2. However, the interfering traffic at S_1D_1 is at constant rate and exponential backoff does not improve the success probability of S_2D_2. This absence of correlation between the change of interference pattern over time makes BEB ineffective in AIS. It can be seen that the link S_2D_2 will get zero throughput until the CW_{min} (of S_1D_1) value is large enough to accommodate the the packet. This suggests that under low CW_{min}, the effect of asymmetric hidden terminals can be reduced by either decreasing the packet size (or increasing the transmission rate). These parameters can be calculated directly from the model.

9.3.4 Preliminary Formulation for Symmetric categories

Symmetric hidden terminals occurs in the SIS and IDIS categories. Computation of the throughput variables p and τ for symmetric categories is hard due to the coupling between the two links. This makes independence assumptions on the probability of collision per backoff stage inaccurate. An accurate model of these cases would require modeling the combined states of the two senders (each of which may take any of the states in the Bianchi model), leading to a very large Markov chain. Nevertheless, we present results with the approximate model. We believe that an accurate model

of SIS cases is an open question that deserves a more thorough treatment.

SIS formulation:

In SIS, the source of a link (S_1 or S_2) causes collision of the packet at the destination of the other link (D_2 or D_1). Reception at D_2 is successful if S_1 does not transmit in slots that overlap with S_2's transmission. Due to symmetry of the hidden terminals, we have $p = p_1 = p_2$ and $\tau = \tau_1 = \tau_2$.

We now derive the the success probability $(1 - p)$. If the value of maximum backoff is lesser than the time required to complete a successful transmission (and ACK), then S_2D_2 cannot find a sufficiently long gap between S_1D_1's transmission and hence $p = 0$. Otherwise, the packet will be transmitted successfully if the interfering link does not transmit a packet such that atleast one slot overlaps with the packet transmission. For example, Figure 9.8 shows the transmission of the data packet by one link (say S_1D_1) in light blue. The slots during which interfering link (S_2D_2) cannot transmit is colored in grey. If τ is the probability that the interfering link will transmit in a given time slot, then the probability that it will transmit in the slots that will collide with the given packet is given by Equation 9.10.

$$\begin{aligned} p = &\quad \tau + (1-\tau)\tau + \ldots + (1-\tau)^{\lceil 2l \rceil - 1}\tau \\ p = &\quad 1 - (1-\tau)^{2\lceil l \rceil} \end{aligned} \tag{9.10}$$

The relationship between p and τ is given by the Equation 9.1 which we term $\tau = b(p)$.

Symmetric hidden terminals have the property of one link being affected by the activity of the other. The probability of drop on link S_1D_1 (p_1) depends on the frequency of packet transmission attempts at link S_2D_2 (τ_2). Let us denote this relation by $p_1 = f(\tau_2)$. Owing to symmetry in the topology, we can represent the above by two relations: (1) $\tau = b(p)$; and (2) $p = f(\tau)$. Equation 9.10 can be used as an approximation for representing the function $p = f(\tau)$. The roots of the above equations can be calculated by standard numerical techniques like Newton method [99]. Improving the expression for f from that in Equation 9.10 is a part of our future work.

Integrating the existing components for calculating p and τ was also attempted. A Markov chain

based approach to calculate τ was proposed in the study [42]. Figure 9.7(d) study the throughput of the links when the CW_{min} and packet sizes are altered. It compares the simulation with the two models (the Garetto model and the one proposed here). Our model matches the simulation only under higher CW_{min} values. The Markov-chain based model captures the throughput trend for larger packet sizes, while a large gap exists under lower packet sizes. We believe that an accurate model of SIS remains an open issue. The model is accurate for No-Retry mechanism(Figure 9.7(a)). At lower values of CW_{min}, BEB scheme outperforms the No-retry scheme. The exponential backoff of one link helps to create enough channel idle time for packet transmissions of the the other link. However, such a scenario exhibits short term unfairness where the throughput of one link dominates for short periods of time.

IDIS formulation: Recall that in IDIS, only receivers are in interference range with each other. A receiver can cause a drop on the other link when it transmits an ACK. Due to the symmetry of the topology, p and the τ are identical for the two links, but are coupled. Their value can be derived in a method similar to symmetric hidden terminals, under the same imperfect assumptions. The results of this model are shown in Figure 9.7(f).

9.4 Conclusions and Future work

The chapter proposes throughput models for the interactions between two-flows discovered under the Two-Disc model of interference [108]. An accurate throughput model for the SCIS and asymmetric scenarios is proposed. The effect of minimum backoff window size on the throughput of the flows is analyzed and the results of the model is verified with the simulations. A refinement to the approximate throughput model for symmetric hidden terminal categories is a part of our future work.

We wish to extend the throughput model to a more realistic SINR/BER model. Deployment studies of two-flow scenarios in network testbeds and measurement based characterization of the interactions will provide the necessary first steps towards analyzing the effect of realistic interference.

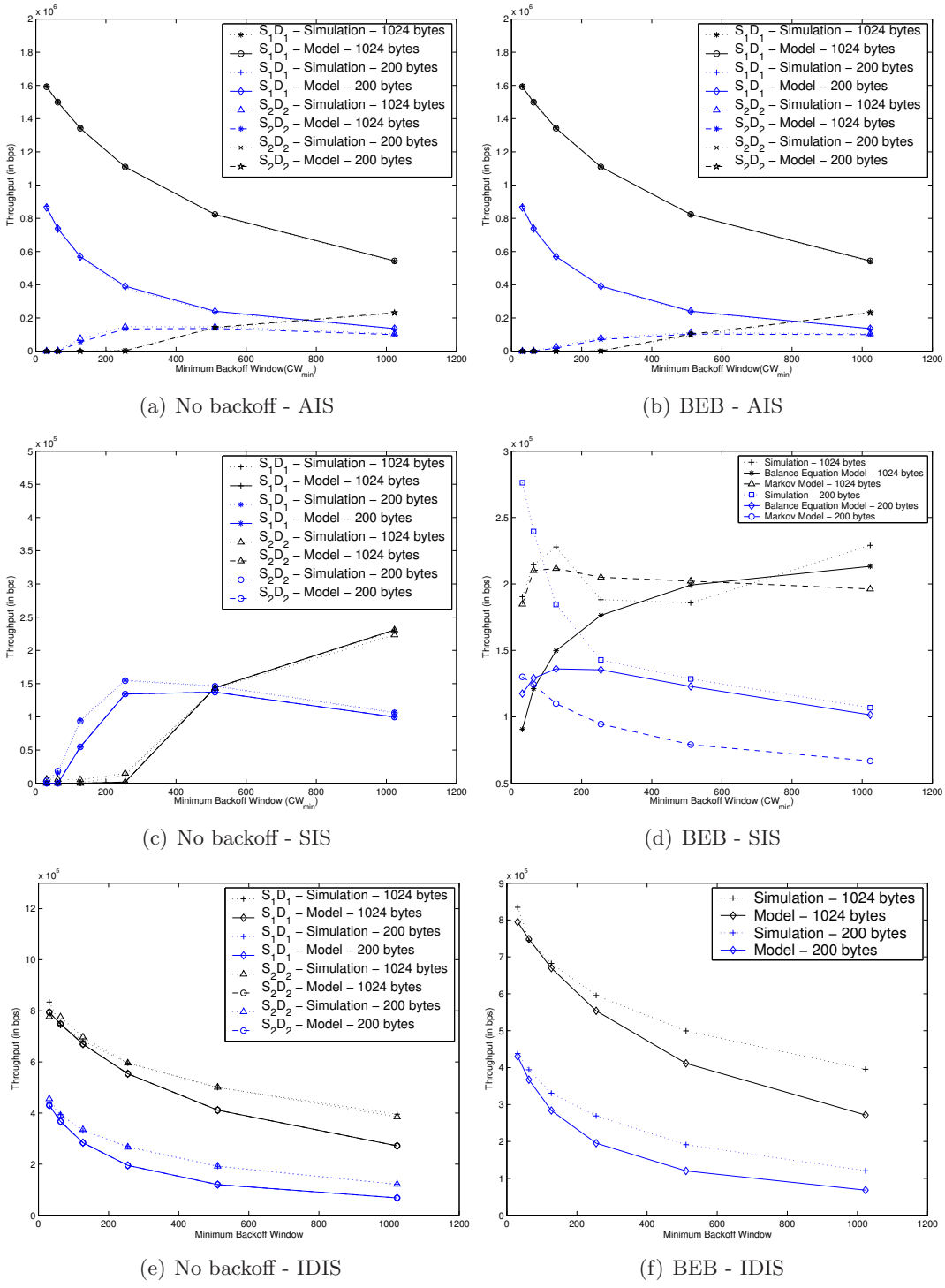

(a) No backoff - AIS

(b) BEB - AIS

(c) No backoff - SIS

(d) BEB - SIS

(e) No backoff - IDIS

(f) BEB - IDIS

Figure 9.7: Effect of Hidden terminals

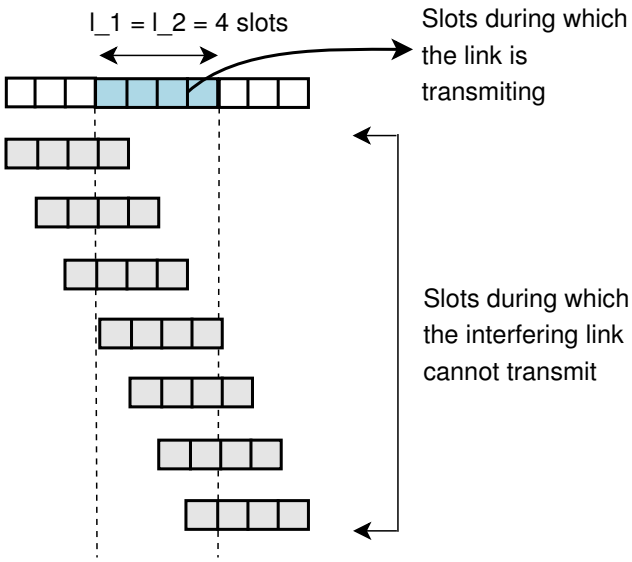

Figure 9.8: Packet success in SIS. l_1 and l_2 represents the slots required to transmit the packet for link S_1D_1 and S_2D_2

Chapter 10

Interaction Models for CSMA Scheduling

In the context of CSMA/CA based MAC protocols these interactions are often simplified under the classification of hidden terminals (essentially, interactions that can cause collisions) and exposed terminals (essentially, interactions that unnecessarily prevent a source from transmission and underutilize the medium). Research studies [13, 84, 88, 119, 128] show that these detrimental interactions have a high impact on the performance of the network. Numerous researchers have investigated solutions to mitigate these effects [4, 13, 37, 74, 92]. However, in-depth understanding of these interactions and their effects is necessary for building effective medium access protocols.

In this chapter, we propose Interaction Graphs(IGs): a framework for depicting and tracking the channel state. We show that hidden and exposed terminal interactions can be captured and estimated by IGs. The effect of different parameters on the hidden and exposed terminals are analyzed using the IGs and an estimation metric for characterizing them is proposed. We design an *ideal scheduler* that operates on a contention mode and is capable of allowing only a certain states of the channel to be active. Through such a scheduler, the analytical model is verified by simulations.

10.1 Introduction

In MHWNs, the medium access problem is that of regulating access from multiple transmitters to a common wireless shared medium. CSMA/CA based protocols are commonly used in this context, including, for example the IEEE 802.11 family of standards. In CSMA protocols, the source transmits on the channel only when the channel is sensed free (the sensed power is below a threshold). A successful packet reception occurs when the channel at the receiver is relatively noise free (the signal to noise and interference ratio is above *the capture* threshold).

The distance between the source, the receiver and interfereres (more accurately, the state of the channel between them), and the radio propagation effects have a significant effect on the observed *channel states*. Furthermore, different nodes can have a different and inconsistent views of the channel, which gives rise to many interesting and destructive interactions, leading to poor performance and unfairness [42, 108].

In this study, we introduce a notion of *Interaction Graphs* (IGs) to model the interactions in wireless networks. The IGs are constructed based on the handshake observed by the MAC protocol and are capable of depicting the set of concurrently active links that are observed on the channel. Representing the interactions through graphs has been studied in the existing literature [16, 41, 63, 123]. In fact, the MICS notion that was proposed in Chapter 5 is also a type of IG. In this study, we identify other forms of interaction graphs that are capable of representing the channel states. Such graphs serve as effective tools to demonstrate the effect of certain interactions in a given MAC protocol. For example, the effectiveness of various protocols can be estimated by comparing the properties of the protocol-specific IGs with the IG of an ideal protocol.

While IGs can be used to depict a majority of the CSMA protocols, we employ this framework to capture two significant interactions in CSMA based protocols (specifically, IEEE 802.11 protocol): the hidden terminals (HT) and the exposed terminals (ET). We evaluate the IEEE 802.11 protocol and its variants and analyze the effects of HT and ET on such MAC protocols. We study the effectiveness of RTS-CTS under different parameters and compare them with the other variations of IEEE 802.11. Eventhough the RTS-CTS scheme was introduced to reduce hidden terminal effects, we conclude that such a scheme, on the contrary, increases both HT and ET effects.

We propose three kinds of IGs, which models this set from three perspectives, namely:

- *Initiation IG (IIG):* IIGs represent the set of concurrent links possible under a given MAC protocol. The interactions in IIG are valid transactions (groups of transmissions) per the MAC protocol and such interactions may include packet drops.
- *Existent IG (EIG):* The *Existent IG* (EIG) track the successful transmissions that can concurrently proceed under a given MAC protocol. Though EIGs remove the hidden terminals, they may contain exposed terminal effects (links that are blocked by the MAC protocol).
- *Optimal IG (OIG):* The OIG consists of the optimal set of concurrent links, essentially removing the hidden terminals, and allow exposed links to transmit. Thus, it maximizes concurrency, and removes all colliding transmissions.

Note that both EIG and OIG are idealized IGs that we use for analysis.

This set of IGs together provide insight into the possible interactions and the loss of performance due to them in a given topology. Under low loads, there is sufficient time on the channel to provide separation between the interacting links; thus, the analysis applies mostly under heavy traffic and serves as an useful tool for quantifying the effectiveness of a MAC protocol.

10.2 Modeling the interactions

In this section, we describe various types of graphs that are capable of capturing the MAC interactions at different levels. We describe the capabilities and uses of such graphs.

Terminology and Assumptions A *transaction* is a sequence of transmissions as defined per the MAC protocol (e.g., RTS-CTS-DATA-ACK under IEEE 802.11). A link is said to be *active* when a transaction is initiated by the source or receiver of the link and the transaction is ongoing, irrespective of whether the transaction is going to be successful or not. We consider a static wireless network topology with l traffic carrying links. Let the source and destination of the link l_i be named by the tuple (s_i, d_i) where $1 \leq i \leq l$. The set of all the traffic carrying links is denoted by the set L.

A transmission is received correctly if the ratio of the *Signal to Interference and Noise Ratio*(SINR) is high. Generally, the higher the SINR, the greater is the probability of reception. We use the *SINR threshold* model to determine if a transmission is received correctly or results in a collision. Although the model does not account for the probabilistic and dynamic radio propagation effects, it serves as a useful abstraction to describe long term behavior.

As illustrated in the Chapters 5, 8, and 9, several MAC level interactions, like packet timeouts, depend upon the combined states of the source and the destination node of the link. Hence, the interactions of the MAC protocol can be effectively captured at a link level, rather than at a node level. The general approach followed is to represent each link as a vertex in the interaction graph and denote various interactions by observing the relationship between these vertices.

10.2.1 Pair-wise interaction graphs

Pair-wise interaction graphs show the relationship between a pair of links. We break the set of links L into a set of links that can be active at the same time. Under a given MAC protocol, a set of such active links interact with each other when the initiation of the the links are allowed by the protocol. For example, under the IEEE 802.11, a link l_1 can be initiated with another link l_2 when the channel and the Virtual Carrier Sensing (VCS) at s_1 indicates a free channel. A graphical notation of the interaction will be helpful to study such a set. Consider each link l_i as a vertex in a graph. If two links are active at the same time, they are connected by an edge. Such a graph will be further referred in the study as *Pair-wise Interaction Graph*. This graph is similar to the *Conflict Graph* proposed by Vaidya et al. [126]. *Pair-wise IG* is similar to the notion of conflict graphs (specifically, a complement of the conflict graph). However, the edges exist between two active links in the Pair-wise interaction graph if and only if they can be initiate transmission together.

While the *Pair-wise Interaction Graph* is able to capture the interaction between a pair of edges, it does not accurately depict the state of the wireless channel. For example, the set of links that can be active at a given point of time cannot be depicted by the Pair-wise IG. Thus, capturing the interactions that occur at different channel states is not possible with Pair-wise IG.

We now define the notations used for describing other interaction graphs that can capture the

state of the wireless channel. The term *Interaction Set (IS)* is used to refer to a set of links l_j that can concurrently initiate a transaction under a given protocol. For example, under the IEEE 802.11 protocol, the sources of these links do not experience busy channel, either by physical carrier sense or virtual carrier sense. As an example, consider the interaction set $IS_1 = \{l_1, l_2, \ldots, l_m\}$. It is possible that a link $l_c \notin IS_1$ has an edge with all the links of IS_1 in the Pair-wise IG, indicating that there are no conflicts with any individual edges in IS_1, but the cumulative interference created by links of IS_1 may disallow the link l_c to initiate. This will exclude l_c from the IS_1.

The problem of finding the interaction set is similar to the problem of finding the *Independent Sets* in the Pair-wise IG. However, it is to be noted that it is possible that the two links have an edge in Pair-wise IG (do not conflict each other) but a link cannot be accommodated into an Interaction Set(IS). This can happen if cumulative interference from the other set of edges can create a busy channel at the source of a link.

A *Maximal Interaction Set (MIS)* is a set of interaction sets such that addition of any other link will invalidate the interaction set properties (similar to the notion of Maximal Independent Sets in graph theory). We denote MIS by L_j. There can be multiple MIS in the scenario, similar to multiple maximal independent sets of a graph. Let $\mathrm{N^I}$ denote the number of MIS present in a given MHWN scenario.

The IS is specific to the MAC protocol being used. Consider the IEEE 802.11 protocol with RTS-CTS-DATA-ACK handshake. Each interaction set IS_j will indicate the set of links whose sources can initiate the RTS transmission together. These correspond the sources whose physical or virtual carrier sensing indicates a free channel when the rest of the links are active. Since the IS only considers the *initiation* of the RTS from the source, it is not necessary to consider the channel state at the receiver even though the IEEE 802.11 protocol is bi-directional. In the case of IEEE 802.11, the Interaction set corresponds to the *source view* of the channel since the source initiates the transmission.

For example, consider the figure 10.1(a) which consists of 6 one-hop links in a 6×6 grid. The Pair-wise IG of the graph for the IEEE 802.11 protocol is shown in Figure 10.1(b).

Based on these notions, we now define three types of interaction graphs that aid in the com-

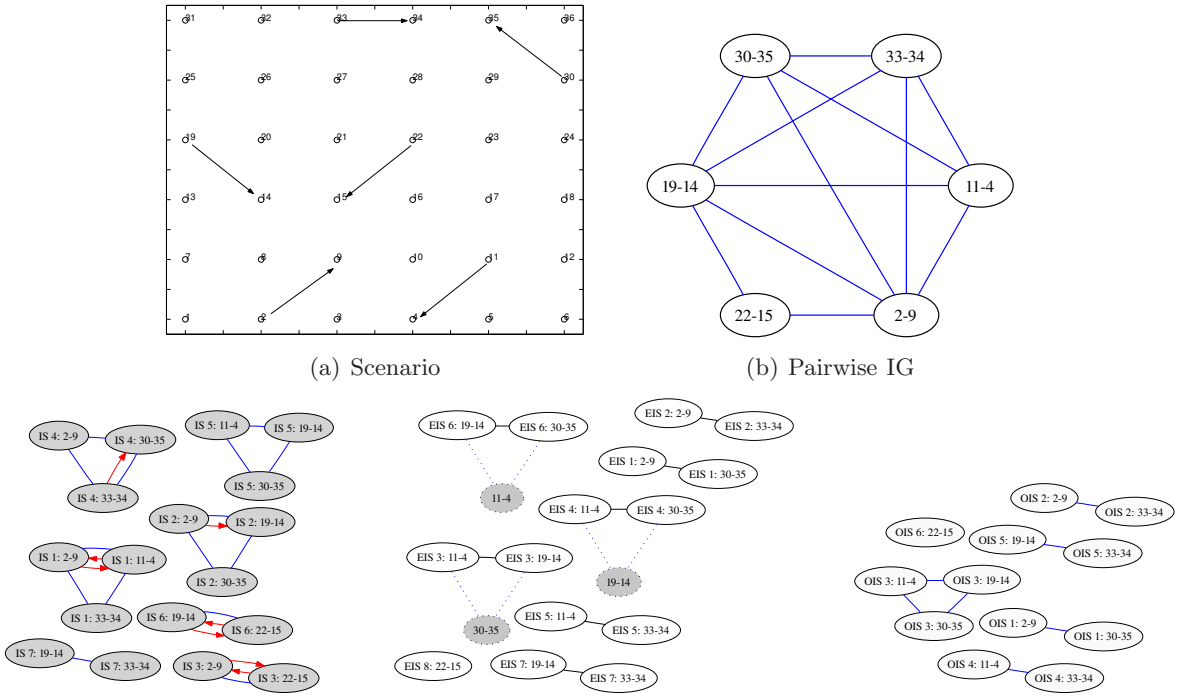

(a) Scenario (b) Pairwise IG

(c) Initiation IG (IIG) (d) Existent IG (EIG) (e) Optimal IG (OIG)

Figure 10.1: Illustrative Interaction Graphs

parison of the effectiveness of a protocol.

10.2.2 Initiation Interaction Graphs(IIGs)

Recall that the Pair-wise IG shows the parallelism between two links. However, it fails indicate the relationship between multiple links. For example, the number of links that can simultaneously be active is hidden from such a graph. Relationship between multiple links is needed for predicting the interactions and the state of the system. We introduce *Initiation IGs*(IIG) as the set of graphs which depict the ISs L_j's described above. Figure 10.1(c) shows the IIG for the topology in Figure 10.1(a). Each clique with a *blue* edges in Figure 10.1(c) represents an IS (The *red* edges are described later). The edge l_m in an interaction set IS_j is named as "*IS j:* s_m-d_m" in the IIG. It can be seen that IIG describes all the relations in Interaction Sets. A link can be present in multiple ISs. Since each clique represents the edges which can initiate transaction together, it can be seen that all the active edges belong atleast one of the cliques in IIG. The interaction between the edges

can now be stated within a single IS (clique). All the cliques in Pair-wise IG does not form an IS in IIG. For example, consider the clique formed by links {*(2,9),(19,14),(22,15)*} in Figure 10.1(b). Though all the three links can go with each other they cannot be initiated together. They break up into two IS in IIG (Figure 10.1(c)), namely, $IS3$ and $IS6$. Even though *(22,15)* can initiate with both the links *(2,9)* (in $IS3$) and *(19,14)* (in $IS3$), the links *(2,9)* and *(19,14)* cannot initiate when either of the link is active with *(22,15)*. This demonstrates the need for IIGs for capturing the actual interactions that occur.

Links in an IS may not achieve successful packet transmission. For example, consider the links *(19,14)* and *(22,15)* in *IS 6* in Figure 10.1(c). The sources initiate the RTS packets when the other link is active, but when *(19,14)* is sending a data packet, the channel at node 15 will be busy. Hence, it fails to respond to the RTS of node 22. Since the IIG represents the *source view* of the channel while IEEE 802.11 is being used, the receiver's inability to complete the transaction successfully leads to packet drops and timeouts in the IIG. Such links are marked with directed *red* edges in the IIGs as shown in Figure 10.1(c). For example, in Figure 10.1(c), a directed red arrow from *(33,34)* to *(30,35)* in *IS 4* indicates that the link *(33,34)* causes an unsuccessful packet delivery attempt on link *(30,35)*.

10.2.3 Existent Interaction Graphs(EIGs)

Although the IIG describes the concurrent transmissions that can go on at a coarse level (links in cliques that do not have a red arrow), it is often helpful to depict the parallel transmissions that are *successfully completed*. Such a graph will represent the actual channel utilization of the network and are useful for predicting the approximate throughput of the links and weakness of an IIG for unsuccessful parallel transmission. We define such graphs as *Existent IGs* (EIGs). Similar to the notion of *Interaction Set*(IS), we define *Existent Interaction Set* (EIS). Each EIS has a set of links that can be active at the same time and finish to completion. Figure 10.1(d) shows the EIG for the topology 10.1(a) under IEEE 802.11. A link l_m in an EIS EIS_j is represented as "*EIS j:* s_m-d_m" in Figure 10.1(d). The dotted nodes and edges are explained later in Section 10.2.4. By comparing the IIG (Figure 10.1(c)) and EIG (Figure 10.1(d)), it can be seen that a red arrow *splits* the IIG

into separate EIS in the EIG. In other words, the link l_a causing an unsuccessful transmission to another link l_b, will break the possibility of both the links l_a and l_b going on concurrently with other members of IIG. The cliques with solid edges and nodes represent different EIS. It is to be noted that the EIG is also specific to the MAC protocol being used.

10.2.4 Optimal Interaction Graphs(OIGs)

The MAC protocol dictates the structure of IIG and EIG for a given topology. However, for measuring the effectiveness of the MAC protocol or for comparing two different MAC protocols, a base-case graph depicting the optimal set of concurrent links is desirable. Note that this optimal set is independent of the MAC protocol, and represents the results of an oracle scheduler. We call such graphs Optimal Interaction Graphs (OIGs). OIGs ignore the restriction placed by the MAC protocol and instead describe the optimal set of links that may be active simultaneously without a reception failures at any link.

Figure 10.1(e) shows the OIG for the topology 10.1(a). Each clique in the OIG represents an Optimal Interaction Set (OIS). A link l_m in OIS j is labelled as "*OIS j:* s_m-d_m" in Figure 10.1(e). The dotted nodes and edges in the EIG (Figure 10.1(d)) show the additional links that could have gone in parallel (as indicated by OIG in Figure 10.1(e)) with the members of EIS but which are blocked by the *source view* (IIGs) of the MAC protocol. Though the construction of the OIS is *Initiation Interaction Set independent*, it is dependent with the fundamental policy of the MAC protocol. A one-way handshake MAC protocol, which transfers packets from source to destination only, should account for the packet loss at the receiver node, while a two-way handshake MAC protocol should account for the packet loss at source and receiver (since receiver sends control packets back to the source). Most of the CSMA/CA based MAC protocols observe a two-way handshake and hence we construct the OIG based on the two-way handshake MAC protocol. However, the generality of the OIG does not prohibit modeling the one-way handshake protocol.

To summarize, we represent the topology and observe interactions in three kinds of graphs. An IIG describes the initiation rules and forms set of links that can initiate concurrently. The EIG represents the links that can initiate concurrently and complete successfully. The OIG represents

the optimal set of links that can complete successfully irrespective of the initiation rules. In Section 10.4.2, we verify through simulations that a vast majority of the concurrent transmissions under IEEE 802.11 are represented by the Existent Interaction sets(EIS) of the EIG. We also verify that the interactions causing the packet drops are covered in the Interaction Sets (IS) of the IIG. The cross-IS packet drops can occur due to rare scenarios like two nodes transmitting at the same point of time without the knowledge of each other's transmission (the *Co-ordinated sources* problem [41]).

10.3 Formulation of the Hidden Link and Exposed Link effects

In this section, we utilize the interaction graphs proposed in the previous section to analyze certain primary interactions in CSMA based protocols. Specifically, we describe the hidden terminal and exposed terminal effects with respect to the interaction graphs.

Analysis of the effect of *Hidden Terminal (HT)* and *Exposed Terminal (ET)* has been done at a *node* level in previous research work like [119]. Since the unicast transmissions predominate in MHWNs, we represent the analysis of HT and ET at the level of a *link* instead of at a *node* level. We propose metrics to quantify the effect of hidden and exposed terminals in a given network scenario.

Terminology and Notations: The number of Interaction Sets in IIG, EIG and OIG is represented by N^I, N^E and N^O respectively. The number of links in the jth interaction set of IIG, EIG and OIG is represented by ${n^I}_j$, ${n^E}_j$ and ${n^O}_j$. The probability of occurrence of the j^{th} Interaction Set (of IIG, EIG and OIG) is represented by ${p^I}_j$, ${p^E}_j$ and ${p^O}_j$ respectively. The derivation of these probabilities are explained in the next section.

10.3.1 Probability of Occurrence of Interaction Sets

Deriving the probability of the occurrence of each Interaction Set is non-trivial and depends upon various protocol parameters like backoffs, retransmission strategy and the number of hidden terminals. A precise estimation of the probabilities of interaction sets has been attempted in past

studies [16, 41]. However, such estimations are computationally expensive and assume a simplistic *Two disk model* of interference (explained in Section 2.2.1). Further, they are iterative in nature, resulting in balance equations and solving them numerically. As a result, they do not expose the processes that lead to the probabilities and provide little insight into how to influence them.

An initial and preliminary model to constructively estimate the occurrence probability values is attempted in Chapter 5. We use a similar approximation to capture the probability of occurrence of the interaction sets. While chapter 8 refines the estimate by precisely calculating the long-term probabilities of occurrence of the MICS, it does not account for the hidden terminals. Hence, in this study, we compute a heuristic estimate of probability of occurrence of each interaction sets in this study. An important component of the future work is to develop accurate and lightweight models for estimating these probabilities, especially under more realistic interference models like the SINR model.

We note that the greater the number of links in an interaction set, the greater the probability of its occurrence. The intuition for this observation is that the more competing links there are in a set, the higher the probability that one of them starts before links in other sets. As a result, only the sets that include the active link compete, and the competition is biased in favor of the sets with higher number of links.

Assuming a linear relationship between the number of links in an interaction set and its probability of occurrence, we estimate the probability of occurrence of the interaction set L_j by Equation 10.1.

$$\mathrm{p}_j = \frac{\mathrm{n}_j}{\sum_{i=1}^{\mathrm{N}} \mathrm{n}_i} \quad \text{where } \mathrm{n}_i \text{ is the size of IS } L_i \tag{10.1}$$

The calculated probability values for IIG, EIG and OIG is represented by ${\mathrm{p}^{\mathrm{I}}}_j$, ${\mathrm{p}^{\mathrm{E}}}_j$ and ${\mathrm{p}^{\mathrm{O}}}_j$. The N is replaced by the respective number of Interaction sets N^{I}, N^{E} and N^{O} for IIG, EIG and OIG. Similarly, the number of links in an interaction set N is replaced by ${\mathrm{n}^{\mathrm{I}}}_j$, ${\mathrm{n}^{\mathrm{E}}}_j$ and ${\mathrm{n}^{\mathrm{O}}}_j$ for IIG, EIG and OIG, respectively.

10.3.2 Hidden Link (HL) effect

At a *node* level, node x is said to be a hidden terminal for node y, if transmission from x can cause a collusion to an actively receiving packet at node y. Under *link* level unicast transmissions, a *hidden link* (HL) causes a packet loss to another active link. Such packet losses can be due to packet collusion or packet timeouts (such as RTS and ACK timeouts). The packet losses are are captured in the IS of the IIG. For example, the red arrows in Figure 10.1(c) captures the packet losses when IEEE 802.11 is being used. Since the packet drops occur between the links of an IS, the HL effect is dependent on the state of the channel that is being active. For example, in Figure 10.1(c), the link *(2,9)* is a hidden link to the *(19,14)* only in the ISs in which both the links exist.

The effect of a Hidden Link can be seen as the difference between the IIG and the EIG. The hidden links observed in the IIG will split and/or merge the IS into different Existent Interaction Set(EIS). The density of the red-arrows in the IIGs (e.g. Figure 10.1(c)) shows the amount of Hidden Link in a given scenario. The goal of the metric is to capture the effect of HL scenario in a given scenario in the range of $[0, 1]$, where an HL effect of 0 indicates no HL effect and 1 indicates maximum HL effect. Examining the extreme ends of the HL effect, a scenario has 0 HL effect when there are no red-arrows in the IIG (IIG will be equal to the EIG). A value of 1 HL effect is present when a each link in an IS is a hidden link for every other link in the IS, i.e a red-arrow between every pair of links in an IS (EIG will a set of single links). The maximum number of red-arrows in a given IS, say L_j, of size $\mathrm{n^I}_j$ will be $\mathrm{n^I}_j \cdot (\mathrm{n^I}_j - 1)$(number of edges in the directed *complete graph*). Let H_{ij} be the set of hidden links for the link i in the IS L_j. Let the number of hidden links for link i in L_j be $\mid H_{ij} \mid$. Then, the density of the hidden links in an Interaction set L_j can be expressed by the simple ratio in Equation 10.2. It can be noted that when there is a single link in an IS (i.e. when $\mathrm{n^I}_j = 1$), then there cannot be any hidden links for the given link and hence will have $\mathrm{D}_j = 0$.

$$\mathrm{D}_j = \begin{cases} \frac{\sum_{i \in L_j} |H_{ij}|}{\mathrm{n^I}_j(\mathrm{n^I}_j - 1)} & \text{if } \mathrm{n^I}_j > 1 \\ 0 & \text{Otherwise} \end{cases}$$

To evaluate the HL effect of the complete the scenario, the effect of HL across all the ISs have to be considered. Let ${p^I}_j$ is the probability of the occurrence of Interaction Set L_j in the IIG, which is approximated by Equation 10.1.

The HL effect for the given scenario will be the weighted average of the HL effects of each IS. An interaction set L_j with probability of occurrence ${p^I}_j$ and having a density of D_j, the HL metric that captures the weighted averages of the hidden link effect of the scenario is represented by Equation 10.2.

$$\mathcal{H} = \sum_{j=1}^{N^I} {p^I}_j \, D_j \tag{10.2}$$

The $\mathcal{H}$ metric quantifies the effect of hidden links in terms of the density of the hidden links in the IIG. A more accurate estimation in terms of the capacity loss due to hidden links involves a detailed accounting for various parameters like the packet lengths and backoff values. This is a part of the future work.

10.3.3 Exposed Link (EL) effect

In this section, we examine and formulate the exposed terminal problem at a *link* level of abstraction. A node that could have successfully completed the transmission is blocked due to a transmission by the neighboring node is termed as an *Exposed Terminal*(ET). At a link level, a link l_a is termed as an Exposed link (EL) if the neighboring link activity would block the l_a eventhough concurrent transmission by both the links would be successful. The exposed terminal/link would under-utilize the channel by preventing valid transmissions. In this section, we quantify the amount of the EL on a given scenario by comparing the interaction graphs.

The OIG depicts the concurrent interactions that can happen without any errors while the EIG represents the actual concurrent transmissions permitted by the MAC protocol. The ratio of the capacity used by an interaction set of OIG (denoted by OISs) and the capacity used by the interaction sets of EIG (denoted by EISs) will denote the effect of the Exposed Link on the given scenario. It is essential to determine the effect of EL on each EIS/OIS and to normalize the effect

across various EIS/OIS in a given scenario. Let $\mathrm{p^E}_j$ be the probability of an EIS j (calculated by Equation 10.1).

The capacity used by a given EIS $\mathrm{L^e}_j$ is dependent upon the number of links that can simultaneous be active. We approximate the overall capacity used by the scenario by weighing the capacity used by different EIS. The overall channel bandwidth utilized by every EIS will be equal to the product of the channel bandwidth and the number of links in the EIS (number of parallele transmissions). The average channel bandwidth utilized by the scenario is approximated as the cumulative sum of the product of the channel bandwidth utilized by each EIS and the probability of the EIS $\mathrm{p^e}$. Similar to the notations used in EIS, let $\mathrm{N^O}$ indicate the number of OISs in the OIG. Let $\mathrm{p^o}$ represent the probability of each OIS occurring in an OIG. Let $\mathrm{L^o}_j$ represent the j^{th} OIS in the OIG. The overall effect of the exposed terminal is determined by the ratio of the channel capacity used by the MAC protocol (by the EISs) to the the optimal capacity utilization (indicated by the OISs). Equation 10.3 shows the formula to measure the effect of the Exposed Links in a given scenario.

$$\mathcal{E} = \frac{\sum_{i=0}^{\mathrm{N^E}} \mathrm{n^E}_i \, \mathrm{p^e}_i}{\sum_{j=0}^{\mathrm{N^O}} \mathrm{n^O}_j \, \mathrm{p^o}_j} \tag{10.3}$$

It is to be noted that we do not consider the effect of the packet drops (hidden links) that can potentially *break* the EIS even though the exposed link effect is tied to the packet drops. This is to isolate the efficiency of the MAC protocol in two aspects: (1) to control the packet losses; and (2) to measure the utilization of the channel capacity.

In Section 7.4, we measure the HL effect for variants of the IEEE 802.11 protocol by altering the Carrier Sense threshold. The HL effect for the given scenario also depends the ability of the physical layer to sense the signals. Higher sensing power would lead to a sensitive source which can sense ongoing transmissions relatively far from it. While such a source avoids hidden links by not trying to initiate, it under-utilizes the channel by adopting a conservative transmission strategy.

10.4 Analysis of the Hidden Link and Exposed Link effects

In this section, initial analysis of the effect of the HL and EL is presented.

The $\mathcal{H}$ and $\mathcal{E}$ metrics is specific to a given scenario. Small changes to the geometry of the network or the traffic flows will lead to different interaction graphs, thus different $\mathcal{H}$ and $\mathcal{E}$. This sensitive dependence of the metrics on a given scenario makes it harder to to predict the changes in these effects on similar network topologies. However, the $\mathcal{H}$ and $\mathcal{E}$ can be determined with high probability on certain network parameter changes. In this paragraph, we discuss the effect of *Carrier Sensing Threshold (CxThresh)* on $\mathcal{H}$ and $\mathcal{E}$. Carrier Sensing Threshold($CxThresh$) is one of the parameter which affects the HL and EL for the given scenario. It denotes the amount of power above which a node observes the channel as busy. As the node decreases the $CxThresh$, it becomes more sensitive, thus avoiding transmissions even due to weaker signals on the channel. A higher $CxThresh$ will result in a damped node which can only capture stronger signals. The $CxThresh$ helps to estimate if the channel is idle or busy (the physical state of the channel). $CxThresh$ affects the state of the channel and is vital for MAC protocols to initiate the packet transmission. Yang et al. [127] has studied the effect of $CxThresh$ variation on IEEE 802.11 by simulations. In this study, we analyze in detail the effect of $CxThresh$ on the HL and the EL effects and verify the analysis by simulation results. We assume that all the nodes in the network are homogeneous and have the same $CxThresh$ value. The dynamic variation of $CxThresh$ under heterogeneous nodes is a part of our future work.

10.4.1 Analytical analysis of HL and EL effects

In this section, we study the effect of Carrier Sense Threshold against the hidden and exposed link parameters on the RTS-CTS and the basic mode in IEEE 802.11. We observe that, irrespective of the carrier sense threshold, the RTS-CTS scheme of IEEE 802.11 creates much greater hidden links than the basic mode which uses only DATA-ACK handshake. The difference between the exposed link effect is negligible between the RTS-CTS and the basic mode. And as observed in the past studies, we see that the hidden link effect grows (and the exposed link effect decreases with) with an increase in Carrier Sense Threshold. The results shown in this section differ from

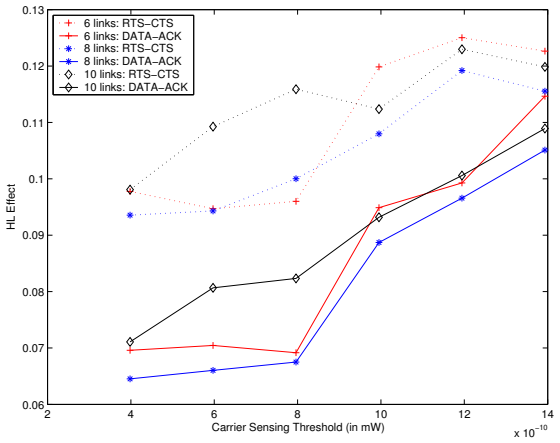

(a) HL Effect in Grid Topology

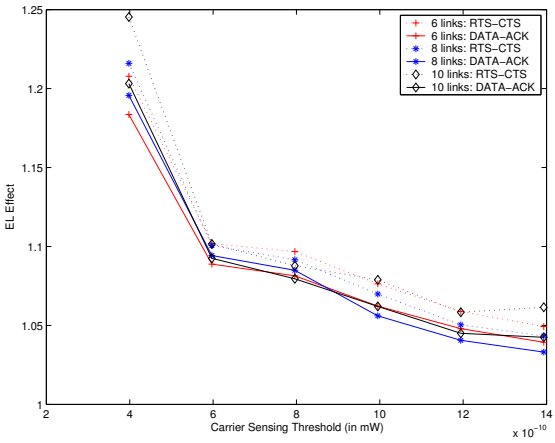

(b) EL Effect in Grid Topology

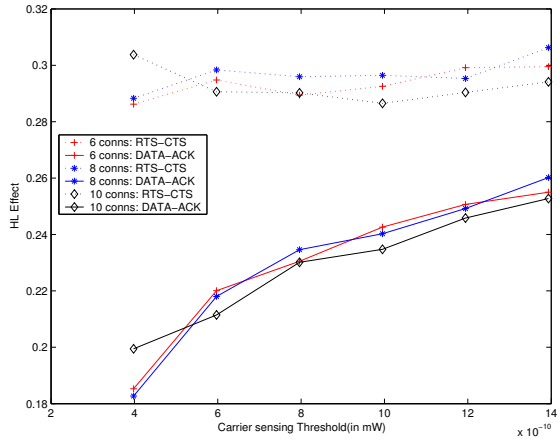

(c) HL Effect in Random Topology

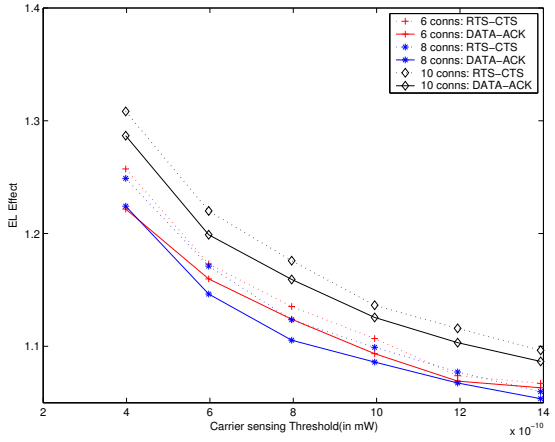

(d) EL Effect in Random Topology

Figure 10.2: Variance of the HL and EL effect due to Carrier Sensing Threshold and the MAC behavior

the previous study [74,128], by quantifying the amount of hidden link (density of hidden links) and exposed links (effective spatial reuse capacity estimation) through the proposed metrics instead of measuring it by estimations of other network metrics like throughput, that encompasses a variety of interactions.

Figure 10.2(c) shows the variation of the HL effect ($\mathcal{H}$) as a function of the $CxThresh$ under IEEE 802.11 protocol. The results are obtained by a random placement of 100 nodes in a 1000×1000 area for 100 different topologies. One hop connections were chosen to eliminate the routing effects. As the $CxThresh$ increases the nodes become more aggressive, thus initiating the transmission even

when the channel noise is higher. This results in greater number of packet collusions (Larger $\mathcal{H}$ metric). However, due to the optimistic estimation of channel interference, it blocks lesser initiations and thus results in a low exposed link effect ($\mathcal{E}$) as shown in Figure 10.2(d). The transmissions that could have completed successfully are now blocked by sensitive $CxThresh$. As the $CxThresh$ decreases, the node becomes more sensitive in initiating transmissions. This increases the EL effect by blocking valid transmissions. However, the HL effect decreases due to the pessimistic initiation of the transmissions.

Recall that IEEE 802.11 has two popular variations that is extensively used. The first one uses the RTS-CTS-DATA-ACK handshake; while the second, and a more popular version, uses just the DATA-ACK handshake. In this study we compare the two approaches analytically to determine the pros and cons of both the variations. Figures 10.2(c) and 10.2(d) shows the $\mathcal{H}$ and $\mathcal{E}$ metrics for both the schemes. The *RTS-CTS* mode is a conservative protocol which was introduced to reduce the number of *Hidden terminals*. On the contrary, we observe that this mode leads to a substantial increase in packet drops and timeouts. The key reason is that the number of *RTS-Timeouts*, which happens when the RTS fails to get a CTS response, is greater due to the pessimistic estimation of the channel. This may happen when there is an RTS collusion or when the channel at the receiver is busy, thus preventing CTS initiation. The receiver sensitivity used to measure the state of the channel is very low when compared to signal strength from the source (Generally, the source and receiver is closer to each other). Hence, even a meek signal on the channel, which could not have corrupted the DATA packet, could block the CTS transmission. This leads to packet drops due to timeouts, which may result in adverse effects like lesser throughput and route failure. The second mode of IEEE 802.11 that uses DATA-ACK handshake is more aggressive in packet transmissions. Such a strategy coupled with the high signal strength between the source and receiver will generally lead to a better $\mathcal{H}$ metric.

10.4.2 Simulation analysis of HL and EL effects

The $\mathcal{H}$ in figure 10.2(c) indicates the *density* of the hidden links (red-arrows in IIG). Hence, while we are able to compare the effect of HL by $\mathcal{H}$, it does not directly translate to the improvement of

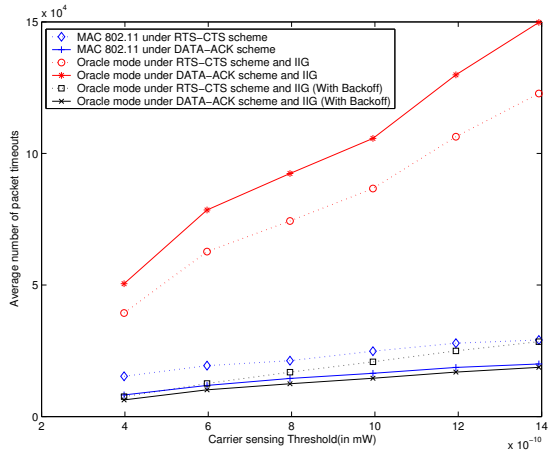

(a) HL effect indicated by average number of packet drops

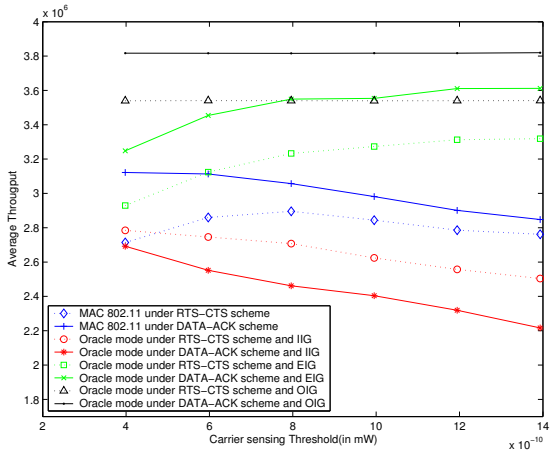

(b) Average Throughput

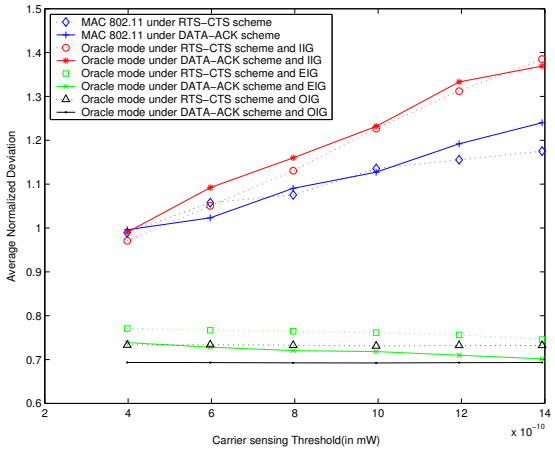

(c) Average Normalized Deviation

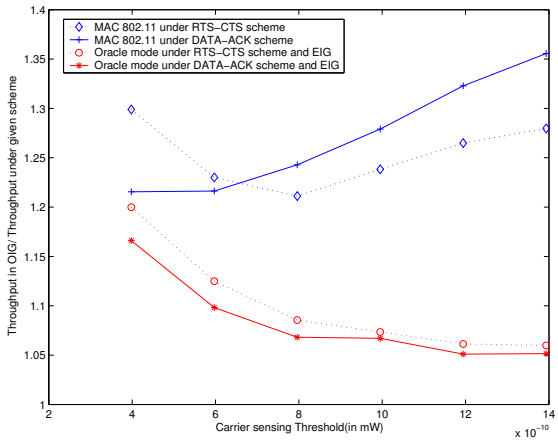

(d) EL effect indicated by throughput ratios

Figure 10.3: HL and EL effects observed in simulations

the other connection metrics. Simulation result analysis was done to observe the effect of HL and EL in terms of connection characteristics.

A generic and globally aware *Oracle MAC protocol* was developed to compare the various MAC strategies for transmission. The oracle MAC can be configured to indicate the parallel transmissions that are permitted. For example, each node under oracle scheme that is provided with the OIG graph transmits only if the currently active links form an interaction set in OIG. While this is not a distributed protocol, this helps to isolate and measure the effectiveness of the proposed graphs, thus enabling measuring the effect of HL/EL through empirical results.

Modeling the supplementary effects like backoff and virtual carrier sensing which are specific to the MAC protocol remains a future work. Oracle mode is simulated with three interaction graphs. For example, under the IIG scheme of 802.11 in RTS-CTS mode, the oracle mode allows the source node for a link to trigger the transmission if the active links on the channel is an allowed Interaction set(IS) for the given link in IIG. With respect to the IIG in Figure 10.1(c), link $(11, 14)$ belongs to $IS1$ and $IS5$. Hence, in oracle mode with IIG, the link $(11, 14)$ will initiate a transmission only if channel is sensed free at node 11 and one of the following three conditions are valid: (a) None of the links are transmitting; (b) Only the links in IS 1 is transmitting; (c) Only the links in IS 5 is transmitting.

The RTS is triggered under such a channel state and transmission of CTS and DATA are also initiated according to the 802.11 rules. An oracle mode under EIG/OIG scheme will obey the rules of the EIS/OIG. In this section, we simulate grid and random networks under oracle modes with IIG, EIG and OIG. We note the effect of throughput and packet drops by altering the configurations of oracle mode and comparing it with each other and the standard 802.11 protocol (both RTS-CTS and basic mode).

Figure 10.3(a) shows the number of packet drops under various schemes. It can be seen that the Oracle mode under IIG scheme has much more packet drops than the IEEE 802.11. This denotes that if the sources were to compete for the channel based on the IIG, the number of packet drops would be much higher than the 802.11 scheme. The effectiveness of the backoff and the VCS schemes in IEEE 802.11 can be observed in this graph. However, we will later show that the throughput and fairness observed in MAC 802.11 indicate that lesser packet drops come at the price of an overly restrictive backoff and VCS scheme. It is to be noted that there are no packet drops under oracle mode for EIG and OIG schemes since they represent the valid transmissions that can complete successfully. As the $CxThresh$ is increased, it can be seen that the number of packet drops increase. This trend is also indicated by the $\mathcal{H}$ in Figure 10.2(c). However, the $\mathcal{H}$ does not directly indicate the number of packet drops. The $\mathcal{H}$ assumes weighted probability of the all the ISs based on the number of links in the IS. A packet drop under one IS may initiate other ISs that favor the currently active links thus prohibiting equal competition by all the ISs. For example,

the $\mathcal{H}$ under RTS-CTS-DATA-ACK scheme in Figure 10.2(c) is not very sensitive to the carrier sense but the number of packet drops increase with $CxThresh$ in Figure 10.3(a). The DATA-ACK scheme has significantly lesser packet drops than the RTS-CTS-DATA-ACK scheme for the 802.11 protocol where as it is vice-versa in under the IIG scheme. We believe that this is because of the aggressive channel contention in the IIG (without backoffs). Figure 10.3(b) also shows that the average overall throughput under IIG scheme is significantly lower than the 802.11 counterparts, indicating again the effectiveness of backoffs. .

Impact on throughput The effect of hidden links for 802.11 on the overall throughput can be measured by comparing the throughput of 802.11 and the oracle EIG scheme counterparts. The oracle EIG scheme indicates the initiation of the links that can be successfully completed without any hidden terminals under a given MAC initiation scheme (source-initiation scheme in 802.11). Comparing the throughput for 802.11 and oracle EIG scheme will show the impact of the hidden links on throughput (Figure 10.3(b)). Increasing $CxThresh$ results in reduced exposed link effect($\mathcal{E}$) which should ideally increase the throughput. However as seen in graph 10.3(a), the throughput is increased under oracle EIG mode, but the throughput decreases for the 802.11 MAC. The difference between their throughput between is also increased when $CxThresh$ increases(due to larger number of packet drops), thus demonstrating that a higher $CxThresh$ may affect the throughput of the network. The oracle mode under OIG denotes the ideal two-way MAC policy with no packet losses. The OIG allows parallel transmissions based on the just the successful packet reception at source and destination and does not consider the state of the channel before transmission. Hence, if the $CxThresh$ is below the signal strength observed between the nodes of the link (which is true in real-world node configurations), the throughput of the OIG mode is insensitive to the variation of the $CxThresh$. Comparing the oracle EIG scheme to OIG scheme, shows the amount of difference in throughput due to a MAC initiation policy(source-initiated MAC in IEEE 802.11).

EL effect In this paragraph, we analyze the effect of EL on a given network topology in terms of the obtained throughput. The throughput achieved under *oracle mode and OIG* will be the ideal value without any exposed link effects and packet drops. We measure the exposed link effect by

comparing the throughputs between the above two schemes. We define the exposed terminal effect measured in simulation ($\mathcal{E}_s$) as the ratio of the throughput under the OIG to the throughput under a given MAC scheme. Figure 10.3(d) compares the $\mathcal{E}_s$ for different MAC schemes. A value of $\mathcal{E}_s = 1$ denotes the absence of the EL effect. The larger the value of the $\mathcal{E}_s$, the larger is the observed EL effect. The throughput obtained under the EIG scheme has exposed terminal effects (due to source initiation) but does not have packet losses. The $\mathcal{E}_s$ for such a scheme indicates the amount of exposed link under a perfect source-initiated scheme. Ideally, as the $CxThresh$ is increased, the amount of throughput that was blocked due to the busy channel at the nodes should be reduced, hence converging towards a value of 1. We also compare the MAC 802.11 for RTS-CTS-DATA-ACK and DATA-ACK schemes. This can be seen that the as the $CxThresh$ is increased, the $\mathcal{E}_s$ is generally increases in MAC 802.11. This is because of the coupled HL and EL effect in MAC 802.11.

Fairness analysis: In this paragraph we analyze fairness under various MAC schemes. We introduce a fairness metric(f) in order to measure the fairness of a given scheme[1]. The standard deviation σ of the throughputs of various connections for a given scenario gives an estimate of fairness. Let μ be the mean throughput of the connections for a given scenario. Lesser the value of σ, lesser the deviation from the mean throughput. Hence, greater will be fairness of a given scenario. However, while comparing against the different MAC schemes(with different mean throughputs), we normalize the metric to show the factor of variation for an unit mean throughput. Hence we define the *Fairness metric* (f) as given in Equation 10.4. The f of 0 will indicate complete fairness and the larger the value of the f, the greater will be the unfairness.

$$f = \frac{\rho}{\mu} \tag{10.4}$$

The unfairness in various scenarios is inherent in the contention based MAC protocols. However, in this analysis we measure the impact of the unfairness due to the given MAC scheme. Figure 10.3(c) shows the average normalized fairness metric across different random runs for various MAC

[1]We wish to exploring the fairness through the use of Jain's fairness metric [64] in the future studies

schemes. The fairness metric under the oracle mode and OIG will show the *average base unfairness* that is introduced due to the contention. The impact of the source-initiation policy (assuming no packet drops) of a MAC protocol can be seen by comparing the oracle OIG scheme with the oracle EIG scheme. The average impact of source-initiation is generally not very sensitive to the changes in $CxThresh$. However, comparison of the IIG and OIG fairness metrics will reveal the effect of source-initiated schemes with packet drops. It can be seen that the effect of packet drops is greater at higher $CxThresh$ values. It can be seen that policies of IEEE 802.11 does not significantly aid to reduce the fairness issues. The difference between the RTS-CTS-DATA-ACK and the DATA-ACK scheme is also not very pronounced.

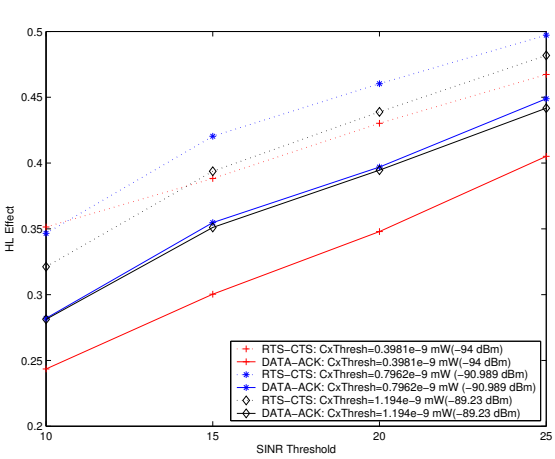

(a) HL Effect for different CxThreshold and SINR Thresholds

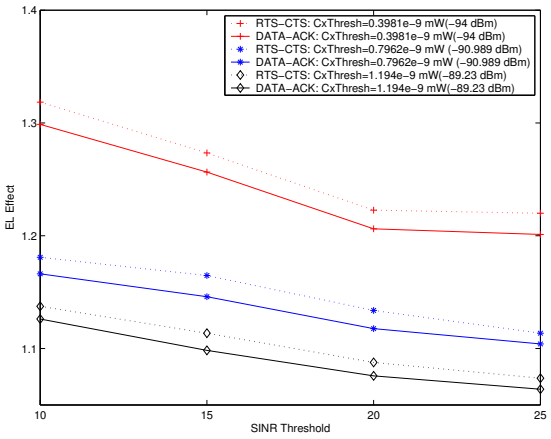

(b) EL effect for different CxThreshold and SINR Thresholds

Figure 10.4: HL and EL Metrics as a function of SINR Threshold

10.5 Conclusions and Future work

We presented the analysis of hidden terminal and exposed terminal in this study. Specifically, 'Interaction Graphs' were proposed to analyze and capture the interactions in MHWNs. Using the IGs, we proposed metrics to quantify the hidden terminal and exposed terminal problems. Methods to empirically estimate the effect of hidden and exposed terminals were proposed by comparing the oracle MAC protocol (under IIG, EIG and OIG) and the 802.11. Initial results indicate that

the proposed metrics match the expected relationship between Carrier Sense threshold and the hidden/exposed terminal effects.

Refining the effectiveness of the metric is a part of the future work. We currently use a simple heuristic to calculate the probability of occurrence of an IS(p). Incorporating the ideas from contention fairness (described in Chapter 8) into this probability calculation will refine the existing metrics. While the existing studies do not isolate and provide the interaction view of hidden and exposed terminals, most of the initial results are already observed by the related work. Simulation of larger type of scenarios can enable insights into the effects of HT/ET. We would like to simulate various other scenarios for this purpose. As a part of ongoing aim of the research, the effect of capturing HT/ET effectiveness with the routing effects can provide valuable feedback to the routing models proposed in this Chapter 4 and Chapter 5.

Chapter 11

Conclusions and Future work

Characterizing the MHWNs is challenging due the effect of interference, which is exhibited in various forms based on the spatial and temporal relationship between the nodes. The dissertation proposed a cohesive framework that captures the effect of interference at different layers of MHWNs. The study formulated *interference-aware routing models* and *CSMA based MAC models* that facilitate traffic-engineering in MHWNs. The design decisions were towards two primary long term goals: (1) Developing an online tool for traffic-engineering in static MHWNs. (2) Formally deriving the functionality of the distributed protocols from the proposed models.

The first contribution of the dissertation was a formulation of *interference-aware routing (IAR) model* using a classical network flow based approach. The IAR model not only accounts for the interference relationships between different edges, but also proposes objective functions that optimize at a connection level. Two flavors of this model were proposed: one for maximizing the throughput and another for minimizing the end-to-end connection delay. It was shown that such a globally co-ordinated routing provides significant improvement over the existing routing protocols under medium traffic conditions.

However, at higher traffic, the assumption of an ideal scheduler in the above model resulted in packet collisions under a more realistic MAC protocol. As a second contribution of the dissertation, we proposed a *scheduling aware routing (SAR) model* that provided interference separated routes by accounting for the scheduling effectiveness. A low-complexity scheduling model and a link-rating

scheme was developed to capture the scheduling effects.

The NP-hard nature of the IAR model limits its applicability in larger networks. The third contribution of the dissertation is a *decomposition based interference-aware routing (d-IAR) model* that is solved in a polynomial time algorithm. The complexity was reduced by applying domain-specific approximations, which resulted in orders of magnitude improvement over the IAR model while still providing efficient routes. Moreover, the application of decomposition techniques have provided formal mechanisms to derive distributed protocols. We wish to pursue the derivation of functionality of protocols using decomposition in the future: one of our primary goals of this line of research.

The next set of contributions was towards improving the accuracy of the CSMA scheduling model while maintaining a low-complexity solution. Towards this end, effective representation of the scheduling interactions were depicted by different *Interaction Graphs*. The versatility of such a framework was demonstrated by applying it for capturing the effect of hidden and exposed terminals. We modeled a fundamental fairness property of CSMA, called *Contention fairness*, using the framework of interaction graphs. The insights from the model enabled us to derive a distributed scheme called "Contention-aware Adaptive Backoff Scheme (CABS)".

Another aspect of CSMA modeling deals with identifying the interactions and quantifying the performance metrics for these interactions. Capturing the interaction between a two-flows forms the basis for the analysis of more complex CSMA interactions. The dissertation formulated throughput models for different categories of interactions between two flows. The accuracy of the model in asymmetric categories were demonstrated. Improving the accuracy of the throughput model in symmetric interaction scenarios is a part of the future work.

The contention fairness and two-flow formulations that were described above were designed as individual models. However, a single low-complexity scheduling model that encompasses primary aspects of CSMA behavior will enable precise characterization of scheduling in a generic scenario. Such a model can be integrated with the routing model, using the SAR or other alternative approaches, for an accurate interference and scheduling aware routing model. This line of research is a part of the future work, that enables us to achieve one of the long term goals, i.e. development

of an online traffic-engineering tool.

In summary, the dissertation formulated primary modeling components to realize a globally co-ordinated routing model that is aware of the effects of interference and CSMA scheduling.

Bibliography

[1] Aad, I., Ni, Q., Barakat, C., and Turletti, T. Enhancing ieee 802.11 mac in congested environments. In *Computer Communications 28 (2005) 16051617* (2005).

[2] Abramson, N. The ALOHA System – Another Alternative for Computer Communications. In *Proceedings of the 1970 Fall Joint Computer Conference* (Montvale, New Jersey, USA, 1970), vol. 36, AFIPS Press, pp. 177–186.

[3] Adya, A., Bahl, P., Padhye, J., Wolman, A., and Zhou, L. A multi-radio unification protocol for ieee 802.11 wireless networks. In *BROADNETS '04: Proceedings of the First International Conference on Broadband Networks (BROADNETS'04)* (Washington, DC, USA, 2004), IEEE Computer Society, pp. 344–354.

[4] Agarwal, S., Krishnamurthy, S. V., Katz, R. H., and Dao, S. K. Distributed Power Control in Ad-hoc Wireless Networks. *12th IEEE International Symposium on Personal, Indoor and Mobile Radio Communications, 2001 2* (2001), 59–66.

[5] Aguayo, D., Bicket, J., Biswas, S., Judd, G., and Morris, R. Link-level measurements from an 802.11b mesh network. In *SIGCOMM '04: Proceedings of the 2004 conference on Applications, technologies, architectures, and protocols for computer communications* (New York, NY, USA, 2004), ACM Press, pp. 121–132.

[6] Ahn, G.-S., Campbell, A. T., Veres, A., and Sun, L.-H. Supporting Service Differentiation for Real-Time and Best-Effort Traffic in Stateless Wireless Ad Hoc Networks (SWAN). *IEEE Transactions on Mobile Computing* (2002).

[7] Ahuja, R. K., Magnanti, T. L., and Orlin, J. B. *Network flows: theory, algorithms, and applications.* Prentice-Hall, Inc., Upper Saddle River, NJ, USA, 1993.

[8] Akyildiz, I. F., Wang, X., and Wang, W. Wireless mesh networks: a survey. In *Computer Networks* (2005).

[9] Bakshi, B. S., Krishna, P., Vaidya, N. H., and Pradhan, D. K. Improving performance of tcp over wireless networks. In *ICDCS '97: Proceedings of the 17th International Conference on Distributed Computing Systems (ICDCS '97)* (Washington, DC, USA, 1997), IEEE Computer Society, p. 365.

[10] Balakrishnan, H., Padmanabhan, V. N., Seshan, S., and Katz, R. H. A comparison of mechanisms for improving tcp performance over wireless links. *IEEE/ACM Trans. Netw. 5*, 6 (1997), 756–769.

[11] Bensaou, B., Wang, Y., and Ko, C. C. Fair medium access in 802.11 based wireless ad-hoc networks. In *MobiHoc '00: Proceedings of the 1st ACM international symposium on Mobile ad hoc networking & computing* (Piscataway, NJ, USA, 2000), IEEE Press, pp. 99–106.

[12] Berger-Sabbatel, G., Duda, A., Gaudoin, O., Heusse, M., and Rousseau, F. Fairness and its impact on delay in 802.11 networks. In *Global Telecommunications Conference, 2004. GLOBECOM '04. IEEE* (2004).

[13] Bharghavan, V., Demers, A., Shenker, S., and Zhang, L. Macaw: a media access protocol for wireless lan's. *SIGCOMM Comput. Commun. Rev. 24*, 4 (1994), 212–225.

[14] Bianchi, G. Performance analysis of the ieee 802.11 distributed coordination function. In *IEEE Journal on Selected Areas in Communications* (mar 2000), vol. 18, pp. 535–547.

[15] Bicket, J., Aguayo, D., Biswas, S., and Morris, R. Architecture and evaluation of an unplanned 802.11b mesh network. In *MobiCom '05: Proceedings of the 11th annual international conference on Mobile computing and networking* (New York, NY, USA, 2005), ACM Press, pp. 31–42.

[16] Boorstyn, R. R., Kershenbaum, A., Maglaris, B., and Sahin, V. Throughput analysis in multihop csma packet radio networks. *IEEE Trans. on Communication* (1987).

[17] Broch, J., Maltz, D. A., Johnson, D. B., Hu, Y.-C., and Jetcheva, J. A performance comparison of multi-hop wireless ad hoc network routing protocols. In *MobiCom '98: Proceedings of the 4th annual ACM/IEEE international conference on Mobile computing and networking* (New York, NY, USA, 1998), ACM Press, pp. 85–97.

[18] Carvalho, M. M., and Garcia-Luna-Aceves, J. J. A scalable model for channel access protocols in multihop ad hoc networks. In *MobiCom '04: Proceedings of the 10th annual international conference on Mobile computing and networking* (New York, NY, USA, 2004), ACM Press, pp. 330–344.

[19] Cavin, D., Sasson, Y., and Schiper, A. On the accuracy of manet simulators. In *POMC '02: Proceedings of the second ACM international workshop on Principles of mobile computing* (New York, NY, USA, 2002), ACM Press, pp. 38–43.

[20] Cerpa, A., Wong, J. L., Potkonjak, M., and Estrin, D. Temporal properties of low power wireless links: modeling and implications on multi-hop routing. In *MobiHoc '05: Proceedings of the 6th ACM international symposium on Mobile ad hoc networking and computing* (New York, NY, USA, 2005), ACM Press, pp. 414–425.

[21] Chaudet, C., Lassous, I. G., Thierry, E., and Gaujal, B. Study of the impact of asymmetry and carrier sense mechanism in ieee 802.11 multi-hops networks through a basic case. In *PE-WASUN '04: Proceedings of the 1st ACM international workshop on Performance evaluation of wireless ad hoc, sensor, and ubiquitous networks* (New York, NY, USA, 2004), ACM Press, pp. 1–7.

[22] Chiang, M., Low, S. H., Calderbank, A. R., and Doyle, J. C. Layering as optimization decomposition: A mathematical theory of network architectures. In *Proceedings of IEEE* (2007).

[23] Chin, K.-W., Judge, J., Williams, A., and Kermode, R. Implementation experience with manet routing protocols. *SIGCOMM Comput. Commun. Rev. 32*, 5 (2002), 49–59.

[24] Clausen, T., (editors), P. J., Adjih, C., Laouiti, A., Minet, P., Muhlethaler, P., Qayyum, A., and L.Viennot. Optimized link state routing protocol (olsr). RFC 3626, October 2003. Network Working Group.

[25] Couto, D. S. J. D., Aguayo, D., Bicket, J., and Morris, R. A high-throughput path metric for multi-hop wireless routing. In *MobiCom '03: Proceedings of the 9th annual international conference on Mobile computing and networking* (New York, NY, USA, 2003), ACM Press, pp. 134–146.

[26] Couto, D. S. J. D., Aguayo, D., Chambers, B. A., and Morris, R. Performance of multihop wireless networks: shortest path is not enough. *SIGCOMM Comput. Commun. Rev. 33*, 1 (2003), 83–88.

[27] Ilog CPLEX. `http://www.ilog.com/products/cplex/`.

[28] D., A., Malcolm, J., Agogbua, J., O'Dell, M., and McManus, J. Requirements for traffic engineering over MPLS, 1999. RFC 2702.

[29] Deng, J., Varshney, P. K., and Haas, Z. J. A new backoff algorithm for the ieee 802.11 distributed coordination function. In *CNDS 2004: Communication Networks and Distributed Systems Modeling and Simulation Conference* (2004).

[30] Draves, R., Padhye, J., and Zill, B. Comparison of routing metrics for static multi-hop wireless networks. In *SIGCOMM* (2004).

[31] Draves, R., Padhye, J., and Zill, B. Routing in multi-radio, multi-hop wireless mesh networks. In *MobiCom '04: Proceedings of the 10th annual international conference on Mobile computing and networking* (New York, NY, USA, 2004), ACM Press, pp. 114–128.

[32] Dube, R., Rais, C. D., Wang, K.-Y., and Tripathi, S. K. Signal stability based adaptive routing (ssa) for ad-hoc mobile networks. *IEEE Personal Communications* (1997).

[33] Durvy, M., and Thiran, P. Understanding the gap between the IEEE 802.11 protocol performance and the theoretical limits. In *IEEE SECON* (2006).

[34] Eckhardt, D., and Steenkiste, P. Measurement and analysis of the error characteristics of an in-building wireless network. In *SIGCOMM '96: Conference proceedings on Applications, technologies, architectures, and protocols for computer communications* (New York, NY, USA, 1996), ACM Press, pp. 243–254.

[35] Feldmann, A., Greenberg, A., Lund, C., Reingold, N., and Rexford, J. NetScope: traffic engineering for IP networks. *IEEE Network 14* (2000).

[36] Fullmer, C. L., and Garcia-Luna-Aceves, J. J. Floor acquisition multiple access (fama) for packet-radio networks. In *SIGCOMM '95: Proceedings of the conference on Applications, technologies, architectures, and protocols for computer communication* (New York, NY, USA, 1995), ACM Press, pp. 262–273.

[37] Fullmer, C. L., and Garcia-Luna-Aceves, J. J. Solutions to hidden terminal problems in wireless networks. *SIGCOMM Comput. Commun. Rev. 27*, 4 (1997), 39–49.

[38] Gallager, R. A minimum delay routing algorithm using distributed computation. *IEEE Transactions on Communications* (1977).

[39] Gambiroza, V., Sadeghi, B., and Knightly, E. W. End-to-end performance and fairness in multihop wireless backhaul networks. In *MobiCom '04: Proceedings of the 10th annual international conference on Mobile computing and networking* (New York, NY, USA, 2004), ACM Press, pp. 287–301.

[40] Gao, Y., Chiu, D.-M., and Lui, J. C. Determining the end-to-end throughput capacity in multi-hop networks: methodology and applications. *SIGMETRICS Perform. Eval. Rev. 34*, 1 (2006), 39–50.

[41] Garetto, M., Salonidis, T., and Knightly, E. W. Modeling per-flow throughput and capturing starvation in csma multi-hop wireless networks. *IEEE INFOCOMM* (2006).

[42] Garetto, M., Shi, J., and Knightly, E. W. Modeling media access in embedded two-flow topologies of multi-hop wireless networks. In *MobiCom '05* (New York, NY, USA, 2005), ACM Press, pp. 200–214.

[43] Garey, M. R., and Johnson, D. S. *Computers and Intractability: A Guide to the Theory of NP-Completeness*. W. H. Freeman & Co., New York, NY, USA, 1979.

[44] Gastpar, M., and Vetterli, M. On the capacity of wireless networks: the relay case. In *Twenty-First Annual Joint Conference of the IEEE Computer and Communications Societies. Proceedings. IEEE INFOCOM 2002* (2002).

[45] Girard, A., and Sansu, B. Multicommodity flow models, failure propagation, and reliable loss network design. *IEEE/ACM Trans. Netw.* (1998).

[46] Goff, T., Abu-Ghazaleh, N., Phatak, D., and Kahvecioglu, R. Preemptive routing in ad hoc networks. In *Proc. ACM Mobicom 2001* (2001).

[47] Gupta, P., and Kumar, P. The Capacity of Wireless Networks. In *IEEE TRANSACTIONS ON INFORMATION THEORY* (2000).

[48] Gupta, R., Musacchio, J., and Walrand, J. Sufficient Rate Constraints for QoS Flows in Ad-Hoc Networks. In *INFOCOMM* (2005).

[49] Gupta, R., and Walrand, J. Approximating maximal cliques in ad-hoc networks. In *Personal, Indoor and Mobile Radio Communications (PIMRC)* (2004).

[50] Gurin, R., and Orda, A. QoS-based Routing in Networks with Inaccurate Information: Theory and Algorithms. In *INFOCOM '97* (1997).

[51] Haas, Z., Pearlman, M., and Samar, P. Zone routing protocol (zrp) for ad hoc networks. Internet Draft, Internet Engineering Task Force, Dec. 2002. http://www.ietf.org/internet-drafts/draft-ietf-manet-zone-zrp-04.txt.

[52] Haas, Z. J., and Deng, J. On optimizing the backoff interval for random access schemes. In *IEEE TRANSACTIONS ON COMMUNICATIONS,* (2003).

[53] He, T., Stankovic, J. A., Lu, C., and Abdelzaher, T. Speed: A stateless protocol for real-time communication in sensor networks. In *ICDCS '03* (Washington, DC, USA, 2003), IEEE Computer Society, p. 46.

[54] Heusse, M., Rousseau, F., Berger-Sabbatel, G., and Duda, A. Performance anomaly of 802.11b. In *INFOCOM* (2003).

[55] Heusse, M., Rousseau, F., Guillier, R., and Duda, A. Idle sense: an optimal access method for high throughput and fairness in rate diverse wireless lans. *SIGCOMM Comput. Commun. Rev. 35*, 4 (2005), 121–132.

[56] Hill, J., Horton, M., Kling, R., and Krishnamurthy, L. The Platforms Enabling Wireless Sensor Networks. In *Communications of the ACM* (2004).

[57] Holland, G., and Vaidya, N. Analysis of tcp performance over mobile ad hoc networks. *Wirel. Netw. 8*, 2/3 (2002), 275–288.

[58] Holland, G., Vaidya, N., and Bahl, P. A rate-adaptive mac protocol for multi-hop wireless networks. In *MobiCom '01: Proceedings of the 7th annual international conference on Mobile computing and networking* (New York, NY, USA, 2001), ACM Press, pp. 236–251.

[59] Huang, X. L., and Bensaou, B. On max-min fairness and scheduling in wireless ad-hoc networks: analytical framework and implementation. In *MobiHoc '01: Proceedings of the 2nd ACM international symposium on Mobile ad hoc networking & computing* (New York, NY, USA, 2001), ACM Press, pp. 221–231.

[60] Huitema, C. *Routing in the Internet*. Prentice-Hall, Inc., Upper Saddle River, NJ, USA, 1995.

[61] Ieee 802.11e: Wireless medium access control (mac) and physical layer (phy) specifications: Medium access control (mac) enhancements for quality of service (qos).

[62] Ioannidis, J., Duchamp, D., and Gerald Q. Maguire, J. Ip-based protocols for mobile internetworking. In *SIGCOMM '91: Proceedings of the conference on Communications architecture & protocols* (New York, NY, USA, 1991), ACM Press, pp. 235–245.

[63] Jain, K., Padhye, J., Padmanabhan, V. N., and Qiu, L. Impact of interference on multi-hop wireless network performance. In *MobiCom* (2003).

[64] Jain, R., Chiu, D.-M., and Hawe., W. A quantitative measure of fairness and discrimination for resource allocation in shared computer system. *Technical Report 301, Digital Equipment Corporation* (Sept. 1984).

[65] Johnson, D. B., Maltz, D. A., Hu, Y.-C., and Jetcheva, J. G. The Dynamic Source Routing Protocol for Mobile Ad Hoc Networks (DSR), 2002.

[66] Jubin, J., and Tornow, J. D. The darpa packet radio network protocols. *Proceedings of the IEEE 75* (1987).

[67] Kamerman, A., and Monteban, L. WaveLAN -II: a high-performance wireless LAN for the unlicensed band. In *Bell Labs Technical Journal* (1997), vol. 2, pp. 118 – 133.

[68] Kang, S.-S., and Mutka, M. W. Provisioning service differentiation in ad hoc networks by modification of the backoff algorithm. In *Computer Communications and Networks* (2001).

[69] Kao, E. P. C. *An Introduction to Stochastic Processes*. Duxbury Press; 1 edition (June 21, 1996), 1996, ch. 3.4.

[70] Karn, P. MACA - a new channel access method for packet radio. In *Proceedings of the ARRL/CRRL Amateur Radio Ninth Computer Networking Conference* (Ontario, Canada, Sept. 1990), pp. 134–140.

[71] Karp, B., and Kung, H. GPSR: Greedy perimiter stateless routing for wireless networks. In *Proc. of ACM International Conference on Mobile Computing and Networking (MobiCom 2000)* (2000).

[72] Keshav, S. A control-theoretic approach to flow control. In *SIGCOMM '91: Proceedings of the conference on Communications architecture & protocols* (New York, NY, USA, 1991), ACM Press, pp. 3–15.

[73] Keshav, S. *An engineering approach to computer networking: ATM networks, the Internet, and the telephone network.* Addison-Wesley Longman Publishing Co., Inc., Boston, MA, USA, 1997.

[74] Kim, T.-S., Hou, J. C., and Lim, H. Improving spatial reuse through tuning transmit power, carrier sense threshold, and data rate in multihop wireless networks. In *MobiCom '06: Proceedings of the 12th annual international conference on Mobile computing and networking* (New York, NY, USA, 2006), ACM Press, pp. 366–377.

[75] Kleinrock, L., and Tobagi, F. A. Random access techniques for data transmission over packet-switched radio channels. In *Proceedings of National Computer Conference* (Anaheim, Californie, USA, May 1975), pp. 187–201.

[76] Kodialam, M., and Nandagopal, T. Characterizing achievable rates in multi-hop wireless networks: the joint routing and scheduling problem. In *MobiCom* (2003).

[77] Kodialam, M., and Nandagopal, T. The Effect of Interference on the Capacity of Multi-hop Wireless Networks. In *Bell Labs Technical Report, Lucent Technologies* (2003).

[78] Koksal, C. E., Kassab, H., and Balakrishnan, H. An analysis of short-term fairness in wireless media access protocols (poster session). *SIGMETRICS Perform. Eval. Rev. 28*, 1 (2000), 118–119.

[79] Kolar, V., and Abu-Ghazaleh, N. The effect of scheduling on link capacity in multi-hop wireless networks. *Technical report under arxiv.org: cs.NI/0608077* (2006).

[80] Kolar, V., and Abu-Ghazaleh, N. The effect of scheduling on link capacity in multi-hop wireless networks. In *CoRR, arXiv:cs.NI/0608077 v1* (2006).

[81] Kolar, V., and Abu-Ghazaleh, N. B. A Multi-Commodity Flow Approach to Globally Aware Routing in Multi-Hop Wireless Networks. In *IEEE Pervasive Computing and Communications (PerCom)* (2006).

[82] Kotz, D., Newport, C., and Elliott, C. The mistaken axioms of wireless-network research. Tech. Rep. TR2003-467, Dept. of Computer Science, Dartmouth College, July 2003.

[83] Li, J., Blake, C., Couto, D. S. J. D., Lee, H. I., and Morris, R. Capacity of Ad Hoc wireless networks. In *MobiCom* (2001).

[84] Li, Z., Nandi, S., and Gupta, A. K. Modeling the short-term unfairness of ieee 802.11 in presence of hidden terminals. *Perform. Eval. 63*, 4 (2006), 441–462.

[85] Lin, C. R. Qos routing in ad hoc wireless networks. In *LCN '98* (Washington, DC, USA, 1998), IEEE Computer Society, p. 31.

[86] Lundgren, H., Nordströ, E., and Tschudin, C. Coping with communication gray zones in ieee 802.11b based ad hoc networks. In *WOWMOM '02: Proceedings of the 5th ACM international workshop on Wireless mobile multimedia* (New York, NY, USA, 2002), ACM Press, pp. 49–55.

[87] Markopoulou, A. P., Tobagi, F. A., and Karam, M. J. Assessment of voip quality over internet backbones. *INFOCOM* (2002).

[88] Medepalli, K., and Tobagi, F. A. Towards performance modeling of ieee 802.11 based wireless networks: A unified framework and its applications. In *INFOCOM* (2006).

[89] Building the business case for implementation of wireless mesh networks, 2004.

[90] Meshdynamics inc. `http://www.meshdynamics.com/`.

[91] Metcalfe, R. M., and Boggs, D. R. Ethernet: distributed packet switching for local computer networks. *Commun. ACM 19*, 7 (1976), 395–404.

[92] Muqattash, A., and Krunz, M. A single-channel solution for transmission power control in wireless ad hoc networks. In *MobiHoc '04: Proceedings of the 5th ACM international symposium on Mobile ad hoc networking and computing* (New York, NY, USA, 2004), ACM Press, pp. 210–221.

[93] Murthy, S., and Garcia-Luna-Aceves, J. J. An efficient routing protocol for wireless networks. *Mob. Netw. Appl. 1*, 2 (1996), 183–197.

[94] Nandagopal, T., Kim, T.-E., Gao, X., and Bharghavan, V. Achieving mac layer fairness in wireless packet networks. In *MobiCom '00: Proceedings of the 6th annual international conference on Mobile computing and networking* (New York, NY, USA, 2000), ACM Press, pp. 87–98.

[95] Nasipuri, A., Castaneda, R., and Das, S. R. Performance of multipath routing for on-demand protocols in mobile ad hoc networks. *Mob. Netw. Appl.* (2001).

[96] Natkaniec, M., and Pach, A. R. An analysis of the back-off mechanism used in ieee 802.11 networks. In *ISCC '00: Proceedings of the Fifth IEEE Symposium on Computers and Communications (ISCC 2000)* (Washington, DC, USA, 2000), IEEE Computer Society, p. 444.

[97] Nemhauser, G. L., and Wolsey, L. A. *Integer and combinatorial optimization*. Wiley-Interscience, New York, NY, USA, 1988.

[98] Nocedal, J., and Wright, S. J. *Numerical Optimization*. Springer Verlag, 2006.

[99] Ortega, J. M., and Rheinboldt, W. C. *Iterative solution of nonlinear equations in several variables*. Society for Industrial and Applied Mathematics, Philadelphia, PA, USA, 2000.

[100] Park, J. C., and Kasera, S. K. Expected data rate: An accurate high-throughput path metric for multi-hop wireless routing. In *SECON: Second Annual IEEE Communications Society Conference on Sensor and Ad Hoc Communications and Networks* (2005).

[101] Park, V., and Corson, S. Temporally-ordered routing algorithm (TORA) version 1 functional specification. Internet Draft, Internet Engineering Task Force, Nov. 2000. http://www.ietf.org/internet-drafts/draft-ietf-manet-tora-spec-03.txt.

[102] Perkins, C. E., Belding-Royer, E. M., and Das, S. Ad hoc On-Demand Distance Vector (AODV) Routing, 2003.

[103] Perkins, C. E., and Bhagwat, P. Highly dynamic destination-sequenced distance-vector routing (DSDV) for mobile computers. *ACM Computer Communications Review 24*, 4 (Oct. 1994), 234–244. SIGCOMM '94 Symposium.

[104] Pioro, M., and Medhi, D. *Routing, Flow, and Capacity Design in Communication and Computer Networks*. Morgan Kaufmann, 2004.

[105] Qualnet network simulator, version 3.6. `http://www.scalable-networks.com/`.

[106] Raniwala, A., Gopalan, K., and cker Chiueh, T. Centralized channel assignment and routing algorithms for multi-channel wireless mesh networks. In *Mobile Computing and Communications Review* (2004).

[107] Rao, A., and Stoica, I. An overlay mac layer for 802.11 networks. In *MobiSys '05: Proceedings of the 3rd international conference on Mobile systems, applications, and services* (New York, NY, USA, 2005), ACM Press, pp. 135–148.

[108] Razak, S., Kolar, V., and Abu-Ghazaleh, N. Modeling and analysis of two-flow interactions in wireless networks. In *Fifth Annual Conference on Wireless On demand Network Systems and Services(WONS)* (2008).

[109] Roberts, J. Traffic theory and the Internet. *IEEE Communications Magazine* (2001).

[110] Rogers, P., and Abu-Ghazaleh, N. B. Analysis of Micro-level Behavior of Ad hoc Network MAC. In *IEEE International Conference on Wireless and Mobile Computing (WiMob)* (2005).

[111] Sadeghi, B., Kanodia, V., Sabharwal, A., and Knightly, E. Opportunistic media access for multirate ad hoc networks. In *MobiCom '02: Proceedings of the 8th annual international conference on Mobile computing and networking* (New York, NY, USA, 2002), ACM Press, pp. 24–35.

[112] Sankar, A., and Liu, Z. Maximum Lifetime Routing in Wireless Ad-hoc Networks. In *INFOCOMM* (2004).

[113] Schrijver, A. *Theory of linear and integer programming.* John Wiley & Sons, Inc., New York, NY, USA, 1986.

[114] Taha, H. A. *Operations Research: An Introduction.* Prentice Hall, 2000.

[115] Takai, M., Martin, J., and Bagrodia, R. Effects of wireless physical layer modeling in mobile ad hoc networks. In *MobiHoc* (2001).

[116] Talucci, F., Gerla, M., and Fratta, L. MACA-BI (MACA By Invitation)-a receiver oriented access protocolfor wireless multihop networks. *The 8th IEEE International Symposium on Personal, Indoor and Mobile Radio Communications, PIMRC '97., 2* (1997), 435–439.

[117] The IEEE Working Group for WLAN Standards. IEEE 802.11 Wireless Local Area Networks. http://grouper.ieee.org/groups/802/11/, 2002.

[118] Tobagi, F. A., and Brazio, J. M. Throughput analysis of multihop packet radio network under various channel access schemes. *IEEE INFOCOM* (1983).

[119] Tobagi, F. A., and Kleinrock, L. Packet switching in radio channels: Part ii–the hidden terminal problem in carrier sense multiple-access and the busy-tone solution. *IEEE Transactions on Communications* (1975).

[120] Vaidya, N. H., Bahl, P., and Gupta, S. Distributed fair scheduling in a wireless lan. In *MobiCom '00: Proceedings of the 6th annual international conference on Mobile computing and networking* (New York, NY, USA, 2000), ACM Press, pp. 167–178.

[121] Valkó, A. G. Cellular ip: a new approach to internet host mobility. *SIGCOMM Comput. Commun. Rev. 29*, 1 (1999), 50–65.

[122] Vutukury, S., and Garcia-Luna-Aceves, J. J. A simple approximation to minimum-delay routing. *SIGCOMM Comput. Commun. Rev. 29*, 4 (1999), 227–238.

[123] Wang, X., and Kar, K. Throughput modelling and fairness issues in csma/ca based ad-hoc networks. In *INFOCOM* (2005).

[124] Xu, K., Gerla, M., and Bae, S. How Effective is the IEEE 802.11 RTS/CTS Handshake in Ad Hoc Networks? In *IEEE Globecom* (2002).

[125] Xu, S., and Saadawi, T. Revealing the problems with 802.11 medium access control protocol in multi-hop wireless ad hoc networks. *Comput. Networks 38*, 4 (2002), 531–548.

[126] Yang, X., and Vaidya, N. H. Priority scheduling in wireless ad hoc networks. In *MobiHoc '02: Proceedings of the 3rd ACM international symposium on Mobile ad hoc networking & computing* (New York, NY, USA, 2002), ACM Press, pp. 71–79.

[127] Yang, X., and Vaidya, N. H. On the physical carrier sense in wireless ad hoc networks. In *INFOCOM '05* (2005).

[128] Yang, Y., Hou, J. C., and Kung, L.-C. Modeling the Effect of Transmit Power and Physical Carrier Sense in Multi-hop Wireless Networks. *INFOCOM* (2007).

[129] Yang, Y., Wang, J., and Kravets, R. Designing routing metrics for mesh networks. In *WiMesh: First IEEE Workshop on Wireless Mesh Networks* (2005).

[130] Yarvis, M. D., Conner, W. S., Krishnamurthy, L., Chhabra, J., Elliott, B., and Mainwaring, A. Real-world experiences with an interactive ad hoc sensor network. *icppw 00* (2002), 143.

[131] Yi, Y., and Shakkottai, S. Hop-by-hop congestion control over a wireless multi-hop network. In *INFOCOM* (2004).

[132] Zhang, H., Arora, A., and Sinha, P. Learn on the fly: Data-driven link estimation and routing in sensor network backbones. In *25th IEEE International Conference on Computer Communications (INFOCOM)* (2006).